Improving the Rainfall and Flood Frequency Analyses Using Stochastic Storm Transposition Method

by

Morteza Kiani

Presented to the Faculty of the Graduate School of

The University of Texas at Arlington in Partial Fulfillment

of the Requirements

for the Degree of

MASTER OF SCIENCE IN CIVIL AND ENVIRONMENTAL ENGINEERING

THE UNIVERSITY OF TEXAS AT ARLINGTON

DECEMBER 2015

Copyright © by Morteza Kiani 2015

All Rights Reserved

Acknowledgements

It is difficult to overstate my gratitude to my advisor, Dr. Nick Z. Fang. Without his active supervision and constant support, this journey would not have been possible. I am also thankful to my committee members Dr. Dong-Jun Seo and Dr. Xinbao Yu for their comments and insights.

In addition, I would like to thank all those who have helped me throughout my M.Sc. program by providing invaluable technical and scientific guidance. Dr. Daniel Wright's insightful comments and constructive criticisms of my research were thought provoking, and they helped me focus my ideas. I am grateful to him. I am grateful to Mr. Jerry Cotter, Matthew Flaming, Simeon Benson and other colleagues at the U.S. Army Corps of Engineers for their encouragement and practical advice. I would like to acknowledge Dr. Ghandehari for numerous discussions on related topics that helped me improve my knowledge in the area.

This thesis would not have been possible without the love and support of my family. My deepest gratitude to my parents and my wife for teaching me the importance of learning and for all the sacrifices they made for me. My special thanks goes to my wife for her endless support during my graduate studies in providing invaluable information, and guidance. She was the source of inspiration and kindness for me. I definitely would not be able to fulfill this research without her technical and mental support.

December 9, 2015

Abstract

Improving the Rainfall and Flood Frequency Analyses Using Stochastic Storm Transposition Method

Morteza Kiani, M.Sc.

The University of Texas at Arlington, 2015

Supervising Professor: Nick Z. Fang

Reproduction and realization of historical rainfall events provides foundations for flood and rainfall frequency analyses and the advancement of meteorological studies. Stochastic storm transposition (SST) is a method for such a purpose and enables us to perform frequency analyses by transposing observed historical storm events over any given watershed. The goal of this study is to stochastically examine the impacts of extreme events on all locations in a homogeneity zone. Storms with the same probability of occurrence on a defined homogenous neighborhood will generate various impacts due to spatial and temporal variations of the storms. Transposing storms occurring in the homogeneity zone will improve our understanding based on any probable rainfall event. This procedure is iterated thousands of times to simulate less frequent storm events over a watershed as the basis to update frequency curves such as the intensity duration frequency (IDF) and flood frequency analysis (FFA). Thousands of storm realizations were utilized along the semi-distributed rainfall-runoff model with low run time enabling the SST to embrace thousands of possible events. A unique characteristic of this study is that applying the SST to a well-defined and commonly used hydrologic model changes the SST method from a theoretical approach to an applied method for frequency analysis. This study focuses on one of the subbasins in the Upper Trinity River watershed, the Mary's Creek River Basin within the Dallas-Fort Worth metroplex. This watershed has a total area of 53 square miles. Ten years of NEXRAD radar rainfall data were used in this study to examine the precipitation and flood frequency curves and a semi-distributed

rainfall-runoff model was coupled with a multi-sensor precipitation estimator (MPE) to create thousands of storm realizations. We used an innovative approach in storm selection to ensure the inclusion of those events that produce high rainfall depth over the study area. The SST approach was successfully used to extend the existing data set temporally and spatially. IDF results from the SST data were compared with other sources such as USGS/TxDOT and iSWM. Results showed that for rainfall with one-hour durations, rainfall intensity from TxDOT/USGS and iSWM IDF curves were consistently higher than SST results at all subbasins. The opposite trend was observed for all other rainfall durations. The FFA results indicate that the design storms (5-year, 10-year, 25-year, 50-year, 100-year, and 200-year) have considerable overestimation at subbbasins with low drainage contributing area compared to the corresponding SST results. The SST and design storms results are similar at downstream locations. As a final objective, we used the SST approach to understand the relationship between return periods of rainfall and discharge information. The results imply that the regional IDF information is subject to large uncertainties due to low correlation between return periods of discharge and rainfall.

Table of Contents

Acknowledgements iii

Abstract iv

List of Illustrations viii

List of Tables xii

Chapter 1 Introduction and Literature Review 1

1.1. Rainfall Frequency Analysis 2

1.1.1. Rainfall Frequency Analysis in Texas 5

1.2. Flood Frequency Analysis 8

1.3. Stochastic Storm Transposition 10

Chapter 2 Approach/Methodology 14

2.1. Data and Study Area 14

2.1.1. Multi-sensor Precipitation Estimator (MPE) 14

2.1.2. Homogeneity Zone 16

2.1.3. Selection of a Study Basin 19

2.2. Hydrologic Model 25

2.3. Methodology 31

2.3.1. Storm Selection 31

2.3.1.1. Developing Preliminary Storm Catalog 32

2.3.1.2. Deterministic Storm Transposition 35

2.3.2. Stochastic Storm Transposition 40

2.3.3. Developing a Module to Perform SST 43

Chapter 3 Results 45

3.1. Historical Analysis 45

3.2. Storm Selection 49

3.3. Rainfall Frequency Analysis 56

3.4. Flood Frequency Analysis (FFA) 72
3.4.1. FFA at USGS gauge location 74
3.4.1. FFA Results at Other Junctions 76
3.5. Correlation between Rainfall and Flood Return Periods 79
Chapter 4 Conclusion and Recommendation for Operational Settings 83
Appendix A Annual Maximum MAP for 54 subbasins 86
References 95
Biographical Information 102

List of Illustrations

Figure 1-1 **a)** Depth of precipitation for 5-year storm for one-hour duration. **b)** Depth of precipitation for 100-year storm for one-hour duration in Texas (Asquith and Roussel 2004)..... 6

Figure 1-2 Intensity-duration-frequency for Tarrant County developed by iSWM..... 7

Figure 2-1 Sample MPE over WGRFC domain (12/24/2012 08z)..... 17

Figure 2-2 AWA defined homogeneity zone (Keppel et al., 2012)..... 18

Figure 2-3 **a)** West Fork Trinity River Basin and its defined homogeneity zone (The grid shows the HRAP pixels, 40 × 40 HRAP pixels), **b)** Location of USGS gauges in West Fork Trinity River Basin, location of 3 selected USGS gauges is enlarged for better illustration, **c)** Upper Trinity River Basin and its defined homogeneity zone (80 × 80 HRAP pixels), **d)** the Mary's Creek River Basin and its defined homogeneity zone (21 × 21 HRAP pixels). 20

Figure 2-4 Streamflow observation at three USGS gauges along the West Fork Trinity River for two different time periods: **a)** 1/20/2010–5/11/2010 and **b)** 5/1/2015–6/15/2015. Gauge Site 8047500 is located at the most downstream location, and Sites 8048000 and 8048543 are located upstream. Flow regulation is apparent at Gauge Site 8047500 at the downstream location. 21

Figure 2-5 **a)** Location of Mary's Creek basin in Upper Trinity River Basin 24

Figure 2-6 Instantaneous discharge (2007), USGS gauge (8047050) Mary's Creek at Benbrook.24

Figure 2-7 **a)** HEC-HMS model of the Mary's Creek River Basin and **b)** histogram of subbasin areas for the Mary's Creek River Basin 27

Figure 2-8 **a)** A sample basin falling on two MPE pixels; hence, the pixel values represent the hourly MPE data for each part of the basin. Actual mean areal precipitation should be 0.98 in while Zonal Statistics return the value of 0.89 in. and **b**) a demonstration of redefined HRAP pixels are used in a MAPCalc package. 28

Figure 2-9 An integrated interface coupling MAPCalc, HEC-DSS and HEC-HMS..... 30

Figure 2-10 Synthetic storms at four consecutive time steps (hourly). 34

Figure 2-11 **a)** Deterministic transposition procedure. Black box shows the initial location of the storm, which is the same as homogeneity zone. Yellow box (Location 2) shows deterministic transposition entry point and the green box shows the location of the storm at the last trial of deterministic storm transposition. **b)** Black dots show all the locations that upper right corner of the black box will experience in deterministic transposition..... 36

Figure 2-12. **a)** A storm with three storm cells **b)** A storm with only one storm cell. Storm (b) will produce a higher MAP compared to storm (a), but storm (a) has a higher chance of creating extreme events when transposed due to having more storm cells. 37

Figure 2-13 Histogram of MAP values from all transpositions of two storms..... 38

Figure 2-14. Summary of the steps required for creating storm catalogue..... 39

Figure 2-15 Probability distribution function for Poisson distribution for **a)** λ =1, **b)** λ=4, and **c)** λ=10..... 40

Figure 2-16 Poisson cumulative distribution function for λ =1, 4 and 10 41

Figure 2-17 Flowchart of the stochastic storm transposition method..... 43

Figure 2-18 Developed module to implement the SST on a user-defined watershed. This module supports ESRI-ASCII and shapefile as the basin definition. 44

Figure 3-1 Annual maximum rainfall intensities for 10 years of radar rainfall values..... 46

Figure 3-2 a) The 500 highest MPE values for each year over the rectangle MPE domain**. b)** The 500 highest MPE values for each year over the homogeneity zone of the Mary's Creek River Basin**. c)** Location of the highest MPE pixels over the rectangle MPE domain **d)** Location of the highest MPE pixels over the homogeneity zone of the Mary's Creek River Basin..... 48

Figure 3-3 **a)** annual peak flow. **b)** monthly peak flow at Mary's Creek at Benbrook USGS gauge. The annual peak flow is for water year not the calendar year, as reported by USGS.3.2. Storm Catalog 49

Figure 3-4 **a)** Center locations of the *deterministically* transposed storms with either 1-hour or 6 hour durations over the homogeneity zone (7,056 points) (transposition increment is ¼ HRAP). **b)** Center locations of the *stochastically* transposed storms over the homogeneity zone after 5,000 realizations with increment of 1/32 HRAP..... 51

Figure 3-5 Histograms of MAP values over the basin from all transpositions of the top 48 storms form the preliminary storm selection (6-hour rainfall duration in 2007). Maximum MAP value over the basin and POE index are given as the title and subtitle of the histograms. 53

Figure 3-6 Cumulative distribution function of MAP values over the Mary's Creek River Basin for the 50 storms from deterministic transposition 54

Figure 3-7 Rainfall frequency analysis for different numbers of annual maximum MAP over the Mary's Creek River Basin (e.g., by iterating SST 500 times, frequency analysis could be extended up to 500 years). Obs refers to the original annual maximum..... 57

Figure 3-8 Spatial locations of the four classified subbasins..... 58

Figure 3-9 IDF curves based on observed values, iSWM, TxDOT-USGS and SST for Subbasins 4, 18, 19, 20, 21 and 23 in Group (I). 61

Figure 3-10 IDF curves based on observed values, iSWM, TxDOT-USGS and SST Group(i)..... 62

Figure 3-11 IDF curves based on observed values, iSWM, TxDOT-USGS and SST Group(i)..... 63

Figure 3-12 IDF curves based on observed values, iSWM, TxDOT-USGS and SST Group(i)..... 64

Figure 3-13 IDF curves based on observed values, iSWM, TxDOT-USGS and SST Group(i)..... 65

Figure 3-14 IDF curves based on observed values, iSWM, TxDOT-USGS and SST Group(i)..... 66

Figure 3-15 IDF curves based on observed values, iSWM, TxDOT-USGS and SST Group(ii).... 67

Figure 3-16 IDF curves based on observed values, iSWM, TxDOT-USGS and SST Group(ii).... 68

Figure 3-17 IDF curves based on observed values, iSWM, TxDOT-USGS and SST Group(iii)... 69

Figure 3-18 IDF curves based on observed, iSWM, TxDOT-USGS and SST for Group(iv) 70

Figure 3-19 Locations of the selected control points and..... 72

Figure 3-20 **a)** All simulated hydrographs were based on 5,000 realizations (~ 5,000 runs) from SST at an upstream junction (J1B) and **b)** at the USGS gauge location (downstream)..... 74
Figure 3-21 Results of the FFA at USGS gauge location for observed annual peak flow (blue dots), design storm (black dots) and SST (green). The solid red line is the fitted Log-Pearson III and the dashed red lines show the 90% confidence interval..... 75
Figure 3-22 FFA results for the basins with low drainage areas 77
Figure 3-23 FFA results of the basins with medium drainage areas..... 78
Figure 3-24 FFA results of the downstream basins with high drainage areas 79
Figure 3-25 Locations of the selected points to study the relationship between rainfall and flow . 80
Figure 3-26 Scatter plots of return periods between rainfall and streamflow..... 81
Figure 3-27 Scatter plots of the return period between rainfall and streamflow 82
Figure 3-28 Scatter plots of the return period between rainfall and streamflow 82

List of Tables

Table 2-1 Land and lake area and their detention effect ratio in the West Fork Trinity River Basin, the Upper Trinity River Basin and the Mary's Creek River Basin. 23

Table 2-2 Column 2 gives the hourly MAP values over the homogeneity zone. Columns 3, 4, 5 demonstrate how to aggregate the hourly MAP values to 6-, 12-, and 24-hr MAP values, respectively. Columns 8, 10, 12 and 14 give the highest MAP values in the year 2007 after sorting columns 2, 3, 4, and 5, respectively. 33

Table 3-1 Annual maximum mean areal precipitation (MAP) values over Mary's Creek and their occurrence date and time for 1-, 6-, 12- and 24-hour rainfall durations over 10 years of radar data (2005-2014). 46

Table 3-2 Selected preliminary storms in 2007 for six hour duration with sorted MAP values over the homogeneity zone 50

Table 3-3 Finalized 6-hours storm catalogue for 10 years based on the preselected list 55

Table 3-4 Four classified subbasins with areas 59

Table 3-5 Classifying the junctions based on drainage area 76

Chapter 1

Introduction and Literature Review

Analyzing the impact of extreme events is a critical topic for hydrologists and water resource engineers as it is an important factor in design and construction of structures and flood management planning. A wide range of hydrologic designs, including roadways, drainage systems, culverts, runways, and so on, are based on rainfall and flood frequency analysis. Also, important structures such as dams and nuclear plants have to be constructed to withstand the most extreme floods, which necessitate construction based on probable maximum precipitation (PMP) and probable maximum floods (PMF). Rainfall is the first building block in frequency analysis and having an accurate estimate is important. Designing water infrastructure accurately and managing flood risk efficiently heavily rely on accurate rainfall information.

Traditional rainfall frequency analysis is based on rain gauge data, which are typically performed using point measurements and in most places are spatially sparse; therefore, additional sources of rainfall information may need to be considered to statistically capture the spatial and temporal variability of extreme rainfall events in a region (Paixao et al. 2015). Advancement in radar-based rainfall estimation provides valuable information on spatial and temporal variations of storms. The U.S. National Weather Service (NWS) established a large network of high-resolution radars called Next-Generation Radar (NEXRAD) in 1988 which has been the main source of rainfall data for severe weather warning and forecasting since the mid-1990s (Fulton 2002). The goal of this study is to benefit from radar information and update existing rainfall and frequency analyses for the study area. One of the drawbacks of using radar information for frequency analysis is the short period of available data (less than 30 years). Rainfall records can be extended by transposing the extreme observed events from other locations, which could have occurred over

the desired catchment (Franchini et al. 1996). This technique is called stochastic storm transposition (SST) and is applied in this research to increase the length of the radar-based rainfall.

This chapter is organized as follows: Section 1.1 presents rainfall frequency analysis, common practices, and previous studies. Section 1.2. describes flood frequency analysis through common approaches as well as previous studies. The stochastic storm transposition concept and its applications are given in Section 1.3.

1.1. Rainfall Frequency Analysis

Intensity–duration–frequency (IDF) curves are widely used in design of hydrosystems and flood risk management in many places. IDF curves are essentially a conditional cumulative distribution function (CDF) of rainfall intensity, conditioned on rainfall duration. IDF curves are usually based on time increments, not the complete storm duration which means they are calculated by sub-dividing the rainfall record into intervals of a desired duration (Eagleson 1970; Chow et al. 1988). Gutknecht (1977) investigated the difference between the IDF curves based on the time increments and the complete storm and concluded that although IDF curves based on a complete storm duration generally have lower rainfall intensity, the difference between two methods is small.

Rainfall frequency analysis is based on rainfall extreme values and there are two common approaches to extract these extreme values called annual maximum series (AMS) and partial duration series (PDS). In AMS, the largest rainfall intensity for a given rainfall duration over a year is selected, while in PDS all the events exceeding a predefined threshold are chosen (Chow et al. 1988). The PDS approach may include some dependent events which are not desired when applying the classical extreme value theory to certain events assumed to be independent (Stedinger et al. 1993). The following explanation is based on the first approach (AMS).

After sub-dividing the rainfall record into intervals of a desired duration, the annual maxima of rainfall intensity (averaged over the duration) is ranked in a descending order. Using a plotting position formula such as Weibull, the conditional return period conditioned on the rainfall duration is calculated. The return period here is the expectation of the number of years between two rainfall events with the chosen duration exceeding (or equal) to a particular intensity. The reciprocal relationship between return period and the probability of rainfall intensity for a given duration exceeding a particular value can be written as follows.

$$\mathrm{P}\{\mathrm{I} \geq i_e | t_r\} = \frac{1}{T} = 1 - \int_0^{i_e} f_I(i \mid t_r)\, di = 1 - F_I(i_e | t_r) \tag{1-1}$$

where $F_I(i_e|t_r)$ is the conditional CDF for rainfall intensity of i_e, given rainfall duration of t_r which is the formal expression of the IDF curves (Sivapalan and Bloschl 1998).

The primary intent of performing rainfall frequency analysis is to estimate the depth of a rainfall for a given return period based on this reciprocal relationship. For example, a 24-hour rainfall with 10% probability of exceedance refers to an event with a return period of 10 years (24-hour storm with this magnitude would likely happen once every 10 years). The values of this return period and duration as well as the rainfall intensity can be found from IDF curves. A typical design return period varies from 2–10 years for small channels or conduits and from to 50–100 years for larger structures such as small dams, large channels or levees. Some critical infrastructures such as spillways and nuclear plants need to be designed for 500 years or more for safety reasons (Chow et al. 1988).

Usually a probability distribution function (PDF) is fitted to the available data points (rainfall intensity for a given duration at different return periods) in order to investigate the statistical properties of extreme rainfall events and also to extrapolate beyond the available data for engineering purposes (Hao and Singh 2013). Many probability distributions have been proposed and applied for rainfall frequency analyses such as generalized extreme value (GEV)

distribution, lognormal distribution, gamma distribution and generalized Pareto distribution (GP), to name a few. GEV distribution is used worldwide and is the most common distribution used for rainfall frequency analysis (Asquith 1998; Alila 1999; Gellens 2002; Fowler and Kilsby 2003; Koutsoyiannis 2004; Overeem et al. 2009; Eldardiry et al. 2015; Marra and Morin 2015). GEV distribution is a combination of three extreme value models of Gumble, Weibull and Frechet. According to NOAA Atlas 14, GEV is a better fit compared to other distributions for the U.S. (Perica et al. 2013).

The IDF curves described above are based on point measurements of rainfall and are valid at the measurement location; however, in most of the studies a catchment-wide estimate is desired. The common approach is using area reduction factors (ARFs), which are empirically-derived functions of the catchment area, that is, rainfall duration and sometimes the return period (US Weather Bureau 1957). Then, rainfall intensity from IDF curves is multiplied by the corresponding ARFs with the desired catchment area, rainfall duration, and return period to develop the catchment IDF curves. When the catchment is small, ARF is close to one (1) and the point IDF curves and catchment IDF curves become almost identical; however, with increasing the size of the catchment the ARFs fall away from unity, and catchment IDF curves become lower and flatter. Sivapalan and Bloschl (1998) introduced an alternative methodology based on the spatial correlation structure of rainfall as an attempt to link scientific theories of spatial-temporal rainfall field with design methods. There have been several studies to develop ARFs based on radar rainfall information to benefit from the better representation of extreme precipitation. Allen and DeGaetano (2005) explored the feasibility of radar-based extreme precipitation to develop ARFs. Results showed considerable differences between radar-based ARFs and gauge-based ARFs. Radar-based ARFs decayed at a faster rate (with increasing area) than gauge ARFs. Olivera et al. (2008) developed ARFs for the 685,000 km^2 of Texas using NEXRAD rainfall estimates. They also reported lower ARFs compared to gauge-based ARFs. Overeem et al. (2009) also reported

similar behavior. But this study mainly focuses on the development of IDF for the Mary's Creek watershed.

There have also been several studies on employing radar information to update IDF curves. Durrans et al. (2000) used seven years of radar data (1993–2000) from the Arkansas-Red Basin River Forecast Center (ABRFC). They concluded that data heterogeneities and lack of data as well as biases found in radar estimates are major factors limiting the development of depth-area relationships based on radar-rainfall data. Wright et al. (2013) conducted a rainfall frequency analysis with stochastic storm transposition using high-resolution radar data that was bias adjusted based on a dense network of rain gauges. They reported a similar behavior between gauge and radar-based frequency analyses despite other studies. Eldardiry et al. (2015) investigated the reasons behind the discrepancies between radar- and gauge-based frequency analyses using 13 years of quantitative precipitation estimates (QPEs) over Louisiana. They found that the limited record of radar rainfall attributed to the majority of the uncertainty associated with the radar-based quantiles; however, the limited radar rainfall records were not directly responsible for the systematic underestimation of the radar-based frequency information. The systematic underestimation was mainly attributed to the existing conditional biases in radar estimates.

1.1.1. Rainfall Frequency Analysis in Texas

Technical Paper 40 (TP-40) is the rainfall frequency atlas of the United States for rainfall durations ranging from 30 min to 24 hours and rainfall return periods of 2–100 years (Hershfield 1962). Later, Fredrick et al. (1977) developed HYDRO-35 for smaller durations and return periods from 2 to 100 years. The U.S. Geological Survey (USGS), in cooperation with the Texas Department of Transportation (TxDOT), developed the depth-duration-frequency (DDF) curves of precipitation for Texas (Asquith, 1998) and areal-reduction factors (ARFs) of the one-day design storm for selected localities in Texas (Asquith, 1999; Asquith and Famiglietti, 2000). Asquith

(1998) provided procedures to develop DDF values for any location in Texas for 12 distinct storm durations from 15 minutes to seven days and recurrence intervals from 2 to 500 years; however, they are cumbersome to apply. Therefore, in 2003, the USGS, again in cooperation with the Texas Department of Transportation constructed an atlas of DDF curves of precipitation for Texas. The maps of the atlas are analogous to the DDF maps prepared by the National Weather Service (NWS) in earlier studies. In total, there are 96 maps depicting the spatial variation of the depth-duration frequency of precipitation annual maxima for Texas for return periods of 2, 5, 10, 25, 50, 100, 250, and 500 years and storm durations of 15 and 30 minutes; 1, 2, 3, 6, and 12 hours; and 1, 2, 3, 5, and 7 days (Asquith and Roussel 2004). Figure 1-1a and b show depths of precipitation for 5-year and 100-year storms of one-hour duration for Texas, respectively as an example.

(a) (b)

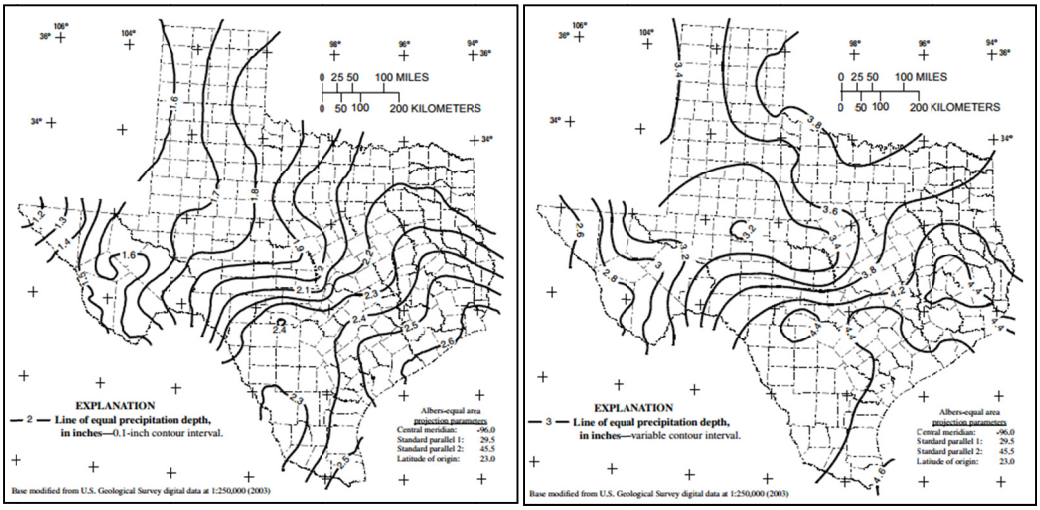

Figure 1-1 **a)** Depth of precipitation for 5-year storm for one-hour duration. **b)** Depth of precipitation for 100-year storm for one-hour duration in Texas (Asquith and Roussel 2004)

IDF curves can also be expressed as empirical equations such as Eq. 1-2 which is widely used in design (iSWM Technical Manual 2014).

$$i = \frac{b}{(t+d)^e} \quad (1\text{-}2)$$

where i is rainfall intensity (inches per hour), t is rainfall duration (minutes) and b, d and e are parameters varying with location and return periods, which are tabulated for each county and can be found in iSWM Technical Manual. This empirical equation is used for their design purposes in Texas and, therefore, is used in this study. Hereafter, we use iSWM IDF curves to refer to IDF curves derived based on Eq. 1-2 and the parameters tabulated in iSWM Technical Manual (2014). Figure 1-2 illustrates IDF curves for Tarrant County as an example of iSWM IDF curves.

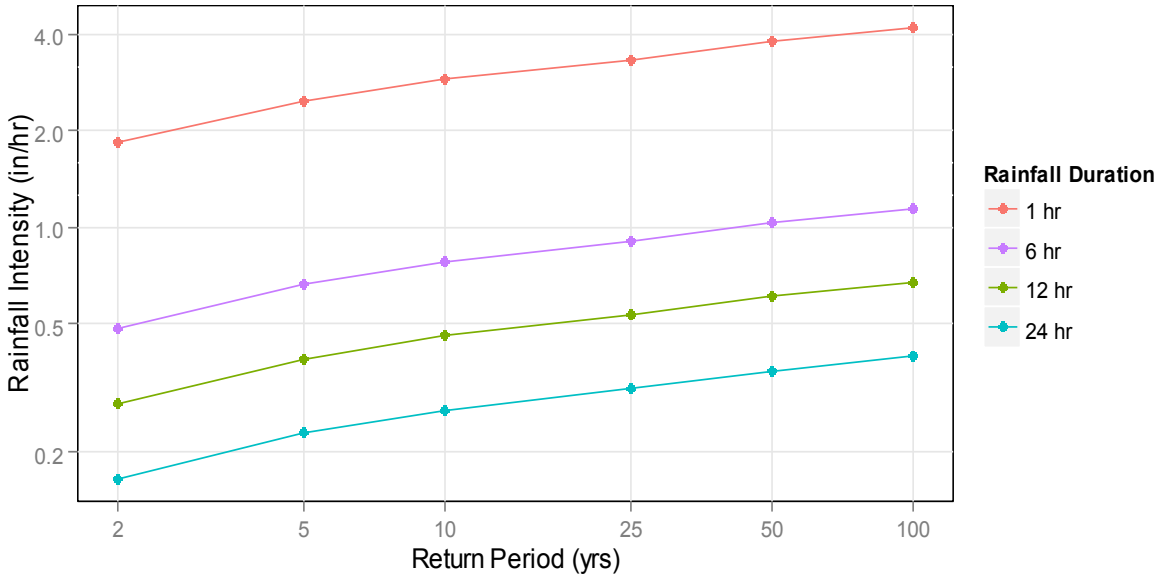

Figure 1-2 Intensity-duration-frequency for Tarrant County developed by iSWM

1.2. Flood Frequency Analysis

Peak discharge information is essential for determining the appropriate size of water conveyance systems such as channels, storm drains, etc. The peak flow frequency is necessary to determine how often the system exceeds its capacity. Usually water-related structures/systems are designed based on socio-economic responses to the inconveniences resulting from exceeding the capacity of the structure and the cost of building the structure/system (Feldman 1979). Flood frequency analysis provides the necessary information to decide how large the system should be with the design based on the risk of exceeding system capacity. In general, there are two common approaches for flood frequency analysis. The first approach uses observed flow data, and the second approach uses a rainfall-runoff model.

There are several statistical approaches when using discharge measurements to perform flood frequency analysis. The process is similar to rainfall frequency analysis. The extreme events and peak flows can be extracted using either annual maximum series (AMS) or the partial duration series (PDS). Annual maximum series is the common approach in flood frequency studies. Then, the peak flow values are treated as a random variable representing a sample of the flood information at the streamflow station. The annual peak flows are assumed to be independent and identically distributed (i.e., homogeneous data set). The annual peak flows are ranked and the return period is calculated using a plotting position formula. There are several distributions which can be fitted in order to have a better representation of the data and to allow extrapolating beyond the available data. The common ones are:

- Normal distribution
- Log-Normal distribution
- Gumbel distribution
- Log-Pearson Type III distribution

Each of these distributions has different properties that can be useful in predicting design floods and has its own merits and demerits. Log-Pearson Type III distribution is the most commonly used technique, and it is also recommended by the U.S. Water Advisory Committee on Water Data (1982) for flood frequency analysis. In this study, the Log-Pearson Type III distribution is used to perform FFA when required.

There are several underlying assumptions in statistical approaches. Stationarity assumption is the most important assumption, which means the process does not change over time. In other words, the change on the peak flow is cyclic, and the cycle is short and repeats in the record of available data. If the stationarity assumption is not met, there should be an adjustment to the data set. Two important factors that can cause non-stationarity are urbanization and climate change. Effects of human activities, river regulation, geomorphological and physiographical modifications and urbanization on flood frequency analyses have been widely investigated (Struoczewski et al. 2001; Villarini et al. 2009a; 2009b; Villarini and Smith 2010; Wright et al. 2012; Villarini et al. 2013). Also Milly et al. 2008 showed how temporal stationarity assumptions in regular frequency analysis undermine the effect of climate change on hydrological studies.

Sometimes, a stationary series of annual peak flows is available, but not at the desired location. In this case, regional frequency analysis is performed by transferring the parameters of the flood frequency distribution from one gauge location to the location of interest (Feldman 1979). However, this is a challenging process and generally not suitable for watersheds which are greatly impacted by human intervention (Wright et al. 2013). The greatest source of error in both rainfall and flood frequency analysis is inadequate data for estimating the distribution. Sampling error can be reduced by extending the data period. In some cases, paleofloods can be used to reduce the sampling error (England et al. 2014).

The second approach is to use the rainfall-runoff model. In this case, a design storm is usually developed based on the IDF curves for a given frequency. The physically based link

between IDF curves and design storm is the time of concentration. For a certain (constant) rainfall intensity, peak flow will be obtained after a duration equal to the time of concentration when the whole catchment contributes to the discharge at the outlet location. Therefore, a design storm is based on IDF curves when rainfall duration is equal to time of concentration of the catchment of interest. Then the selected rainfall intensity is shaped into a design storm hyetograph that conforms to the appearance of historical or synthetic hyetograph patterns (Adams and Howard 1986).

The rainfall-runoff model is then forced by the design storm to analyze the response of the catchment. It is common practice to assume that the design storm hyetograph and the runoff hydrographs resulting from hydrological model have the same frequency (return period). This assumption has been questioned (Adams and Howard 1986; Wright et al. 2014), and we also investigated this assumption herein. Wright et al. (2014) showed that the rainfall with a *T*-year return period does not necessarily cause *T*-year flooding. In other words, there is no one-to-one relationship between rainfall frequency and flood frequency. Therefore, the conventional flood frequency analysis is subject to errors arising from the assumptions explained in this section.

1.3. Stochastic Storm Transposition

Traditional rainfall and flood frequency analysis are based on several assumptions which are often not met. One of the recent approaches applied in frequency analysis is stochastic storm transposition (SST), which addresses some of the problems arising from applying traditional approaches in frequency analysis. The concept of the SST is very similar to the Monte-Carlo approach (Weidi 1987) and provides an opportunity to analyze the probability of exceedance of the extreme storms and their recurrences. Stochastic transposition of storms consists of "transposing extraordinary storm data from one place to another within a meteorologically

homogenous region" (Weidi 1987). A comprehensive mathematical form of SST was given by Foufoula-Georgiou (1989), and it has been used in frequency analyses and in estimating probable maximum precipitation (PMP) and probable maximum flood (PMF).

One of the main drawbacks of traditional frequency analysis are sampling errors due to inadequate records, which can be addressed by using stochastic storm transposition (SST). SST uniformly transposes observed extreme events to lengthen the data record, which enables us to estimate rainfall and floods for higher return periods (beyond 100 years). SST is simply trading space with time (Wright et al. 2013).

Franchini et al. (1996) applied the SST technique to estimate exceedance probabilities of extreme design floods. Each storm was linked to a flood peak using rainfall-runoff transformation and stochastic description of antecedent moisture conditions and storm depth temporal distributions. Cumulative average catchment depths produced by the SST approach was converted to a range of possible flood peak values using a rainfall-runoff model (the ARNO model). Franchini et al. (1996) further concluded that even regionalization and standard flood frequency analysis methods (based on extrapolation of a hypothesized probability distribution function for floods) are not appropriate for estimation of design events of return periods greater than 500-1000 years.

England et al. (2014) applied an integration of collaborative work in hydrometeorology, flood hydrology, and paleoflood hydrology. The SST model was applied for the first time to the large and mountainous Arkansas River Basin with an area of 4,633 mi^2. The two-dimensional Runoff, Erosion and Export (TREX) model was coupled with SST to estimate extreme flood hazards with very low annual exceedance probabilities ($\leq 10^{-4}$). About 110 extreme storms with some depth-area-duration (DAD) information were located in their study area. Soil moisture was incorporated on hydrological model internalizations. England et al. (2014) also considered three saturation levels for sensitivity analysis: 0.05 (dry), 0.2 (slight saturation) and 0.8 (near

saturation). They concluded that the size and location of extreme storms are substantially important for flood frequency analysis, and the runoff model results were improved.

Wright et al. (2013) presented an alternative framework for rainfall frequency analysis that coupled SST with "storm catalogs" developed from 10 years of bias, i.e., corrected radar rainfall data. The transposition method applied was similar to that used in the estimation of probable maximum precipitation (PMP) and probable maximum flood (PMF) in Hansen (1987). The results of NOAA Atlas 14 and SST-based IDF curves for 1, 3, 6 and 12-hour rainfall durations were similar at point/radar—pixel scale for Little Sugar Creek at Archdale. For a longer period (500 and 100 years) the SST-based estimates for a one-hour duration are larger than Atlas 14. Wright et al. (2013) concluded that SST can be a useful alternative to conventional approaches for flood risk assessment

Wright et al. (2014) used SST to synthetize long records of rainfall over the Charlotte, North Carolina, US metropolitan area by reshuffling radar rainfall data. The resampled radar rainfall data was used to force a physics-based distributed hydrologic model for a heavily urbanized watershed in Charlotte. They estimated the discharge return periods along the mainstream flow without having any assumptions for rainfall structure or its interactions with watershed features that are usually required in conventional methods. They concluded SST can provide a rigorous probabilistic approach for examining the spatial extent of flooding and also incorporated nonstationarity in rainfall or land use into the flood risk assessment process. Wright et al. (2014) also demonstrated a considerable difference between rainfall and peak flood return periods for a particular event, contrary to the conventional one-to-one assumption between the return period of the rainfall and peak flow.

This study presents a modified version of the SST along with the physically based rainfall-runoff model for rainfall and flood frequency analysis. The procedure of selecting extreme events has been modified (Section 2.3.1.) in order to increase the probability of having extreme

events on the study area when transposing stochastically. To the best of author's knowledge this is the first study to apply SST and updated IDF curves and flood frequency analysis for an urbanized watershed in Texas. Radar rainfall information was obtained from NWS's West Gulf River Forecast Center (WGRFC) for this study. Also parallel processing programming techniques were implemented in this study to significantly reduce the run time, enabling us to relocate thousands of storm realizations in the SST procedure within a reasonable timeframe.

Chapter 2

Approach/Methodology

A multi-sensor precipitation estimator (MPE) was used in this study due to the availability of data and relatively long period covered by the records. This approach is explained in Section 2.1.1. Definition of the homogeneity zone from where the storm can be transposed to the location of interest is given in Section 2.1.2. The size of the zone and unregulated flow information are two important factors in choosing the case study. The coarse resolution of MPE data, flow regulation, and constraints in choosing the homogeneity zone posed some limitations on the choice of case study. All the case studies considered and the final choice is explained in Section 2.1.3. HEC-HMS is the hydrologic model used in this study and the challenges in using HEC-HMS for SST are described in detail in Section 2.2. Section 2.3 describes the methodology in three main subsections: 1) storm selection (Section 2.3.1.), 2) stochastic storm transposition procedure (Section 2.3.2.), and 3) the modules developed for SST (Section 2.3.3).

2.1. Data and Study Area

2.1.1. Multi-sensor Precipitation Estimator (MPE)

Precipitation information is the first building block in any hydrological modeling. Existing errors in precipitation data can grow nonlinearly in streamflow simulation; thus, it is very important to have an accurate data set. In the late 1980s, the U.S. National Weather Service (NWS) installed the Next-Generation Weather Radar (NEXRAD) system consisting of a network of WSR-88D (Weather Surveillance Radar, 1998 Doppler) radars at 159 sites throughout the United States and at selected locations overseas (Klazura and Imy 1993). Reflectivity measurements from WSR-88D radars apply as a basis to estimate the quantitative precipitation

estimates (QPE). Reflectivity is converted to rainfall intensity using Z-R relationships (Battan 1973; Lovejoy and Austin 1979; Rinehart 1991). There are different Z-R relationships for various types of rainfall events (Smith et al. 1990). A forecaster and hydrologist decided at NWS which to use based on their experience and understanding of the storm types. Thus, this was a subjective approach of calculating QPE solely relying on the expertise of the human forecaster (Olson et al. 1995). Upgrading the WSR-88D radars began in 2010 and was completed in 2013. WSR-88D sites across the nation were upgraded to polarimetric radars, which added vertical polarization to horizontal radar waves in order to more accurately detect different types of hydrometeors and reduce the possible chances of misclassification as well as automating the whole process (Hagen and Meischner 2000; Melnikov et al. 2003; Bachmann 2004; Ivics et al. 2008).

NEXRAD radar rainfall products have four stages (I-IV) based on the amount of processing and quality control for different uses. Stage I is the hourly rainfall estimate using radar alone with the nominal spatial resolution of 4 km x 4 km based on the Hydrologic Rainfall Analysis Project (HRAP) grid coordinate system (Reed and Maidment 1999). Stage II includes mean bias correction and local adjustments using rain gauge data. Stage III product mosaics are the result of multiple radar QPEs combined into one product at the River Forecast Center (RFC) scale, which also has interactive quality control of both gauge and radar data (Briendenbach et al. 1998). Finally, Stage IV mosaics are based on the RFC level Stage III products, which is the most widely used product at the national scale. Other rainfall products have different temporal and spatial resolutions. For example, the Multi-Radar Multi-Sensor (MRMS) system built at the National Severe Storms Laboratory (NSSL) and implemented at the National Center for Environmental Prediction (NCEP) ingests ~146 S-band dual-polarization WSR-88D radars across the conterminous United States (CONUS) and ~ 30 C-band single polarization across southern Canada. It has a horizontal resolution of 0.01° and temporal resolution of 2 min (Zhang et al.

2015). Ideally, we would like to perform SST with such fine resolution rainfall information; however, the length of the record is too short (less than 2 years) at this time.

In this study, we have used the multi-sensor precipitation estimator (MPE) (Seo et al. 2010, Kitzmiller et al. 2011). MPE is a near real-time product that merges rainfall measurements from rain gauges, rainfall estimates from NEXRAD, and the Geostationary Operational Environmental Satellite (GOES) products (Seo et al. 2010). The MPE product obtained from the West Gulf River Forecast Center (WGRFC) has a temporal resolution of one hour and nominal spatial resolution of 4 km at mid-latitudes in the Hydrologic Rainfall Analysis Project (HRAP) grid (Greene and Hudlow 1982). The MPE product is subject to different sources of errors that are variable in space and time. One of the well-known errors existing in MPE is the truncation error, which results in underestimation of the rainfall value and accordingly underestimates streamflow simulation prior to 2004 (Fulton et al. 2003). To avoid having bias adjustment in this study, we used MPE from the last 10 years spanning from 2005–2014. There are numerous studies on evaluating MPE (Wang et al. 2008, Wescott et al. 2008, Habib et al. 2009, Habib et al. 2013), bias adjustment (Zhang et al. 2011) and improving the accuracy via fusion (Rafieeinasab et al. 2015). Due to the inaccessibility of the rain gauge data in the study area, we relied on the accuracy of MPE and did not perform evaluation or bias adjustment of MPE. Figure 2-1 shows an example of MPE and WGRFC borders.

2.1.2. Homogeneity Zone

The main goal of the SST was to transpose storms occurring at other locations to the location of interest which can increase the length of available data and make the frequency analysis feasible for return periods beyond 100 years without relying on extrapolation. The SST is implemented over a domain called the homogeneity zone. The storm transposition area or so-called homogeneity zone is the area wherein all past storms can be transposed anywhere in the

region either with the same depths and an adjustment to their probability of occurrence, or with the same probability of occurrence but with an adjustment to their depths (Foufoula-Georgiou 1989). For example, transposing a hurricane from a coastal area to inland places without any adjustment to the moisture amount will introduce error because the air mass would lose moisture when traveling inland (US Army Corps of Engineers, HMR52, 1984).

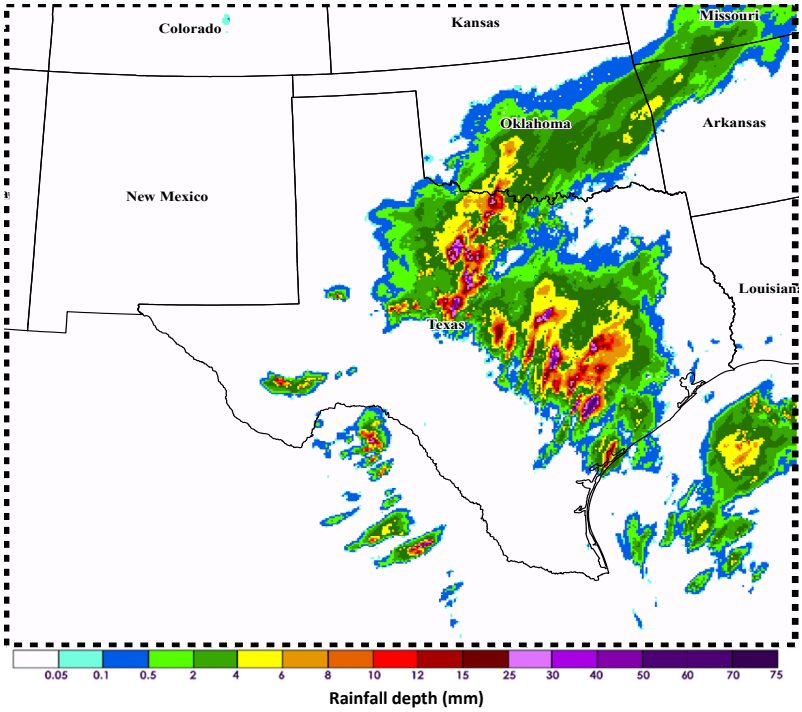

Figure 2-1 Sample MPE over WGRFC domain (12/24/2012 08z)

An analytical study was performed by the Applied Weather Associates (AWA) with the Tarrant Regional Water District (TRWD), using a homogeneity zone as depicted in Figure 2-2 for TRWD watersheds (Kappel et al. 2012). Figure 2-2 shows an area with similar meteorological conditions and topography and storms can be transposed from any point in this area to the location of interest.

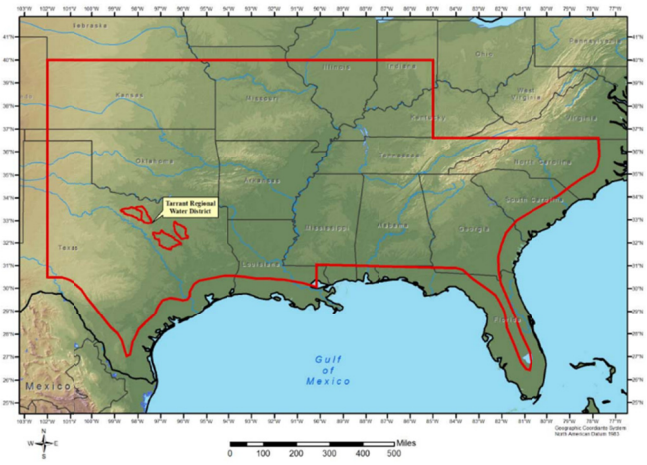

Figure 2-2 AWA defined homogeneity zone (Keppel et al., 2012)

Although larger homogeneity zone can include more storms into the analysis, overextending the homogeneity zone can introduce more complexity. To avoid such complexity and rainfall depth adjustment, we define the homogeneity zone in such a way that no adjustment is required. Also, the ratio between the area of the homogeneity zone and desired basins are important to the SST approach. This ratio varies from 10 to 60 in different studies (Foufoula-Georgiou 1989; England et al. 2014; Wright et al. 2014). In PMP/PMF studies, storms are transposed deterministically; therefore, the homogeneity zone is only a search domain for extreme events. However, when SST is used for frequency analysis, storms are selected from the homogeneity zone and then stochastically transposed within the homogeneity zone (refer to Section 2.3.2 for more detail). Having a very large homogeneity zone for our application will yield many incidents where the storm does not fall on the location of interest since storms are transposed stochastically. On the other hand, if the homogeneity zone is too small, the number and value of added storms to the historical record for the location of interest would be limited, which consequently affects the flood frequency analysis. Therefore, the homogeneity zone should be

defined in a way that is large enough to generate extreme events to the existing record of rainfall over the study area, but not so large as to indicate too many incidents with no rainfall.

2.1.3. Selection of a Study Basin

Even though our primary goal was to perform SST over the Dallas–Fort Worth area and beyond, we had to change our case study for several reasons as explained below. Due to the coarse resolution of MPE, the first choice for the study area was the West Fork Trinity River Basin (Figure 2-3a). This case study was large enough to show the effect of storm transposition as well as being sensitive to the coarse resolution of MPE. The ratio between the homogeneity zone and watershed area is about 20, which falls into the range used in the previous studies. However, flow was regulated heavily at several locations, and the hydrological model could not reflect the regulation effect properly. The resultant hydrographs were biased in both peak flow and volume. The observed values from three USGS stream gauges (8048543, 8047500 and 8048000) downstream of the West Fork Trinity River are shown in Figure 2-4 to demonstrate the effect of regulated flow. Geographic location of the gauges with respect to the study area is shown in Figure 2-3b. The USGS gauge at Beach St. along the West Fork Trinity River (8048543) is located at the most downstream point about 20 miles near the downstream outlet. Two more USGS gauges were placed at the Clear Fork Trinity River (8047500) and at Fort Worth along the West Fork Trinity River (8048000) upstream of gauge 8048543.

Figure 2-4a and Figure 2-4b illustrate observed flow from two time periods of Jan-May 2010 and May-July 2015, respectively. The impact of the regulated flow on the observed flow is apparent in Figure 2-4. Reservoir management, flood control or other regulations can drastically change the runoff volume during extreme events. Streamflow information does not reflect the natural response of watershed to rainfall events due to flood control operations. The streamflow information at the two upstream gauges (8047500 and 8048000) has natural looking hydrographs

while the gauge (8048543) at the downstream location is like a step-wise function and cannot be captured by the model if the regulation information is not fed into the hydrologic model properly. The human interruptions in heavily regulated basins make the flood frequency analysis unreliable. Thus, the West Fork Trinity River Basin was not selected.

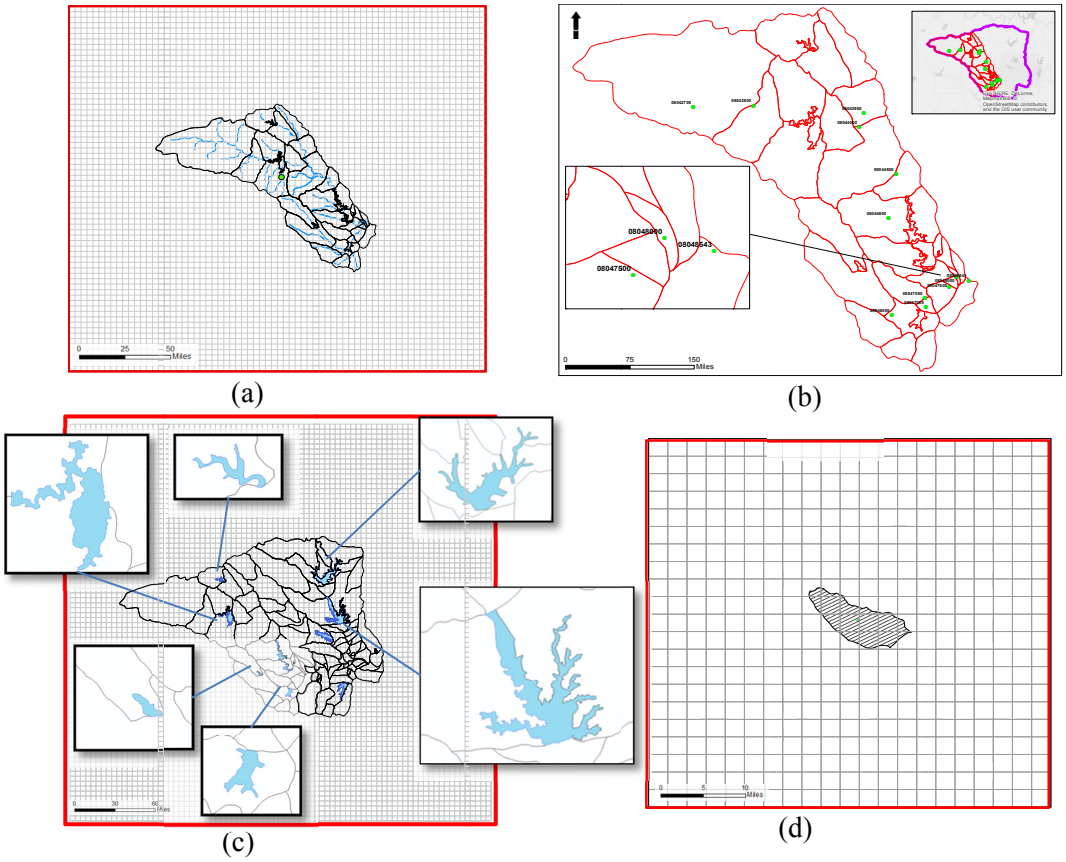

Figure 2-3 **a)** West Fork Trinity River Basin and its defined homogeneity zone (The grid shows the HRAP pixels, 40 × 40 HRAP pixels), **b)** Location of USGS gauges in West Fork Trinity River Basin, location of 3 selected USGS gauges is enlarged for better illustration, **c)** Upper Trinity River Basin and its defined homogeneity zone (80 × 80 HRAP pixels), **d)** the Mary's Creek River Basin and its defined homogeneity zone (21 × 21 HRAP pixels).

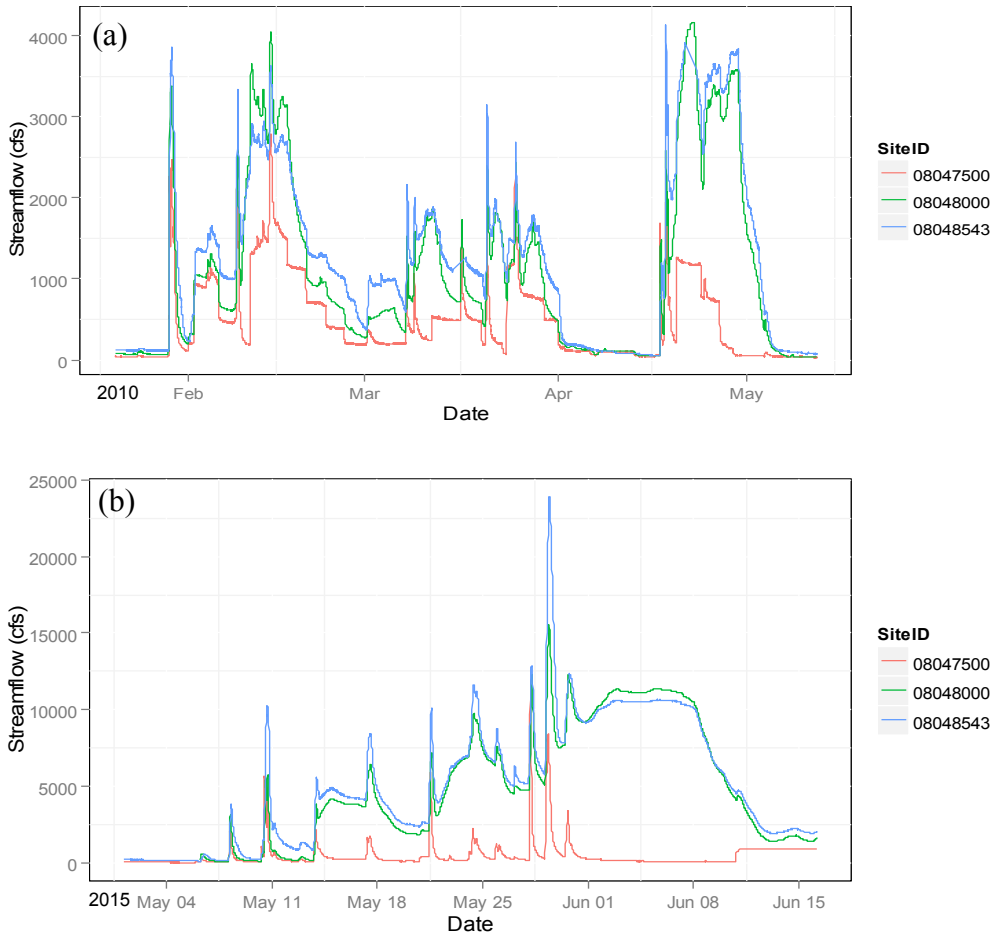

Figure 2-4 Streamflow observation at three USGS gauges along the West Fork Trinity River for two different time periods: **a)** 1/20/2010–5/11/2010 and **b)** 5/1/2015–6/15/2015. Gauge Site 8047500 is located at the most downstream location, and Sites 8048000 and 8048543 are located upstream. Flow regulation is apparent at Gauge Site 8047500 at the downstream location.

Our second considered study area was the Upper Trinity River Basin (Figure 2-3c). The Upper Trinity River Bain is ~ 6,500 square miles and includes 116 subbasins. Since the watershed is located on the north east side of the West Gulf River Forecasting Center, the homogeneity zone could not be expanded from the north side. One could use another rainfall product such as Stage

IV, which is a dataset for the ccontiguous US (Seo et al. 2010) to overcome the constraint at the north side, or we could have used an irregular shape for the homogeneity zone expanding only from other sides. The ratio between the area of homogeneity zone and the watershed would be about eight in this case. This low ratio would reduce the chance of transposing enough storms to lengthen the number of historical data.

We approached the rainfall frequency analysis for the Upper Trinity River Basin; however, in the course of study we found out that it was too large to perform rainfall frequency analysis in an *integrated* manner. By *integrated*, we mean in a manner where one can randomly transpose one storm from any location within the homogeneity zone and calculate mean areal rainfall over all the subbasins at once. We found that a very large basin like the Upper Trinity River Basin tends not to accommodate large storm events that can generate significant amount of rainfall. In other words, an extreme rainfall most likely will not cover the whole case study. As a result, mean areal precipitation (MAP) values for some of the basins would be zero or close to zero which causes a significant underestimation on frequency analysis. Thus, smaller subbasins must be used or the SST approach must be repeated for individual subbasins.

Another reasoning for not approaching the problem with this case study was the large number of lakes and reservoirs in the Upper Trinity River Basin. The hydrologic model applied in this study was capable of simulating the reservoir effects and other regulations through the storage-discharge relationship; nevertheless, reservoir operation and flood control operations did not obey the predefined storage-discharge functions or other regulations in critical conditions. The lake-to-land ratio for all cases is given in

Table 2-1.

The Mary's Creek River Basin was selected as the final study area (Figure 2-3d). Mary's Creek, the largest contributor to the Clear Fork Trinity River with the release of Benbrook Dam, which has a 52.8 square mile drainage area. The basin extends from the Clear Fork Trinity River

(Clear Fork) near SH 183 to a distance of approximately 14 miles northwest into Parker County. Frequency analysis of the annual peak discharges since 1952 (about 60 years ago), indicates that the 100-year discharge on Mary's Creek is about 30,000 cfs (Mary's Creek, Findings from adjustments to hydrologic model, 2014).

Table 2-1 Land and lake area and their detention effect ratio in the West Fork Trinity River Basin, the Upper Trinity River Basin and the Mary's Creek River Basin.

	West Fork Trinity River Basin	*Upper Trinity River Basin*	*Mary's Creek River Basin*
Watershed area (mi^2)	2670	6316	53
Lake area (mi^2)	44	156.58	0.61
Ratio (%)	1.65	2.48	1.15

Figure 2-5a shows the Mary's Creek location in the Upper Trinity River Basin. Figure 2-5b also shows the detailed watershed delineation on Mary's Creek. There is only one USGS gauge (8047050) within the Mary's Creek River Basin, Mary's Creek at Benbrook(Figure 2-5b) shows the instantaneous streamflow from this site since 2007 when the data first became available. The daily peak flow reports of the gauges go back to 1988 (http://waterdata.usgs.gov/nwis). We selected the Mary's Creek River Basin because we did not observe any drastic impact from flow regulations or existing detention effect. In addition, Mary's Creek has a lower ratio between total catchment area and the total lake area (

Table 2-1). As shown on Figure 2-5b, the watershed delineation in Mary's Creek hydrologic model is very detailed; therefore, it will avoid any mismatch between point and radar pixel during the MAP calculation.

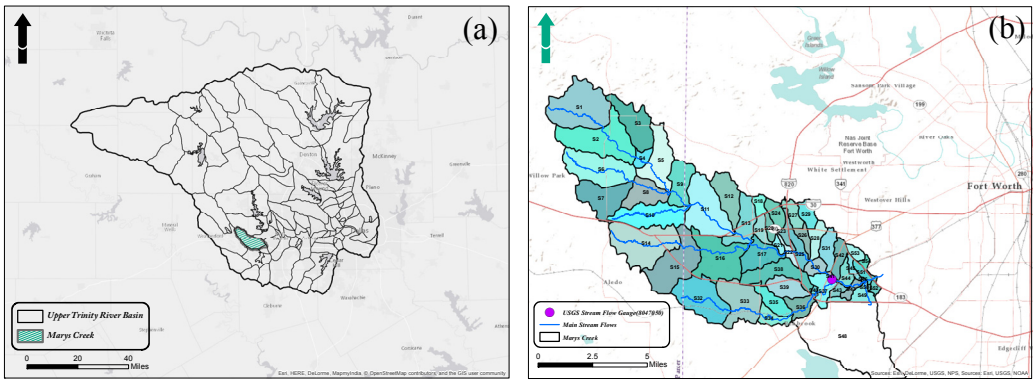

Figure 2-5 **a)** Location of Mary's Creek basin in Upper Trinity River Basin

and **b)** Mary's Creek and the delineated subbasins

(Mary's Creek, Findings from adjustments to hydrologic model, 2014)

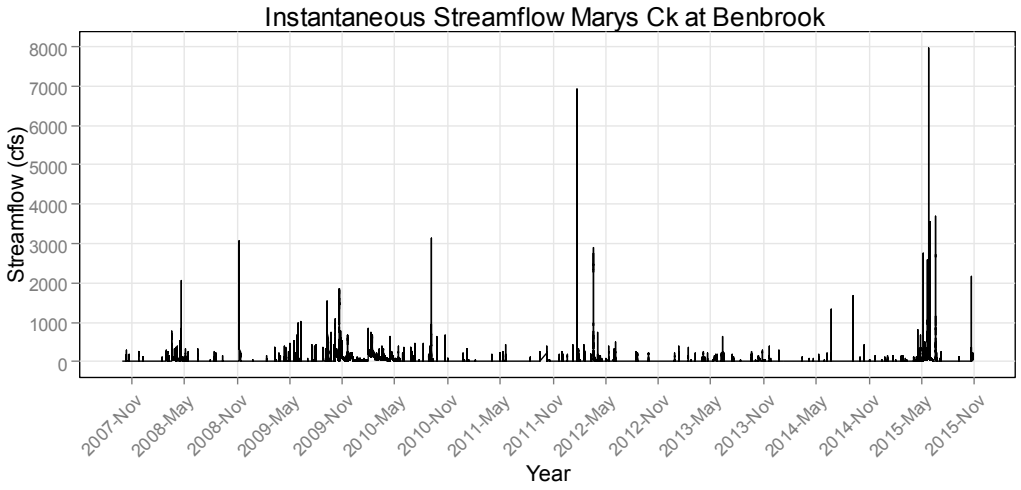

Figure 2-6 Instantaneous discharge from 2007, USGS gauge (8047050) Mary's Creek at Benbrook

2.2. Hydrologic Model

Flood forecasting based on SST is a computationally expensive exercise. To apply the SST, rainfall-runoff model is iterated thousands of times to calculate the maximum annual flow values. This procedure requires a hydrological model with low runtime. The Dallas-Fort Worth area also has many small detention ponds, lakes and reservoirs. Therefore, the hydrologic model should be able to simulate the detention effects throughout the watershed. HEC-HMS is the hydrological model used widely in the Dallas-Fort Worth area by different agencies such as the U.S. Army Corps of Engineers, Tarrant Regional Water District (TRWD), Texas Water Development Board (TWDB) and many consulting firms. Therefore, the HEC-HMS model was used in this study.

HEC-HMS is the hydrologic modeling software developed by the Hydrologic Engineering Center (HEC) at the Army Corps of Engineers. This model uses separate components such as the basin model, meteorological model and control model (Feldman 2000). The basin model includes basin parameters such as infiltration characteristics, time of concentration, and routing parameters as well as the geometry of each subcatchment. The control model manages simulation periods and the time window used to run the model. Capable of simulating various routing methods with reservoir operations is one of the advantages in this model. The meteorological model can be used to supply data from design storms, statistical analysis, and the frequency storm method, or from observed rainfall data. Point rainfall can be used by the gauge or may be converted to the areal rainfall by using surface interpolation methods such as the inverse distanced weighted method (IDW).

The HEC-HMS model for the Mary's Creek watershed was developed for the City of Benbrook in conjunction with the efforts from the Tarrant Regional Water District, the City of Fort Worth, and the U.S. Army Corps of Engineers (2014). It was used as the rainfall-runoff

model in this study. This model has 54 subbasins with 3 small detention elements, which are not located along the main channel (Figure 2-7a). The infiltration method used in the model is the initial-loss/constant loss-rate (IACL) method. The parameters used in the loss method were calibrated using three historical events in the study area (Mary's Creek, Findings from adjustments to hydrologic model, 2014). Modified pulse and lag time methods were used as the channel routing method in this model. The Snyder's unit hydrograph method was used to account for overland rainfall transformation.

To perform the FFA through the SST method, the number of required iterations is the product of number of years (highest return period) and number of simulations per year (for each year, the model is run multiple times). For the simplest scenario of applying SST, this value would exceed 5,000 times. An integrated graphical user interface (GUI) was developed to iterate the HEC-HMS using parallel processing to reduce the run time. HEC-DSS (Data Storage System) was used as a vehicle to feed transposed rainfall data to the HMS for each trial. Then the outputs of the HEC-HMS will be converted to ASCI format for further analysis like finding the peak flow for each transposition.

HEC-HMS requires MAP values for each subbasin to obtain rainfall information. Point rainfall data should be translated to MAPs when using HEC-HMS. Various deterministic approaches like spline and IDW or geostatistical methods like kriging can be used to convert point data to surface data. All these interpolation methods have uncertainties on pinpointing the peak rainfall or depth of the rainfall for the ungauged locations. Regardless of the common errors in translating the radar reflectivity to the depth in radars, two-dimensional radar data provides valuable information about the spatial variability of the storm, and there is no need to convert point measurements to areal rainfall. Hence, there is less uncertainty in using MPE data.

Figure 2-7b illustrates a histogram of the distribution of the subbasin area in Mary's Creek River Basin. All of the subbasins have an area less than one HRAP pixel which is about

8.76 square miles. The area of the largest subbasin (#54) in the Mary's Creek River Basin is 7.23 mi^2 which is lower than the area of a HRAP cell. Therefore, error resulting from mismatching of the point (radar pixel) and mean areal rainfall (over the subbasin) will be negligible. The average of the subbasin area is about 1.19 mi^2, which means that the resolution of the model is sufficient for our purpose.

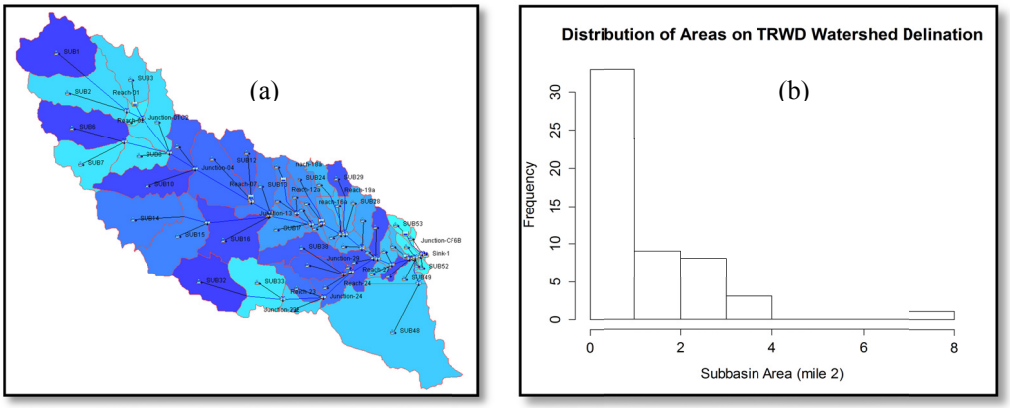

Figure 2-7 **a)** HEC-HMS model of the Mary's Creek River Basin and **b)** histogram of subbasin areas for the Mary's Creek River Basin

In order to calculate MAPs, we developed a software called MAPCalc that calculates the MAP over any given domain in a platform independent from ArcGIS for two reasons. First, ArcGIS is a computationally demanding software when it comes to performing iterations or a high number of processes. Second, the ArcGIS spatial analysis tool for MAP calculation (called Zonal Statistic, for calculating different statistics on values of a raster within the zones of another data set) is not accurate at the resolution of this study. To illustrate, Figure 2-8a shows a basin, which falls into two MPE pixels with 0.76 and 1.017 inches of rainfall. Two sections of the basin falling into these two MPE pixels have areas of 0.61 and 4.07 $miles^2$, respectively. It is found that the actual MAP using the areal weighted average is 0.98 inch while the Zonal Statistics method returns the value of 0.89 inch.

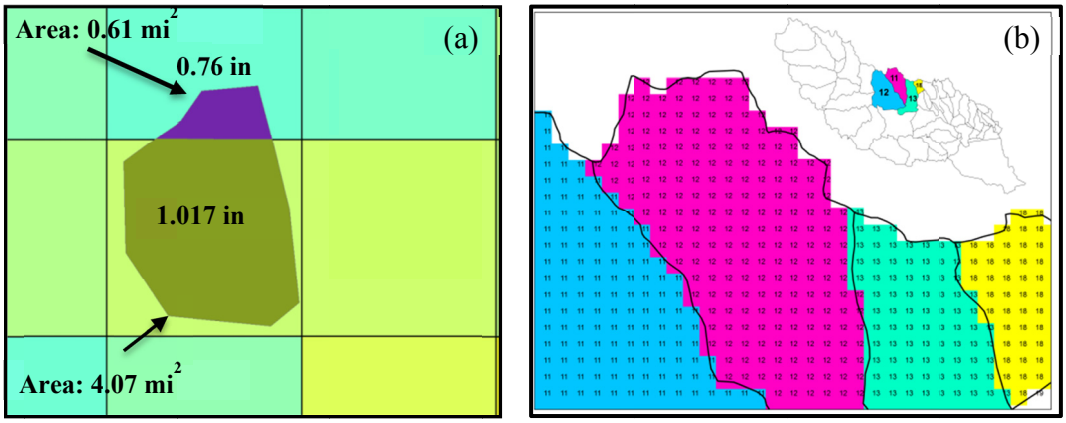

Figure 2-8 **a)** A sample basin falling on two MPE pixels; hence, the pixel values represent the hourly MPE data for each part of the basin. Actual mean areal precipitation should be 0.98 in while Zonal Statistics return the value of 0.89 in. and **b)** a demonstration of redefined HRAP pixels are used in a MAPCalc package.

The only remedy to this problem when using ArcGIS is to resample the raster file into a much finer resolution. In that case, runtime increases exponentially and makes it impossible to use ArcGIS for our purpose. Therefore, we developed the MAPCalc that speeds up the calculation and provides accurate MAP results. In addition, it integrates the MAP values in a suitable format compliant with the HEC-HMS model and significantly reduces the preprocessing time for flood frequency analysis. MAPCalc simply divides the MPE pixels into finer cells (it is optional, here 1/32 HRAP is used as shown in Figure 2-8b), and calculates the MAP by averaging the MPE values of all cells. At this time, the MAPCalc package can only be adjusted by various HRAP fractions (1/2, 1/4, 1/8, 1/32) but will provide flexible options of resolutions for MAP calculations in the near future. The main components of the MAPClac are:

MPE Reader: This component will read the XMRG binary files and convert them to one object with HRAP coordinates (XHRAP, YHRAP).

Basin File Reader: Subbasin polygons (any projections) are converted to the HRAP projection system.

Data Processor: This element organizes the resultant MAP from each MPE to a time series rainfall information that can be fed into HEC-HMS.

Model Runner: Series of classes and objects that iterate HEC-HMS through the scrip files. This component updates the whole HEC-HMS main files such as Control file, Basin File, Run and the Met file.

Calculating the MAP values for 10 years using MAPcalc has a considerably low runtime compared to other similar products such as ArcGIS–Zonal Statistics or HEC-MetVue developed by the U.S. Army Corps of Engineers (Fort-Worth District). A developed interface as shown in Figure 2-9 integrates MAPCalc with HEC-HMS for iterations. Reusability and a decent runtime for each transposition trial are some of the advantages of this integrated package. The inputs of this model are watershed polygon and gridded radar rainfall in a XMRG or ASCI ESRI format.

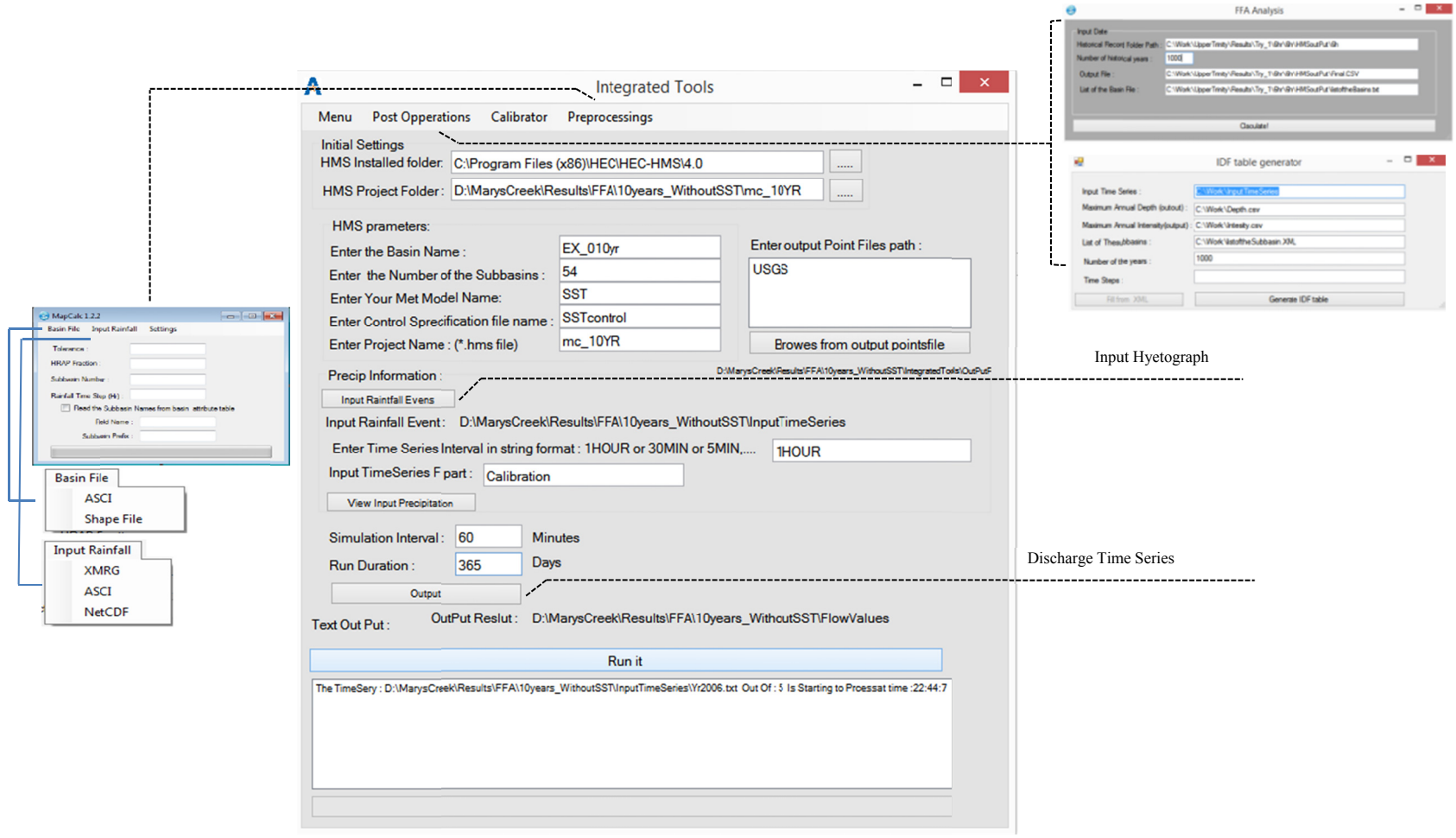

Figure 2-9 An integrated interface coupling MAPCalc, HEC-DSS and HEC-HMS

2.3. Methodology

2.3.1. Storm Selection

Concerning the main application of SST, recognizing and selecting the extreme events in historical records is of significant importance. Rainfall frequency analysis is to identify the *m* largest *t*-hour duration rainfall accumulations within the domain. In this research, 1-, 6-, 12- and 24-hour rainfall durations were selected for the rainfall frequency analysis, and 24-hour duration rainfall is used for flood frequency analysis. The collection of these *m* largest *t*-hour duration rainfall events is, henceforth, referred to as a "storm catalog." Previous studies have used different strategies in selecting extreme events. Foufoula-Georgia (1989) used a simplified geometric shape to simulate the spatial variation of the storm and implemented SST logic. England et al. (2014) assumed that the storm is single-centered, and isohyets are geometrically similar in the form of an ellipse. Wright et al. (2013; 2014) used the original shape and orientation of the storms without any modifications on storms. In this research, the original characteristics of storms with some modification to the methodology were applied.

Wright et al. (2013; 2014) used maximum possible total depth over the watershed as the main criteria to select storms for the storm catalogue. They numerously transposed the watershed throughout a homogeneity zone to find the extreme events, which resulted in the highest MAP over their study area. They developed a storm catalog of the 50 largest 12-h rainfall events with varied sizes and shapes for their flood frequency analysis and repeated the same procedure for another duration in 24 hours. However, they implicitly considered the shape and orientation of the watershed by applying this technique. We found that storms with the same shape, extent and rainfall depth, but having different orientations relative to the orientation of a watershed of interest would generate very different MAP values.

Transposing all the storms to find the maximum rainfall depths is computationally expensive. Wright et al. (2013; 2014) had to use a pattern recognition technique to find storms, which had the possibility of producing heavy rainfall over the duration of their case study. They transposed the watershed over the homogeneity zone to select the extreme events (personal communication). But in this study, we used a simpler approach to find the preliminary storms. First, the MAP values over the homogeneity zone were calculated for historical rainfall events from the past ten years. This process enabled us to extract useful storms out of the huge data set. Then, a deterministic transposition approach was performed based on the previous step to generate a series of MAP values over the Mary's Creek River Basin. Finally, storms with the highest possibility of producing extreme events over the Mary's Creek River Basin were selected as a preliminary storm catalog. Details of the procedure are explained in the following subsections.

2.3.1.1. Developing Preliminary Storm Catalog

The aim of the storm selection was to archive a set of storms based on the storm size and orientation in order to maximize the probability of obtaining the highest precipitation depth when transposing stochastically. The storm selection process follows two steps: Firstly, the hourly MAP values over the homogeneity region were calculated by the MAPCalc tool for ten years of MPE data. Then, *t*-hourly rainfalls would be calculated by simply aggregating hourly MAP values from *t* consecutive time steps (hourly). For example, the 6-hour rainfall event for time t was calculated by accumulating the rainfall depth from time $(t-6)$ to t (See Table 2-2). The aggregated MAP values were also converted to rainfall intensity with respect to corresponding durations for IDF analysis later. This procedure was repeated for 12- and 24-hour durations. Then, MAPs of *t*-hour rainfall events were sorted in a descending order for each year (columns 8, 10, 12, 14 in Table 2 for 1-, 6-, 12- and 24-hr rainfalls, respectively). Only the top 50 rainfall events with higher rainfall depths in every year would be selected for each duration. For simplicity, we refer to the selected

storms as S1, S2, …, S50. Although this step did not necessarily give us detailed information about the spatial structure of the storm; it eliminated many insignificant events with low rainfall depths from the pre-selection process.

Table 2-2 Column 2 gives the hourly MAP values over the homogeneity zone. Columns 3, 4, 5 demonstrate how to aggregate the hourly MAP values to 6-, 12-, and 24-hr MAP values, respectively. Columns 8, 10, 12 and 14 give the highest MAP values in the year 2007 after sorting columns 2, 3, 4, and 5, respectively.

(1)	**(2)**	**(3)**	**(4)**	**(5)**	(6)	(7)	**(8)**	(9)	**(10)**	(11)	**(12)**	(13)	**(14)**
Time	**1Hr**	**6Hr**	**12Hr**	**24Hr**	**Strom #**	Time	**1 Hour**	Time	**6 Hour**	Time	**12 Hour**	Time	**24 Hour**
1/1/2007 0:00	0				**S1**	03/31/2007 01:00	0.68	03/31/2007 03:00	1.91	03/31/2007 04:00	2.25	06/27/2007 12:00	2.64
1/1/2007 1:00	0				**S2**	06/26/2007 23:00	0.58	03/31/2007 04:00	1.89	03/31/2007 03:00	2.17	06/27/2007 11:00	2.61
1/1/2007 2:00	0				**S3**	05/03/2007 00:00	0.45	03/31/2007 02:00	1.78	03/31/2007 05:00	2.17	06/27/2007 13:00	2.58
1/1/2007 3:00	0				**S4**	03/31/2007 02:00	0.42	06/27/2007 01:00	1.74	03/31/2007 06:00	2.16	06/27/2007 14:00	2.50
1/1/2007 4:00	0				**S5**	10/15/2007 13:00	0.42	03/31/2007 05:00	1.73	04/25/2007 03:00	2.12	06/27/2007 10:00	2.50
1/1/2007 5:00	0	0			**S6**	03/31/2007 00:00	0.38	06/27/2007 02:00	1.71	04/25/2007 04:00	2.11	06/27/2007 15:00	2.45
1/1/2007 6:00	0	0			**S7**	06/26/2007 22:00	0.36	06/27/2007 00:00	1.62	04/25/2007 05:00	2.10	06/27/2007 19:00	2.44
1/1/2007 7:00	0	0			**S8**	04/24/2007 20:00	0.35	04/25/2007 00:00	1.51	03/31/2007 07:00	2.09	06/27/2007 16:00	2.43
1/1/2007 8:00	0	0			**S9**	06/27/2007 00:00	0.35	06/27/2007 03:00	1.48	03/31/2007 08:00	2.07	06/27/2007 17:00	2.43
1/1/2007 9:00	0	0			**S10**	04/24/2007 21:00	0.34	04/25/2007 01:00	1.44	04/25/2007 06:00	2.05	06/27/2007 18:00	2.43
1/1/2007 10:00	0	0			**S11**	11/25/2007 08:00	0.31	03/31/2007 01:00	1.39	03/31/2007 09:00	2.04	06/27/2007 20:00	2.41
1/1/2007 11:00	0	0	0		**S12**	05/24/2007 21:00	0.31	03/31/2007 06:00	1.38	03/31/2007 02:00	2.02	06/27/2007 09:00	2.38
1/1/2007 12:00	0	0	0		**S13**	06/03/2007 14:00	0.29	04/24/2007 23:00	1.36	04/25/2007 02:00	1.97	03/31/2007 08:00	2.31
1/1/2007 13:00	0	0	0		**S14**	09/05/2007 06:00	0.29	06/26/2007 23:00	1.28	03/31/2007 10:00	1.94	03/31/2007 09:00	2.31
1/1/2007 14:00	0	0	0		**S15**	10/15/2007 12:00	0.29	04/25/2007 02:00	1.28	06/27/2007 01:00	1.91	03/31/2007 10:00	2.31
1/1/2007 15:00	0	0	0		**S16**	03/26/2007 23:00	0.28	04/24/2007 22:00	1.20	06/27/2007 02:00	1.88	03/31/2007 11:00	2.31
1/1/2007 16:00	0	0	0		**S17**	09/10/2007 17:00	0.27	03/27/2007 00:00	1.16	06/27/2007 08:00	1.86	03/31/2007 12:00	2.31
1/1/2007 17:00	0	0	0		**S18**	04/24/2007 19:00	0.27	06/27/2007 04:00	1.12	06/27/2007 07:00	1.85	03/31/2007 07:00	2.31
1/1/2007 18:00	0	0	0		**S19**	09/05/2007 07:00	0.26	03/27/2007 01:00	1.12	06/27/2007 00:00	1.85	03/31/2007 13:00	2.31
1/1/2007 19:00	0	0	0		**S20**	03/29/2007 23:00	0.25	04/25/2007 03:00	1.09	06/27/2007 03:00	1.84	03/31/2007 14:00	2.31
1/1/2007 20:00	0	0	0		**S21**	03/26/2007 21:00	0.25	09/10/2007 18:00	1.07	06/27/2007 04:00	1.82	03/31/2007 06:00	2.31
1/1/2007 21:00	0	0	0		**S22**	06/26/2007 21:00	0.25	03/26/2007 23:00	1.06	06/27/2007 06:00	1.82	03/31/2007 15:00	2.30
1/1/2007 22:00	0	0	0		**S23**	05/02/2007 23:00	0.25	09/10/2007 17:00	1.05	06/27/2007 05:00	1.82	03/31/2007 16:00	2.30
1/1/2007 23:00	0	0	0	0	**S24**	06/25/2007 23:00	0.24	04/24/2007 21:00	1.03	04/25/2007 01:00	1.78	03/31/2007 05:00	2.27
1/2/2007 0:00	0	0	0	0	**S25**	09/10/2007 16:00	0.24	09/10/2007 19:00	1.01	04/25/2007 07:00	1.78	03/31/2007 04:00	2.26
1/2/2007 1:00	0	0	0	0	**S26**	06/02/2007 06:00	0.24	09/05/2007 11:00	1.01	03/31/2007 11:00	1.77	06/27/2007 21:00	2.25
1/2/2007 2:00	0	0	0	0	**S27**	06/18/2007 06:00	0.24	09/05/2007 09:00	1.00	06/27/2007 09:00	1.75	06/27/2007 08:00	2.25

One of the assumptions in frequency analysis is that events are independent. Selecting the highest MAP values over the homogeneity region will not necessarily yield independent storms and, in fact, many of the resultant storms belong to the same event. For example in 2007 (Table

2-2), S1, S4 and S6 for 1-hr rainfall duration belong to the 3/31/2007 event. Another example would be S1, S2, S3, S5, S11 and S12 for 2-hr rainfalls, which all happened on the 3/31/2007 event.

A typical storm has a dynamic spatial variation over the time. For instance as shown in Figure 2-10, a synthetic storm changes with its corresponding orientations at four different time steps within a homogeneity zone. If a definition of 2-hour rainfall events is desired; one can find three available sets of storms (See Figure 2-10). According to the assumption of the frequency analysis, only one of the three 2-hour storms can be selected as an independent event. The MAP value over the homogeneity region is constant; the MAP values over the Mary's Creek River Basin varies with respect to time and can be used as a criterion to identify a storm with the maximum possible rainfall depth. In this example, S1 should be identified as such because it generates the highest MAP value over the Mary's Creek River Basin with the largest coverage over the watershed compared to the others (S2 and S3). In this study, we decided to use the MAP values over the Mary's Creek River Basin as a major criterion to identify independent storms for the deterministic transposition approach to be introduced in the following section.

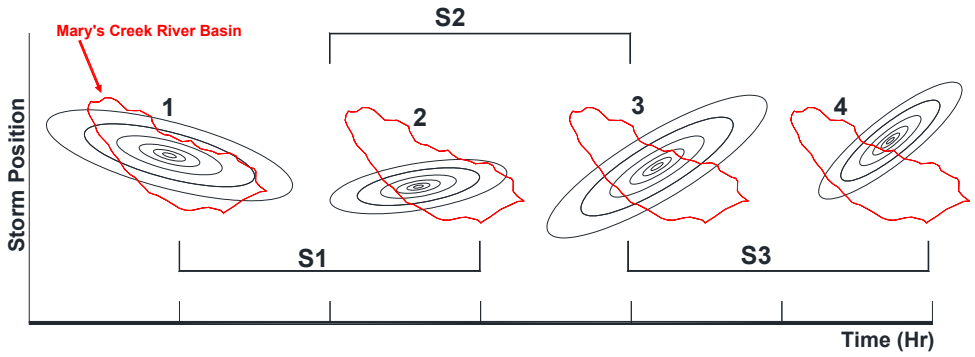

Figure 2-10 Synthetic storms at four consecutive time steps (hourly).

2-hr S1, S2 and S3 storms are dependent storms.

2.3.1.2. Deterministic Storm Transposition

As mentioned in Section 2.3.1.1, selecting storms solely based on MAP over the homogeneity zone is not a comprehensive criterion. For example, a small storm may not have a high MAP value over the homogeneity zone but can produce a lot of rainfall with a high MAP value over the study area due to its orientation aligned with the study area. If the MAP value over the homogeneity zone was used to select impactful storms as the sole criterion, this particular small storm may be ignored during the selecting process. But in fact, after the storm transposition process, this small storm can be possibly turned into a storm generating a very large impact on the study area. To avoid missing the possible storm events, we transposed the pre-selected preliminary set of storms deterministically across the homogeneity zone and calculated the MAP values over the study area (Mary's Creek River Basin); then, we finally chose the storms with the highest probability of producing extreme rainfall depths over the Mary's Creek River Basin.

Figure 2-11a shows the concept of deterministic transposition during storm selection at three different statuses (original-1, initial-2, and ending-3) using black, yellow, and green boxes, respectively. The goal is to transpose the storm in a way that any point of the storm within our homogeneity zone (black box) experiences falling on Mary's Creek River Basin at least once. The total transposition distance (Δx , Δy) would vary between $(-\frac{X}{2}, -\frac{Y}{2})$ and $(+\frac{X}{2}, +\frac{Y}{2})$ where X (21 × ~4 km) and Y (21 × ~4 km) are the width and height of homogeneity zone, respectively. We start with transposing the lower left corner of storm, point (1) in the black box, to point (2) in the yellow box. In this case, transposition distance is equal to $(-\frac{X}{2}, -\frac{Y}{2})$. Then the storm is shifted to the right direction, until the transposition distance becomes $(+\frac{X}{2}, -\frac{Y}{2})$. Next, it is shifted in Y direction with a predefined HRAP fraction as a transposition interval. The last location which point (1) would experience is at point (3) in the green box.

The transposition distance should be a fraction of the HRAP cell size (e.g., ½ HRAP). For example, in the case of Mary's Creek, the number of the deterministic transposition for a single storm is 42×42 times if a half of HRAP is used for transposition. Corresponding MAP values over Mary's Creek were then calculated for all transpositions of one storm. This procedure is repeated for all storms in the preliminary storm catalogue.

After calculating all the possible MAP values over the Mary's Creek basin, we need further criteria to finalize storm selection. We believe solely choosing the highest MAP values over the basin will not be the best procedure. In SST procedure, storms including multiple storm cells tend to have a higher probability to be placed over the basin when being transposed stochastically compared to those storms with one storm cell. Figure 2-12a is a storm with three separate storm cells and has a higher probability of creating extreme events on the Mary's Creek River Basin compared to Figure 2-12b. The storm in Figure 2-12a has a higher probability of creating extreme events.

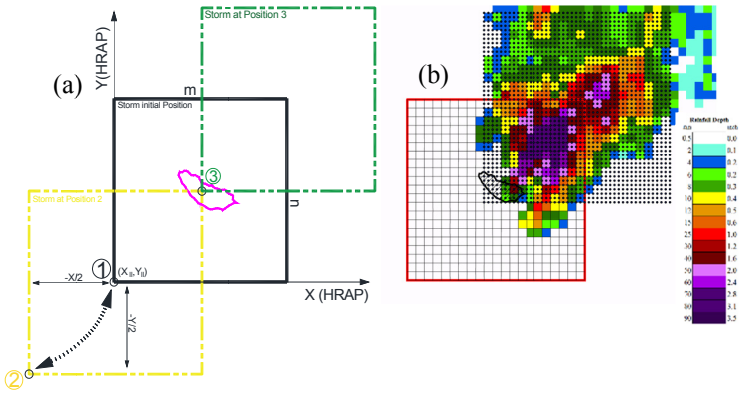

Figure 2-11 **a)** Deterministic transposition procedure. Black box shows the initial location of the storm, which is the same as homogeneity zone. Yellow box (Location 2) shows deterministic transposition entry point and the green box shows the location of the storm at the last trial of deterministic storm transposition. **b)** Black dots show all the locations that upper right corner of the black box will experience in deterministic transposition

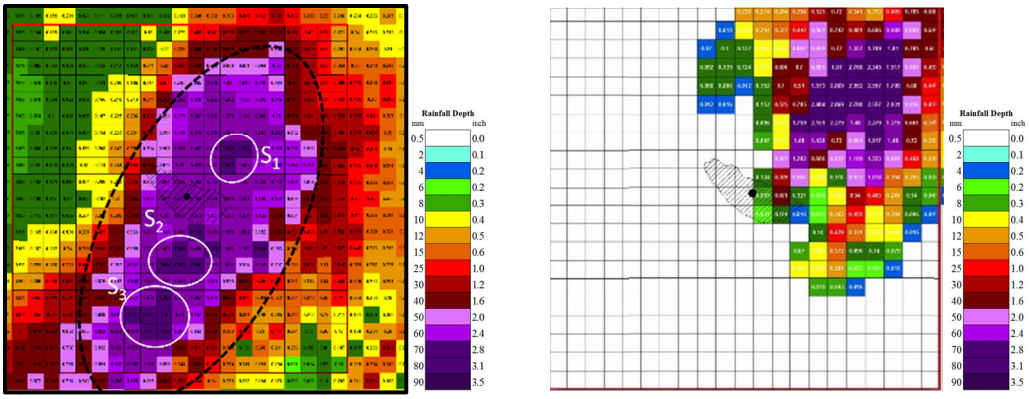

(a) (b)

Figure 2-12. **a)** A storm with three storm cells **b)** A storm with only one storm cell. Storm (b) will produce a higher MAP compared to storm (a), but storm (a) has a higher chance of creating extreme events when transposed due to having more storm cells.

The goal is to maximize the chance of having significant events when transposing stochastically as well as creating high MAP values. The probability of exceedance (POE) index was used in the further storm selection, which is comparable to the exceedance probability.

$$POE = \sum_{i=THR}^{Max\ depth} i \times Frequency \quad (2\text{-}1)$$

where i is the bin midpoint and THR is the threshold value. The observed annual maximum MAP value over the Mary's Creek River Basin for each year is used as the threshold value. For example, Figure 2-13 shows the histogram of all calculated MAP values over the Mary's Creek River Basin from deterministic transposition for two different storms (Storms 10 and 20) in 2007. The maximum MAP values achieved by transpositions, are given in the figure subtitle. The maximum possible MAP values of Storms 10 and 20 (Figure 2-13a and b) over the watershed are 5.23 and 5.47 inches, respectively. They have a similar maximum possible MAP value; however, the POE for Storm 10 is slightly higher than that of Storm 20, implying that Storm 10 has a higher probability of creating extreme events compared to Storm 20. The process of using POE index in conjunction with MAP values enabled us to finalize the storm selection. Therefore, the POE index

will serve as supplementary information. Figure 2-14 summarizes the whole storm selection procedure in a flow chart.

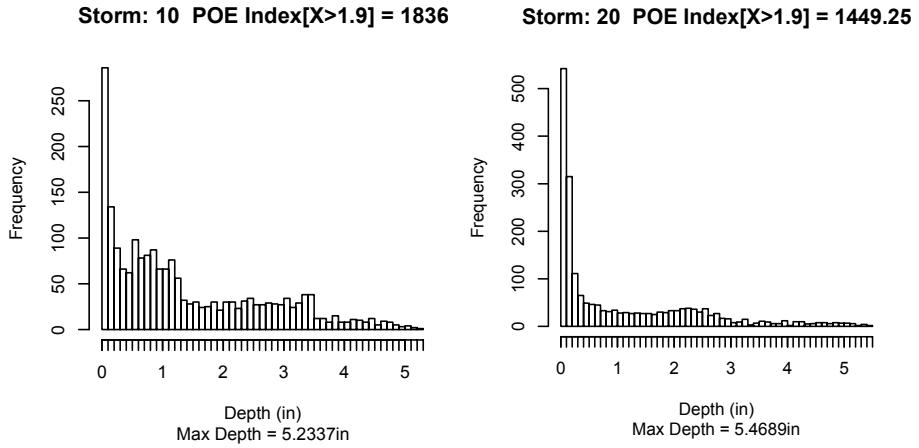

Figure 2-13 Histogram of MAP values from all transpositions of two storms over Mary's Creek River Basin.

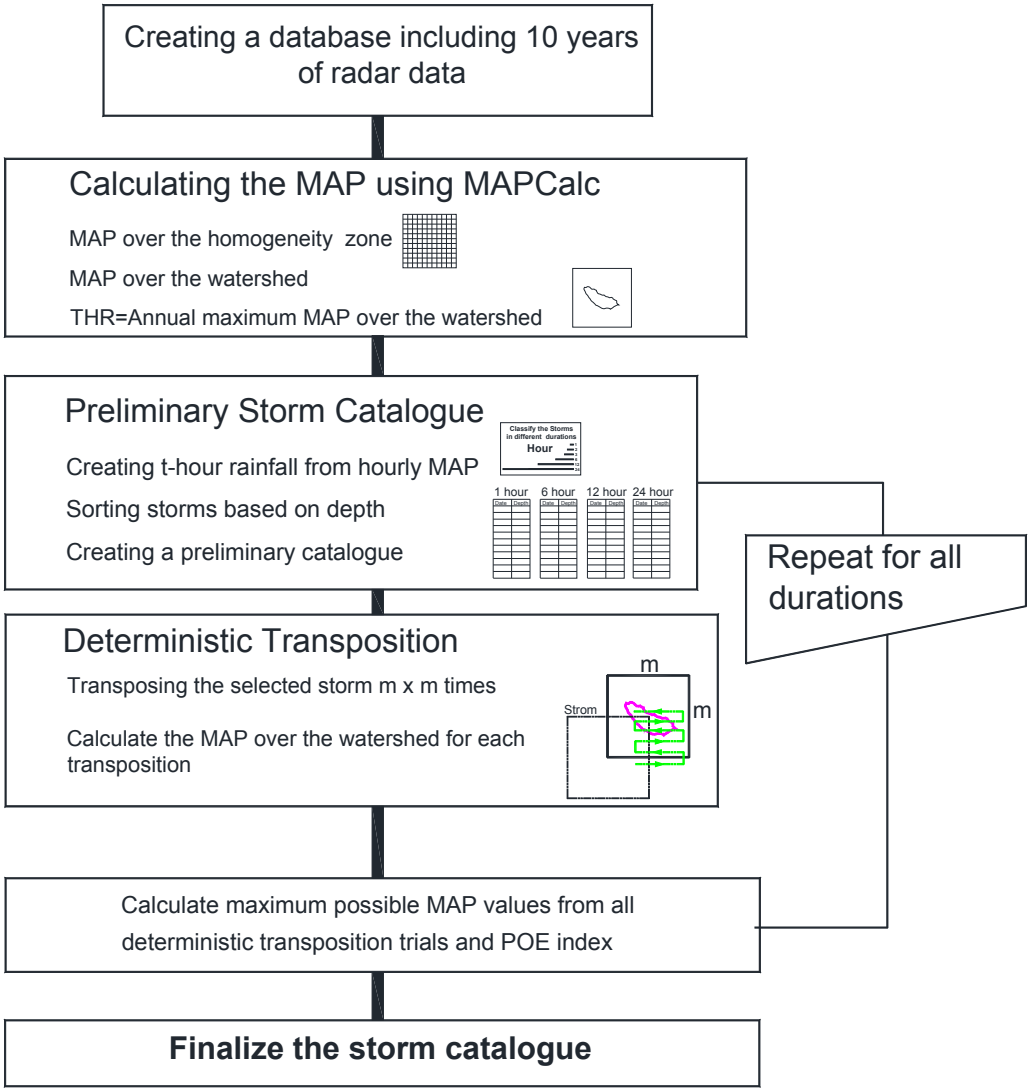

Figure 2-14. Summary of the steps required for creating storm catalogue.

The flowchart shown in Figure 2-14 is used as a basis to automate the storm selection process. This procedure finalized the storm catalogue. One of main advantages of this automated method is avoidance of common human errors such as missing severe storms or misallocating the storms to measure the maximum possible depths.

2.3.2. Stochastic Storm Transposition

The storm catalogue developed (as explained in the previous section) refers to the selection of extreme storms used in the SST procedure. The number of storm occurrences per year is assumed to follow the Poisson distribution with a rate parameter equal to the average number of storms per year. The Poisson distribution function is for discrete random variables such as the number of possible floods or earthquakes in a year. In this study, 50 storms over 10 years of data were selected; therefore, the expectation E[x] for the number of storms occurring in a given year is (50/10) = 5. This parameter is used for generating realizations from the Poisson distribution function explained later in the SST procedure. Probability density function (PDF) and cumulative distribution functions (CDF) of the Poisson distribution function are given in Eq. 2-2 and 2-3, respectively.

$$P(k;\lambda) = \Pr(X = k) = \frac{\lambda^k e^{-\lambda}}{k!} \tag{2-2}$$

where $\lambda = E[X]$, the expected number of storms per year.

$$CDF = e^{-\lambda} \sum_{i=0}^{[k]} \frac{\lambda^i}{i!} \tag{2-3}$$

Figure 2-15 and Figure 2-16 show the probability density and cumulative distribution functions for three different expectation values of one, four and ten storms per year.

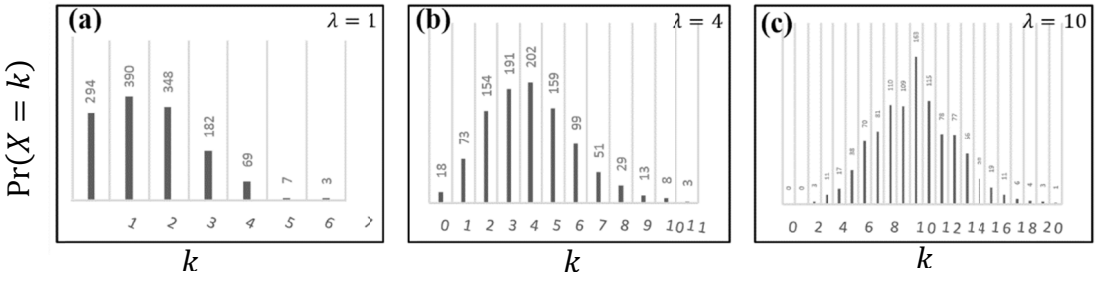

Figure 2-15 Probability distribution function for Poisson distribution for **a)** λ =1, **b)** λ=4, and **c)** λ=10

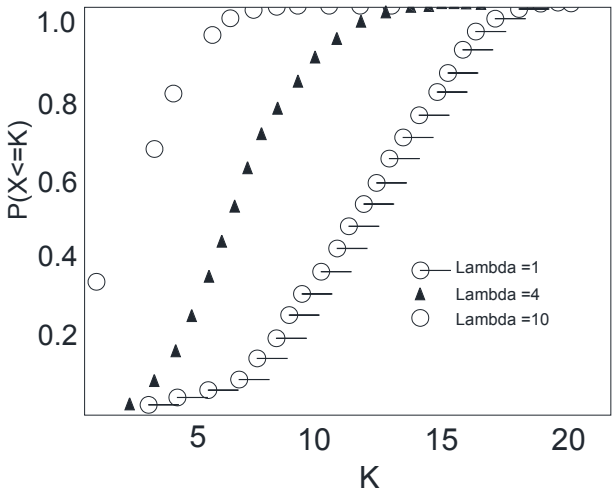

Figure 2-16 Poisson cumulative distribution function for λ =1, 4 and 10

Figure 2-17 shows the flow chart of stochastic storm transposition (SST). We have explained the steps as follows:

1. To identify the homogeneity zone (explained in Section 2.1.2. and 2.1.3.) that contain the watershed of interest and over which the extreme rainfall climatology is homogeneous. The homogeneity zone for this study is defined as a rectangle domain of 21 × 21 HRAP pixels, including theMary's Creek River Basin at the center of the homogeneity zone.

2. To create the storm catalogue containing the *m* storms within the domain at the *t*-hour. The number of annual storm occurrences is assumed to follow the Poisson distribution with a rate parameter equal to λ storms per year (5 in this study); therefore, 50 storms were selected for each rainfall duration. Prior climatological studies in the selected region revealed that the number of the severe storms (exceeding than defined thresholds for each year) varies from three to six storm per year. Sensitivity analysis on Poisson distribution rate parameter (λ) value from three to six indicated that the SST results were not

sensitive to the variation of the λ within the declared range, therefore; we assumed the rate parameter λ=5 to simulate the occurrence of five storms in each year. This procedure was conducted for t = 1-, 6-, 12- and 24-h rainfall durations (Section 2.3.1.).

3. To generate a random number (k) from Poisson distribution with the rate parameter of $\lambda = 5$.
4. To randomly select a storm from the storm catalog.
5. To generate two random numbers from uniform distribution for Δx and Δy which are used to transpose the storm in x and y direction. The motion and evolution of the storm at all periods is unaltered during transposition (i.e., for t-hour rainfall, all the *t* hourly rainfall is transposed with the same Δx and Δy)
6. To repeat steps 4 and 5 with k times.
7. For each of the transpositions (k times), to calculate MAP over the Mary's Creek River Basin; to identify the maximum MAP values from the k transposition trial and assign that to the annual maximum MAP value of the basin.
8. To repeat steps 3 to 7 for a thousand times to recreate 1,000 years of t-hour ''annual'' rainfall maxima for the watershed of interest.

The flow chart in Figure 2-17 was used to develop a module to perform the SST for user-defined watersheds. The results of SST from 1-, 6-, 12- and 24-hr rainfall durations were used in rainfall frequency analysis. Only results of 24-hr rainfall duration were used in flood frequency analysis. The 24-hr extreme events were ingested to the hydrologic model to simulate the streamflow values, which were used in FFA later.

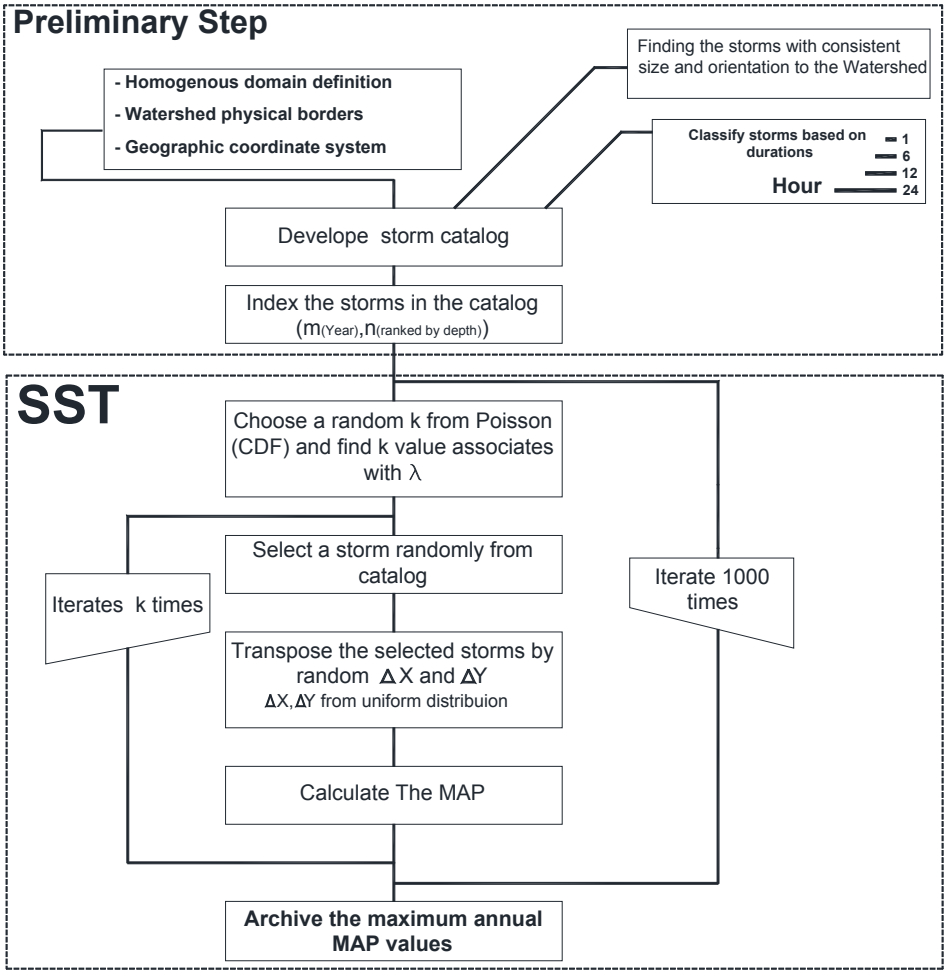

Figure 2-17 Flowchart of the stochastic storm transposition method

2.3.3. Developing a Module to Perform SST

A module was developed to implement the SST approach based on logic explained in Section 2.3.2. The module was developed using programming languages such as on C#.NET C++ and many open source libraries such as DOT spatial and complex sorting algorithms. Open source GIS library was also applied to read and display the GIS features. This module can be used for any user-defined watershed with radar rainfall in XMRG, NetCDF or ESRI standard ASCII format. This module contains three main components (See Figure 2-18). Watersheds of interest can be

defined through (shapefile) or either standard ASCI format. This component can convert any geographic coordination system to HRAP. Defining the physical paths for the preliminary storm catalogue and deterministic transposition are done in the storm catalogue component. The last component includes defining and setting some of the parameters for the SST such as transposition range and number of the desired years for frequency analysis. Advanced programming techniques such as multi-threading reduced the run time and provides the capability for us to run the SST module for several rainfall durations simultaneously.

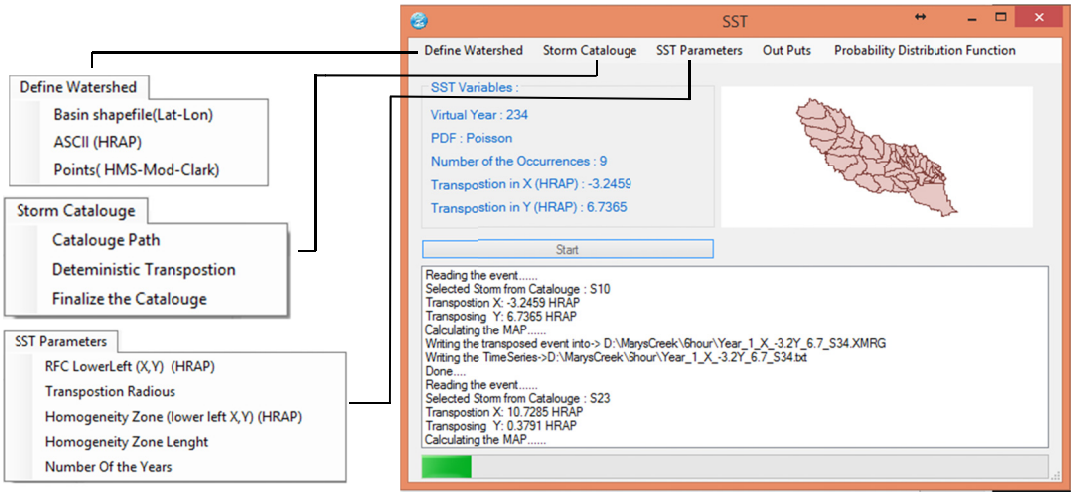

Figure 2-18 Developed module to implement the SST on a user-defined watershed. This module supports ESRI-ASCII and shapefile as the basin definition.

Chapter 3

Results

3.1. Historical Analysis

A sufficiently long data period is required for FFA and IDF; however, the reality does not always behave as expected. Rainfall and streamflow measurements are not available at every desired location, and even if there is a gauge, it does not have a long enough data record for the frequency analysis. For instance, the Mary's Creek River Basin has one USGS gauge with about 16 years of data. The daily minimum and maximum stage values are available from 1998 and instantaneous streamflow has been continually recorded since 2007. Unfortunately, there is no rain gauge available in the Mary's Creek River Basin to be used to compare the IDF curves from SST with the observed rainfall values. Therefore, we set the IDF information that was developed based on the maximum annual MAP values from 10 years of radar data without any transposition as our baseline information. The maximum MAP values over the Mary's Creek River Basin for each year and different rainfall durations as well as their date and time of occurrences are listed in Table 3-1. Figure 3-1 also illustrates the same information visually. Similar information for all the subbasins can be found in **Appendix A**. According to Figure 3-1, 2008 had the highest rainfall intensity for 1, 6 and 12 hours over the Mary's Creek River Basin, while 2005 had the lowest MAP value among all.

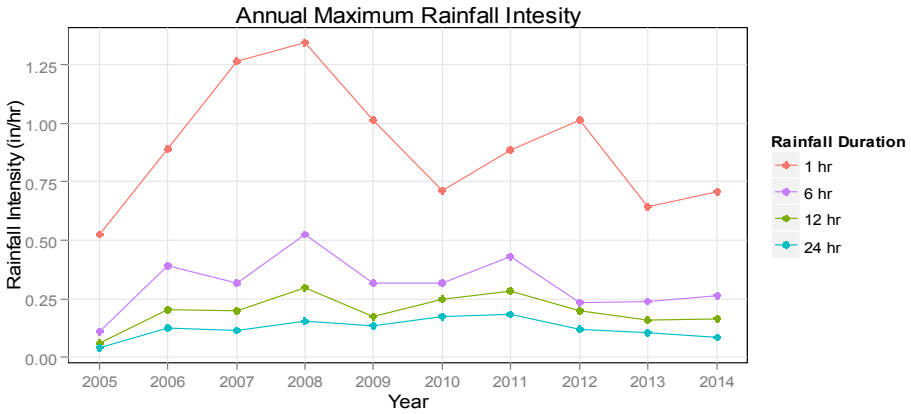

Figure 3-1 Annual maximum rainfall intensities for 10 years of radar rainfall values for Mary's Creek River Basin

Table 3-1 Annual maximum mean areal precipitation (MAP) values over Mary's Creek and their occurrence date and time for 1-, 6-, 12- and 24-hour rainfall durations over 10 years of radar data (2005-2014).

		RAINFALL DURATION							
		1 hr		**6 hr**		**12 hr**		**24 hr**	
		Maximum Annual MAP (in)	Date	Maximum Annual MAP (in)	Date	Maximum Annual MAP (in)	Date	Maximum Annual MAP (in)	Date
YEAR	**2005**	0.52	8/16/2005 00:00	0.67	6/1/2005 8:00	0.73	3/26/2005 21:00	1.04	3/27/2005 11:00
	2006	0.89	11/06/2006 06:00	2.36	11/6/2006 10:00	2.44	11/6/2006 11:00	2.99	2/25/2006 21:00
	2007	1.26	3/31/2007 01:00	1.91	6/27/2007 2:00	2.40	6/27/2007 9:00	2.77	6/27/2007 21:00
	2008	1.34	11/11/2008 03:00	3.14	11/11/2008 5:00	3.59	11/11/2008 10:00	3.67	11/11/2008 14:00
	2009	1.01	9/22/2009 01:00	1.90	9/12/2009 6:00	2.09	9/12/2009 12:00	3.28	10/22/2009 10:00
	2010	0.71	5/14/2010 18:00	1.91	9/8/2010 11:00	2.98	9/8/2010 14:00	4.15	9/8/2010 12:00
	2011	0.88	5/23/2011 16:00	2.59	10/9/2011 8:00	3.37	10/9/2011 14:00	4.39	10/9/2011 18:00
	2012	1.02	6/06/2012 20:00	1.39	6/7/2012 1:00	2.37	3/20/2012 10:00	2.89	3/20/2012 14:00
	2013	0.64	2/10/2013 09:00	1.44	1/9/2013 7:00	1.94	1/9/2013 11:00	2.52	9/21/2013 0:00
	2014	0.71	11/06/2006 20:00	1.58	10/13/2014 11:00	1.97	6/22/2014 20:00	2.12	6/23/2014 12:00

Figure 3-2a and b show the highest MPE values over the rectangle domain of MPE data as well as over the homogeneity zone of the Mary's Creek River Basin over the 10 years of data recorded. Figure 3-2c and d show the locations in which the highest MPE values occurred on WGRFC and the Mary's Creek River Basin. There are several incidents where MPE values are extremely high (greater than 200_{mm} / $25.4=7.87_{in}$) and clustered at the upper right corner of the rectangle domain. Since this area is located outside of the WGRFC boundary, MPE values are not reliable due to the uncertainty existing in the data quality control for the area. There are also several spots with rainfall depths as high as 6 inches mostly around the gulf coastline. According to Figure 3-2d the maximum MPE pixel value is inside of the homogeneity zone, where the highest rainfall depth is about 3.5 inches which is considerably higher than the observed values over Mary's Creek River Basin (center of the homogeneity zone). Therefore, one would expect that storm transposition to drastically change the MAP values over the Mary's Creek Basin for at least a one-hour rainfall duration.

As explained, there was only one available USGS gauge for Mary's Creek (Mary's Creek at Benbrook -8047050). The historical annual and monthly peak flow for this station is depicted in. Figure 3-3a and b. We used 16 years of available data for FFA comparison. It is found that the highest peak flow in the 10 years between 2005 and 2014 happened on 03/30/2007 (local time) with 21,200 cfs, which reflected a watershed response to the second highest 1-hour MAP value as shown in Table 3-1. There were several significant events occurring before the 03/30/2007 event, which generated a near saturated soil condition with a severe flood as a consequence. On the other hand, the highest rainfall event occurring on 11/11/2008 did not generate the highest peak flow value. The corresponding peak streamflow to that rainfall event was only 3,070 cfs due to the antecedent dry conditions prior to the 11/11/2008 event. In other words, the Creek was almost dry in the preceding months.

This implies that the relationship between return periods of rainfall and streamflow is not at one-to-one and in fact the preceding soil moisture condition, as well as spatial variation of rainfall have a great impact on the return period of the streamflow. This topic will be discussed in detail in Section 3.5.

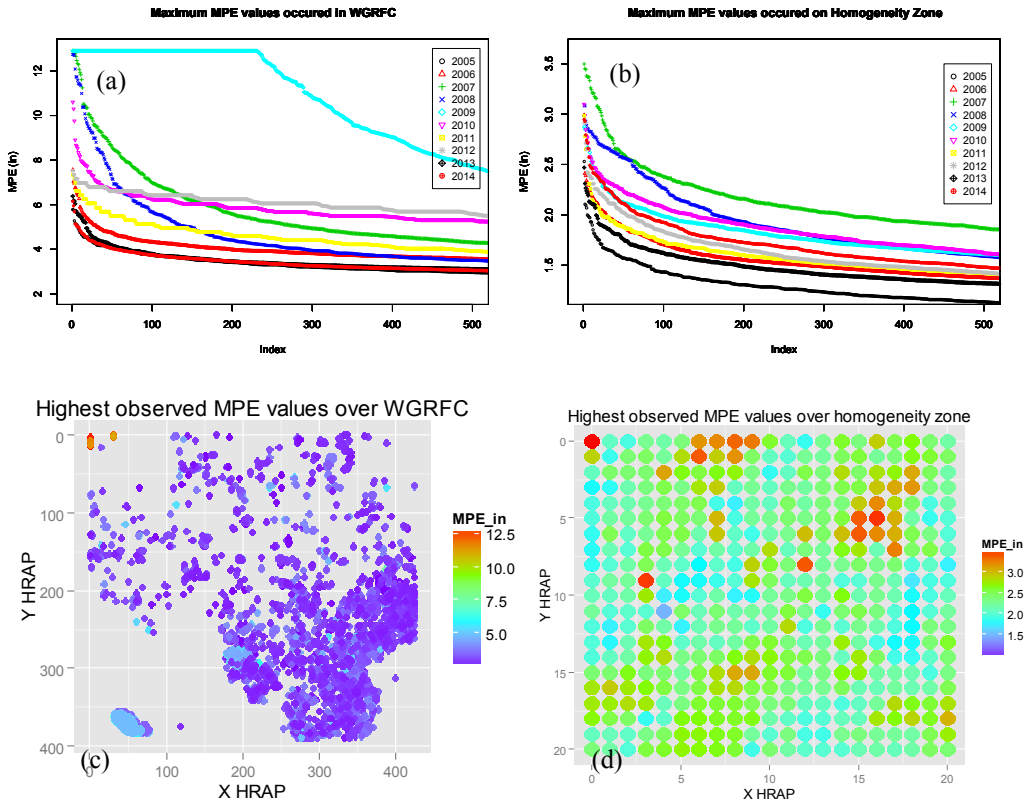

Figure 3-2 a) The 500 highest MPE values for each year over the rectangle MPE domain**. b)** The 500 highest MPE values for each year over the homogeneity zone of the Mary's Creek River Basin**. c)** Location of the highest MPE pixels over the rectangle MPE domain **d)** Location of the highest MPE pixels over the homogeneity zone of the Mary's Creek River Basin.

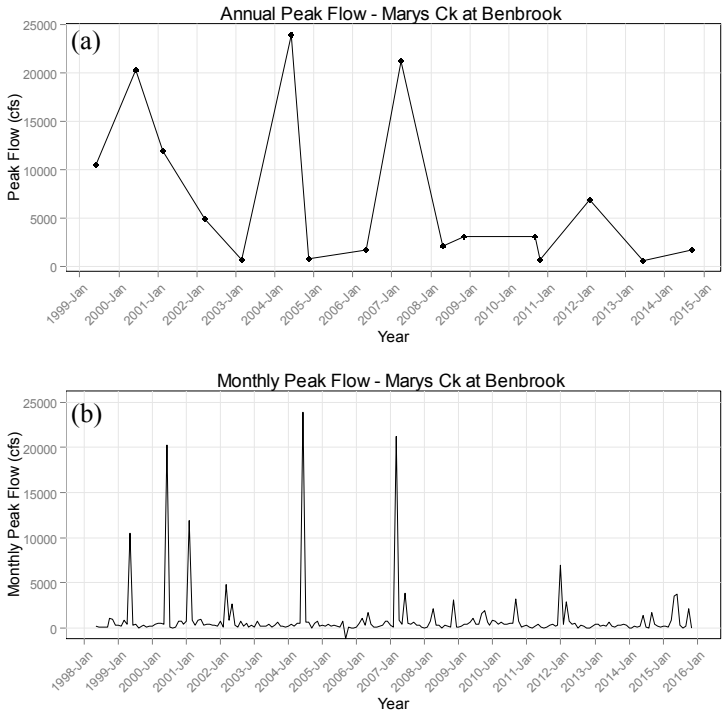

Figure 3-3 **a)** annual peak flow. **b)** monthly peak flow at Mary's Creek at Benbrook USGS gauge. The annual peak flow is for water year not the calendar year, as reported by USGS.3.2. Storm Catalog

3.2. Storm Selection

As explained in Section 2.3.1, selecting preliminary storms based on the maximum MAP over the homogeneity region helps to eliminate many insignificant events from the storm selection process. In this section, a series of six-hour rainfall events in 2007 are selected as an example to demonstrate the process of creating a storm catalogue. The preselected MAP values over the homogeneity zone with a 6-hour duration are listed in Table 3-2.

Table 3-2 Selected preliminary storms in 2007 for six hour duration with sorted MAP values over the homogeneity zone.

Storm Name	Date and Time	MAP (in)	Storm Name	Date and Time	MAP (in)
S1	3/31/2007 3:00	1.91	**S26**	9/5/2007 11:00	1.01
S2	3/31/2007 4:00	1.89	**S27**	9/5/2007 9:00	1
S3	3/31/2007 2:00	1.78	**S28**	9/5/2007 10:00	0.99
S4	6/27/2007 1:00	1.74	**S29**	10/15/2007 17:00	0.99
S5	3/31/2007 5:00	1.73	**S30**	10/15/2007 16:00	0.99
S6	6/27/2007 2:00	1.71	**S31**	9/5/2007 8:00	0.97
S7	6/27/2007 0:00	1.62	**S32**	10/15/2007 15:00	0.97
S8	4/25/2007 0:00	1.51	**S33**	3/30/2007 1:00	0.95
S9	6/27/2007 3:00	1.48	**S34**	3/30/2007 2:00	0.93
S10	4/25/2007 1:00	1.44	**S35**	11/25/2007 11:00	0.92
S11	3/31/2007 1:00	1.39	**S36**	4/25/2007 10:00	0.92
S12	3/31/2007 6:00	1.38	**S37**	9/10/2007 20:00	0.91
S13	4/24/2007 23:00	1.36	**S38**	11/25/2007 12:00	0.91
S14	6/26/2007 23:00	1.28	**S39**	3/30/2007 3:00	0.9
S15	4/25/2007 2:00	1.28	**S40**	3/27/2007 2:00	0.9
S16	4/24/2007 22:00	1.2	**S41**	10/15/2007 14:00	0.89
S17	3/27/2007 0:00	1.16	**S42**	5/26/2007 13:00	0.86
S18	6/27/2007 4:00	1.12	**S43**	9/10/2007 16:00	0.86
S19	3/27/2007 1:00	1.12	**S44**	5/3/2007 3:00	0.86
S20	4/25/2007 3:00	1.09	**S45**	5/3/2007 2:00	0.86
S21	9/10/2007 18:00	1.07	**S46**	5/3/2007 4:00	0.85
S22	3/26/2007 23:00	1.06	**S47**	9/5/2007 7:00	0.85
S23	9/10/2007 17:00	1.05	**S48**	5/26/2007 12:00	0.85
S24	4/24/2007 21:00	1.03	**S49**	11/25/2007 10:00	0.84
S25	9/10/2007 19:00	1.01	**S50**	5/3/2007 1:00	0.83

The preliminary storm catalogue is only a means to reduce the number of deterministic transpositions as explained in Section 2.3.1.1. The only parameter to define for the deterministic transposition is the spatial increment as a fraction of HRAP pixel size. In this study, ¼ HRAP was used to transpose 1hour and 6-hour storms; while ½ HRAP was used for 12 and 24-hour storms. Consequently, the total number of transpositions for one trial of either 1- hour or 6-hour storms over the homogeneity zone of 21×21 HRAP pixels is 7,056 times (84×84); while the total number of transpositions for one trial of either 12- hour or 24-hour storms over the homogeneity zone is 1,764 times (42×42). Figure 3-4a shows the center locations of the *deterministically*

transposed storms with either 1-hour or 6 hour durations over the homogeneity zone (7,056 points). Changing the increment from ½ HRAP to ¼ HRAP will increase the number of the transpositions 4 times. For the limited computational power at this stage, we believe that the selection of ½ HRAP and ¼ HRAP serves the current research purpose because the main goal of this process is to identify the most impactful 50 storms from 10 years for each duration (1, 6, 12, and 24 hours).

It is worth mentioning that the increment used in the *stochastic transposition* approach (in the SST procedure) is set to be 1/32 HRAP. Figure 3-4b shows the center locations of the *stochastically* transposed storms over the homogeneity zone after 5,000 realizations. The transposition distance (Δx , Δy) is generated from the uniform distribution as described in Section 2.3.2.

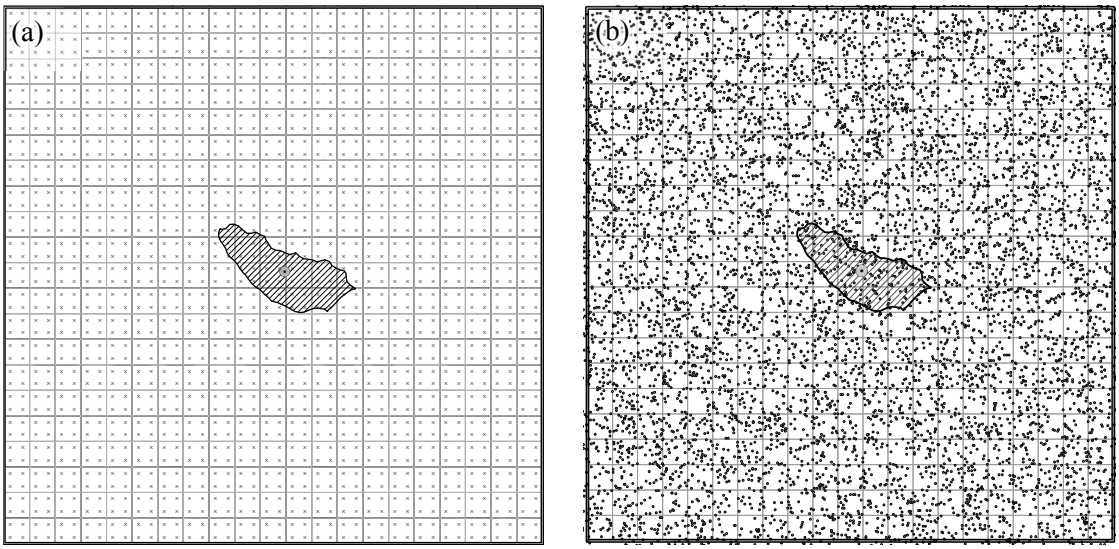

Figure 3-4 **a)** Center locations of the *deterministically* transposed storms with either 1-hour or 6 hour durations over the homogeneity zone (7,056 points) (transposition increment is ¼ HRAP). **b)** Center locations of the *stochastically* transposed storms over the homogeneity zone after 5,000 realizations with increment of 1/32 HRAP.

Once each of the storms listed in Table 3-2 was transposed 84 × 84 times, corresponding MAP values over the Mary's Creek River Basin were calculated and plotted in histogram for each trals as illustrated in Figure 3-5. To clarify, the n^{th} histogram refers to the ***Sn*** storm in Table 3-2 (e.g. the first histogram is for S1 with the highest MAP over the homogeneity zone). The subtitle of each histogram in Figure 3-5 indicates the Maximum MAP values over the Mary's Creek River Basin from all transpositions for each storm. According to Table 3-1 the observed maximum MAP value over the Mary's Creek River Basin for a 6-hour duration in 2007 is 1.91 inches from S1 (3/31/2007 03:00, see Table 3-2) . But the maximum MAP value generated from the deterministic transposition was 5.65 inches. This high MAP value (5.65 inches) was derived from transposing S15 (04/25/2007 02:00, see Table 3-2) with a transposition distance ($\Delta x = -5_{HRAP}$, $\Delta y = -11_{HRAP}$) which originally produced a MAP of 0.518 inches over the Mary's Creek River Basin.

Figure 3-6 is another illustration of the results from the deterministic transposition using the cumulative distribution function. It gives a quick insight about which storms should be selected to finalize the storm catalog. As discussed in Section 2.3.1.1., some of the selected storms in the preliminary storm catalogue are not independent. We used the deterministic transposition approach to calculate the MAP values over the Mary's Creek River Basin as a first step to identify independent storms from the preliminary storm catalog. Then the POE index was used to distinguish the effective storms from other storms selected in the previous step. If there is little difference among the highest MAP values from the selected storms, then the storm with higher POE index is chosen. In other words, the higher POE index, the higher probability of producing extreme events over the study area.

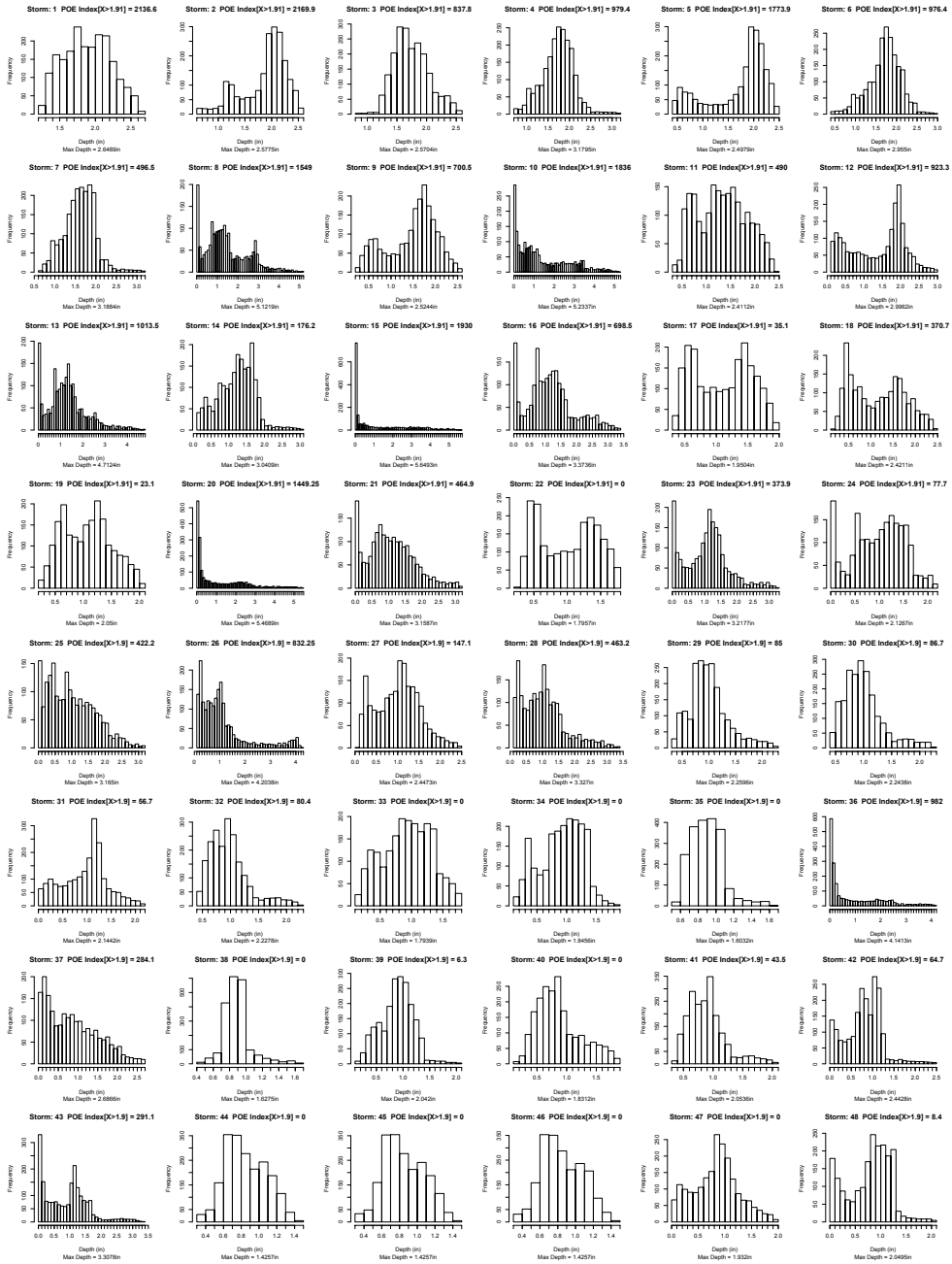

Figure 3-5 Histograms of MAP values over the basin from all transpositions of the top 48 storms form the preliminary storm selection (6-hour rainfall duration in 2007). Maximum MAP value over the basin and POE index are given as the title and subtitle of the histograms.

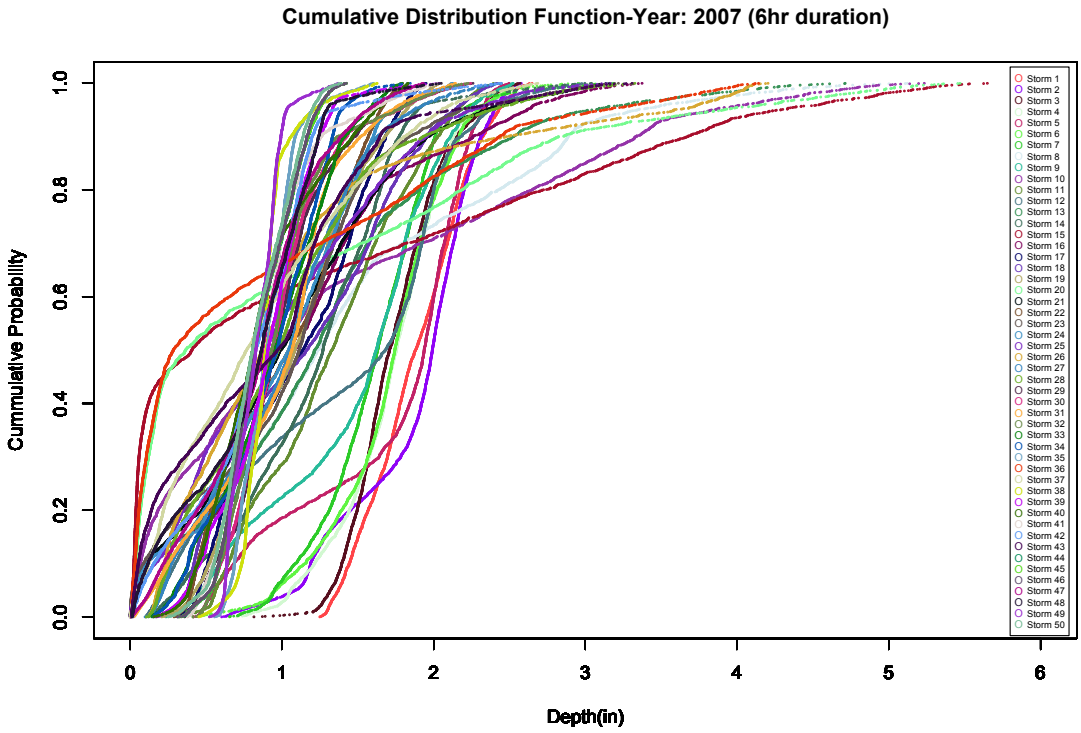

Figure 3-6 Cumulative distribution function of MAP values over the Mary's Creek River Basin for the 50 storms from deterministic transposition

After removing the dependent events and the storms with low chance of producing the extreme events, we combined all the remaining storms from the past 10 years. The finalized storms were ranked according to the maximum MAP values over the Mary's Creek River Basin; only the top 50 storms were selected for each duration regardless of the year of occurrence. The final 50 storms in the storm catalog for 6-hour duration are listed in Table 3-3. It is worth mentioning that no storms were selected from some of the years such as 2005 due to low rainfall depths from these years.

Table 3-3 Finalized 6-hours storm catalogue for 10 years based on the preselected list

Order	Yr : Storm Name	Depth over basin(in)	Order	Yr : Storm Name	Depth over basin(in)
1	**2007:S20**	5.47	26	**2010:S8**	3.26
2	**2014:S2**	5.18	27	**2010:S18**	3.25
3	**2014:S11**	4.98	28	**2012:S1**	3.24
4	**2006:S4**	4.84	29	**2007:S23**	3.22
5	**2014:S26**	4.80	30	**2014:S32**	3.20
6	**2006:S1**	4.60	31	**2010:S21**	3.20
7	**2010:S7**	4.37	32	**2007:S7**	3.19
8	**2010:S17**	4.32	33	**2006:S23**	3.17
9	**2007:S26**	4.20	34	**2007:S25**	3.17
10	**2014:S17**	4.17	35	**2009:S12**	3.15
11	**2007:S36**	4.14	36	**2012:S17**	3.15
12	**2010:S32**	4.10	37	**2010:S4**	3.10
13	**2006:S11**	3.98	38	**2006:S17**	3.09
14	**2006:S9**	3.85	39	**2008:S10**	3.07
15	**2006:S18**	3.85	40	**2011:S7**	3.07
16	**2011:S1**	3.84	41	**2010:S45**	3.06
17	**2014:S3**	3.83	42	**2007:S14**	3.04
18	**2008:S3**	3.68	43	**2009:S25**	3.03
19	**2008:S25**	3.67	44	**2014:S10**	3.02
20	**2010:S6**	3.67	45	**2008:S19**	3.01
21	**2014:S4**	3.46	46	**2007:S12**	3.00
22	**2007:S16**	3.37	47	**2009:S38**	2.99
23	**2010:S13**	3.34	48	**2010:S20**	2.99
24	**2008:S46**	3.30	49	**2012:S43**	2.98
25	**2008:S7**	3.29	50	**2012:S29**	2.81

3.3. Rainfall Frequency Analysis

The first application of SST in this study is to perform rainfall frequency analyses and develop IDF curves for all the subbasins in the Mary's Creek River Basin. To address such questions, we need to understand the sufficient number of SST iterations for all durations to conduct proper frequency analysis. A simple sensitivity analysis was performed for a one-hour rainfall duration on the entire Mary's Creek River Basin as a single basin. It is assumed in this study that the total number of iterations represents the number of return periods. The sensitivity analysis was performed for a one-hour rainfall duration only. Based on 1,000 iterations of one-hour rainfall data for the Mary's Creek River Basin representing 1,000 years of return periods, the annual maxima values were obtained. The first 10 maxima values (before sorting) were chosen from the 1,000 years of results, which is comparable to 10-years of annual maximum rainfall data. Finally, the Weibull plotting position formula was used to calculate the conditional return period conditioned on the rainfall duration.

$$Return\ Period = \frac{n+1}{m} \tag{3-1}$$

where m is the rank for the sorted data in a descending order and n is the total number of available data points. The highest value is given the 1st, which is the lowest value given the nth rank. We plotted the rainfall intensity over the Mary's Creek River Basin for 10-year return periods in black circles as shown in Figure 3-7. In the same manner, 20 annual maxima values were chosen from the 1,000 years of data to represent the 20 year return period; they are plotted in red circles in Figure 3-7. The aforementioned steps were repeated for 25, 50, 100, 200, 500 and 1000 annual rainfall maxima values and corresponding one-hour rainfall intensities were plotted with respect to return periods in Figure 3-7.

As shown in Figure 3-7, the annual maximum MAP values increase by extending the number of years. This trend demonstrates that the SST is capable of increasing the return period

extent for the frequency analysis. We have successfully increased the record of data from 10 to more than hundreds of years by relocating numerous storms that occurred at different locations with an equal probability of occurrence over the Mary's Creek River Basin.

Interestingly, as shown in Figure 3-7, the MAP values do not increase significantly from 500 to 1,000 return periods. We think that it may be due to the lack of the extreme storms with a large return period like 1,000 years. Based on the results with little difference between 500 year and 1,000 year return periods from this sensitivity analysis, we decided to use 1,000 years as the highest return period to conduct frequency analysis in this study.

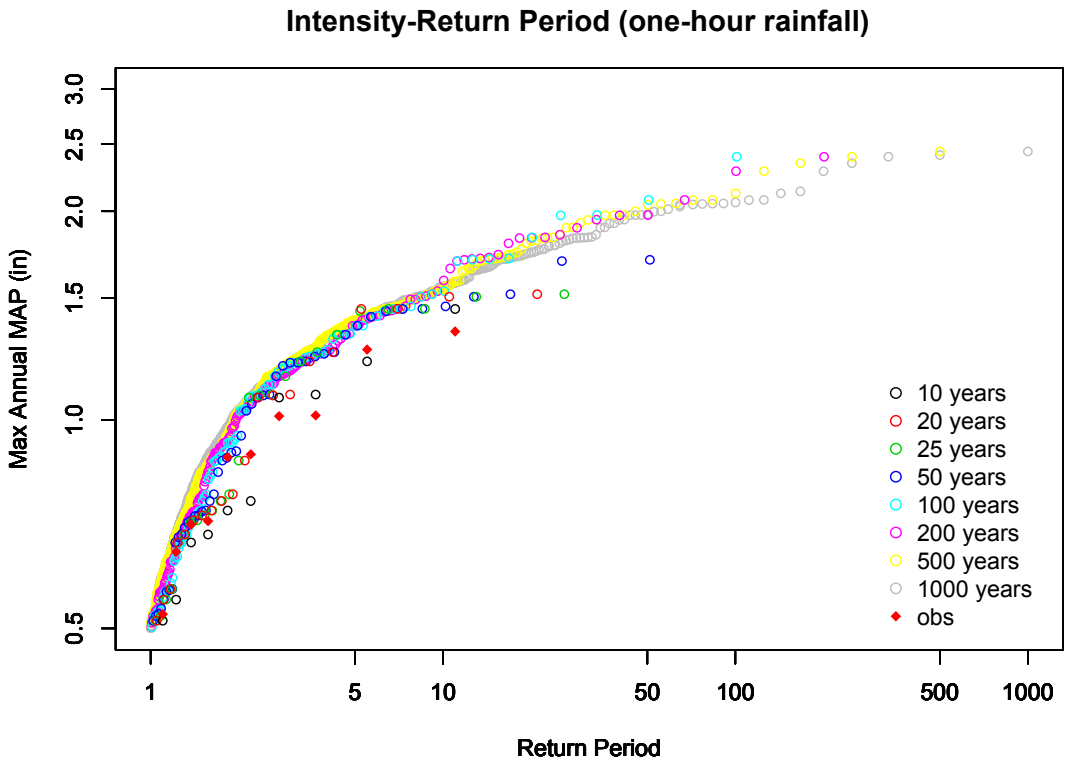

Figure 3-7 Rainfall frequency analysis for different numbers of annual maximum MAP over the Mary's Creek River Basin (e.g., by iterating SST 500 times, frequency analysis could be extended up to 500 years). Obs refers to the original annual maximum MAP from MPE without any transposition

Since the area of the subbasins is an important factor to calculate MAP values and develop IDF curves, all the subbasins within the Mary's Creek River Basin were divided into four categories based on their areas (Figure 3-8). The goal is to understand the relationships between the areas of the subbasins and the IDF information in the rainfall frequency analysis. The same basin information is provided in Table 3-4. One can see in Table 3-4 that the majority of the subbasins have an area smaller than 0.8 mi^2.

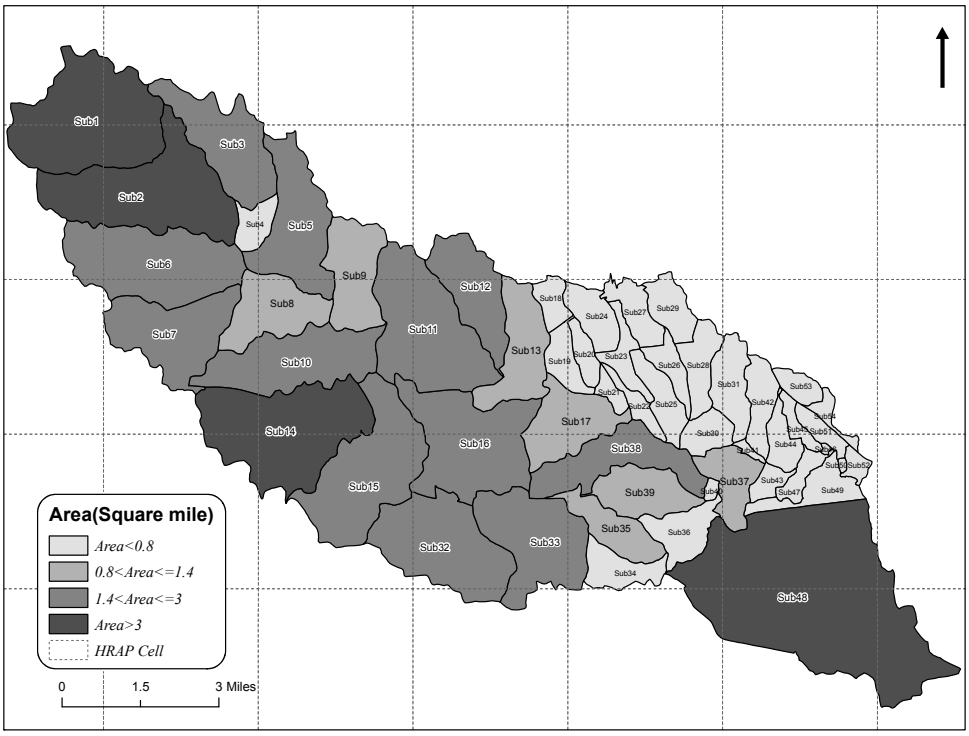

Figure 3-8 Spatial locations of the four classified subbasins

Table 3-4 Four classified subbasins with areas

(I) *Area ≤ 0.8 mi²*		*(II)* *0.8 < Area ≤ 1.4 mi²*	*(III)* *1.4 < Area ≤ 3 mi²*	*(IV)* *Area > 3 mi²*
Sub 4	Sub 36	Sub 37	Sub 32	Sub 1
Sub 18	Sub 40	Sub 39	Sub 6	Sub 14
Sub 19	Sub 41	Sub 9	Sub 10	Sub 48
Sub 20	Sub 42	Sub 35	Sub 16	Sub 2
Sub 21	Sub 43	Sub 13	Sub 38	
Sub 22	Sub 44	Sub 8	Sub 11	
Sub 23	Sub 45	Sub 36	Sub 15	
Sub 24	Sub 46	Sub 17	Sub 3	
Sub 25	Sub 47		Sub 5	
Sub 26	Sub 49		Sub 7	
Sub 27	Sub 50		Sub12	
Sub 28	Sub 51			
Sub 29	Sub 52			
Sub 30	Sub 53			
Sub 31	Sub 33			
Sub 34	Sub 54			

The developed IDF information from the SST approach was compared with three kinds of data sources: the observed annual maximum MAP values, the IDF information provided by iSWM (iSWM Technical Manual 2014), and the IDF information provided by the TxDOT/USGS (Asquith and Roussel 2004). The observed annual maximum MAP refers to the computed MAP values from 10 years of MPE data without any transposition. The observed annual maximum values for various rainfall durations (1, 6, 12, and 24 hours) are tabulated in **Appendix A**. The Weibull plotting position formula was used to determine the corresponding return period for each observed MAP without fitting any function. Secondly, the IDF information provided from the iSWM technical manual was developed based on the empirical equation (1-2) (iSWM Technical Manual 2014). The IDF information developed in a collaborative efforts of TxDOT and USGS is widely used for engineering designs in Texas (Asquith and Roussel 2004). It is referred as the TxDOT-USGS in many plots hereafter.

Figure 3-9 to Figure 3-14 show the estimated IDF curves based on SST, observation, TxDOT-USGS and iSWM for Group (I) subbasins in logarithmic scales for both x-axis and y-axis The x axis indicates the rainfall return periods, starting from 2-year to 1,000-year return periods.

Some of the values with return periods of less than two years are not shown in Figure 3-9 to Figure 3-14.

In general, it was found that the SST results match closely with observed values for one-hour rainfall durations; while the SST-based IDF curves are higher than the observed values for other rainfall durations such as 6, 12 and 24 hours. It was also found that the TxDOT-USGS and iSWM IDF curves are consistently higher than the observed values. The SST-based IDF curves are consistently lower than those of the iSWM and TxDOT-USGS IDF curves for one-hour duration; while the SST-based IDF curves are similar to other curves (observed, iSWM, and TxDOT/USGS for the rest of the durations (6, 12, and 24 hours). In addition, we found that the rainfall intensity values generated from the SST are generally larger than those of the TxDOT/USGS information for smaller return periods of less than 100 years, while the opposite is observed for higher return periods.

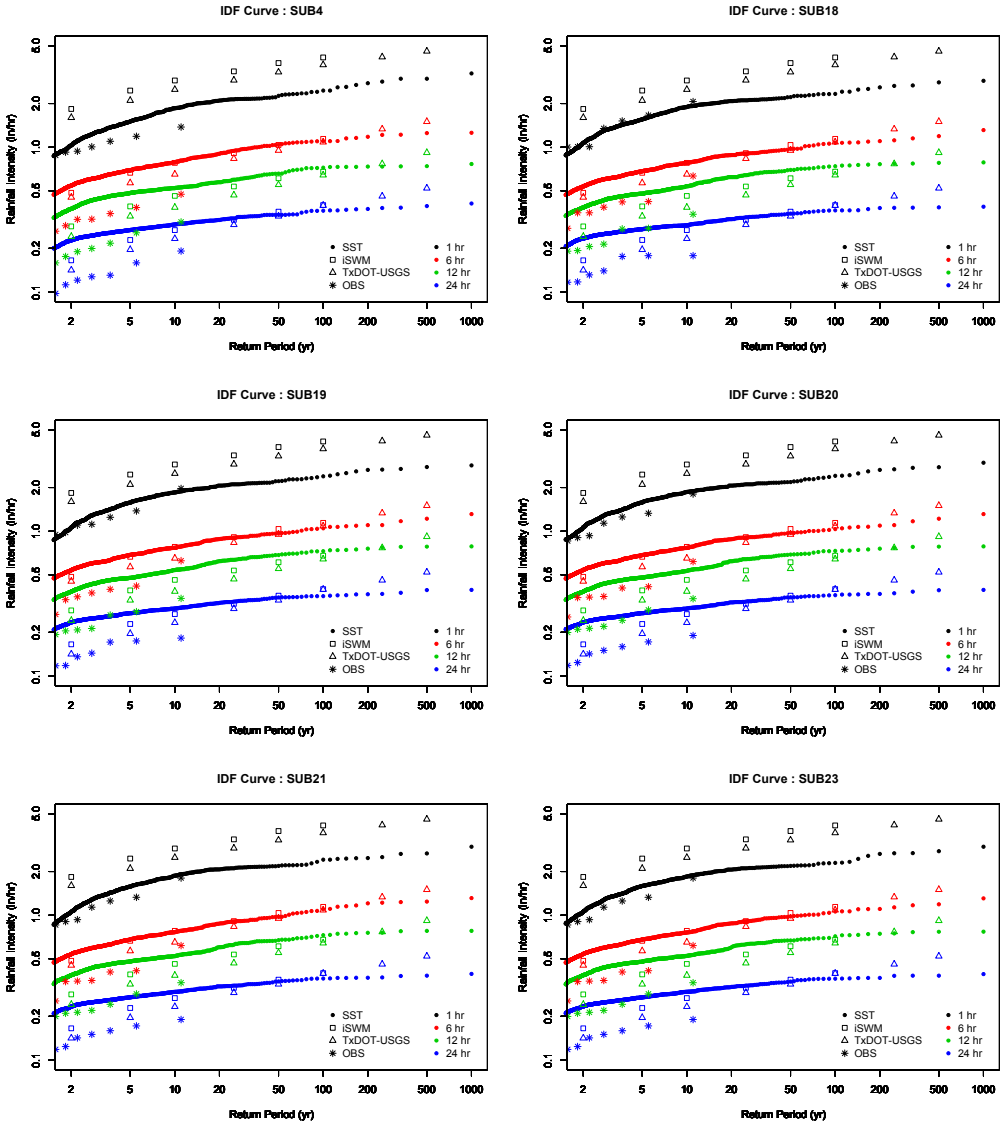

Figure 3-9 IDF curves based on observed values, iSWM, TxDOT-USGS and SST for Subbasins 4, 18, 19, 20, 21 and 23 in Group (I).

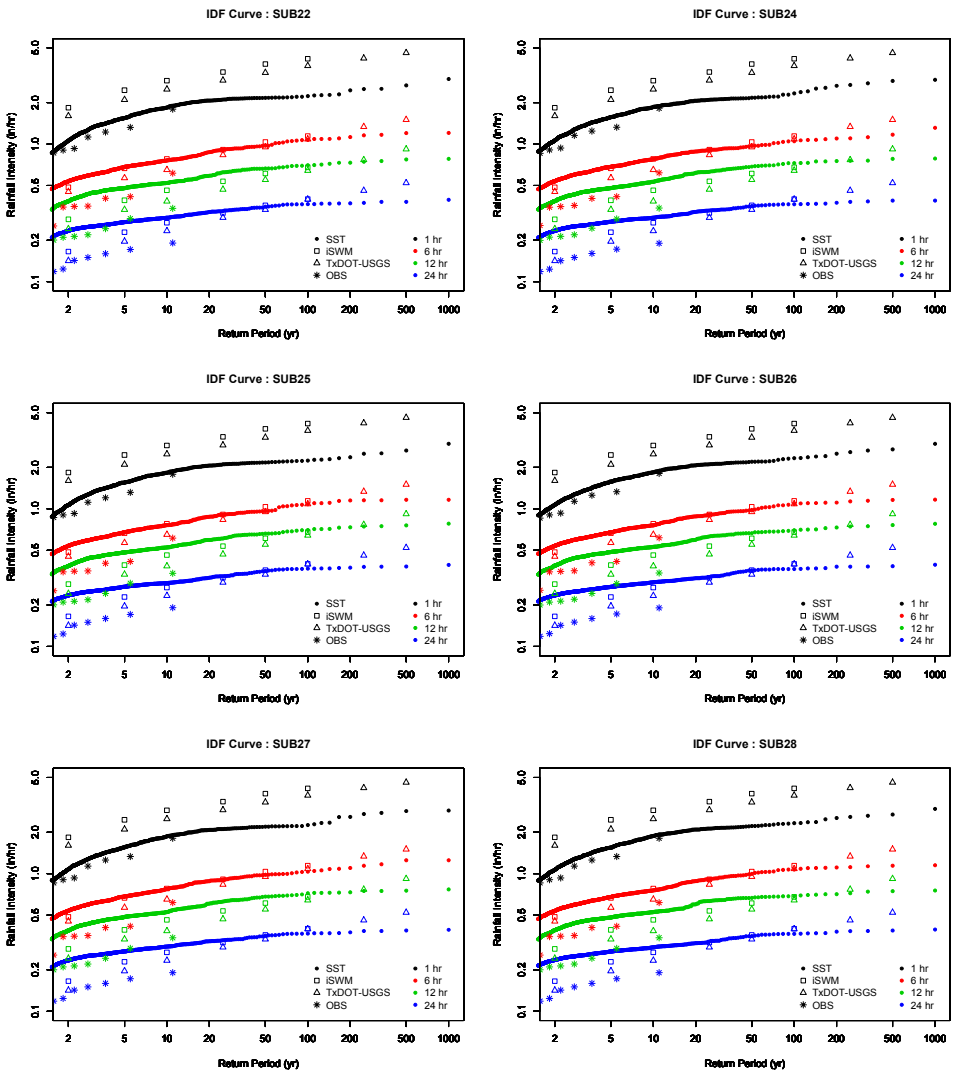

Figure 3-10 IDF curves based on observed values, iSWM, TxDOT-USGS and SST for Subbasins 22, 24, 25, 26, 27 and 28 in Group (I).

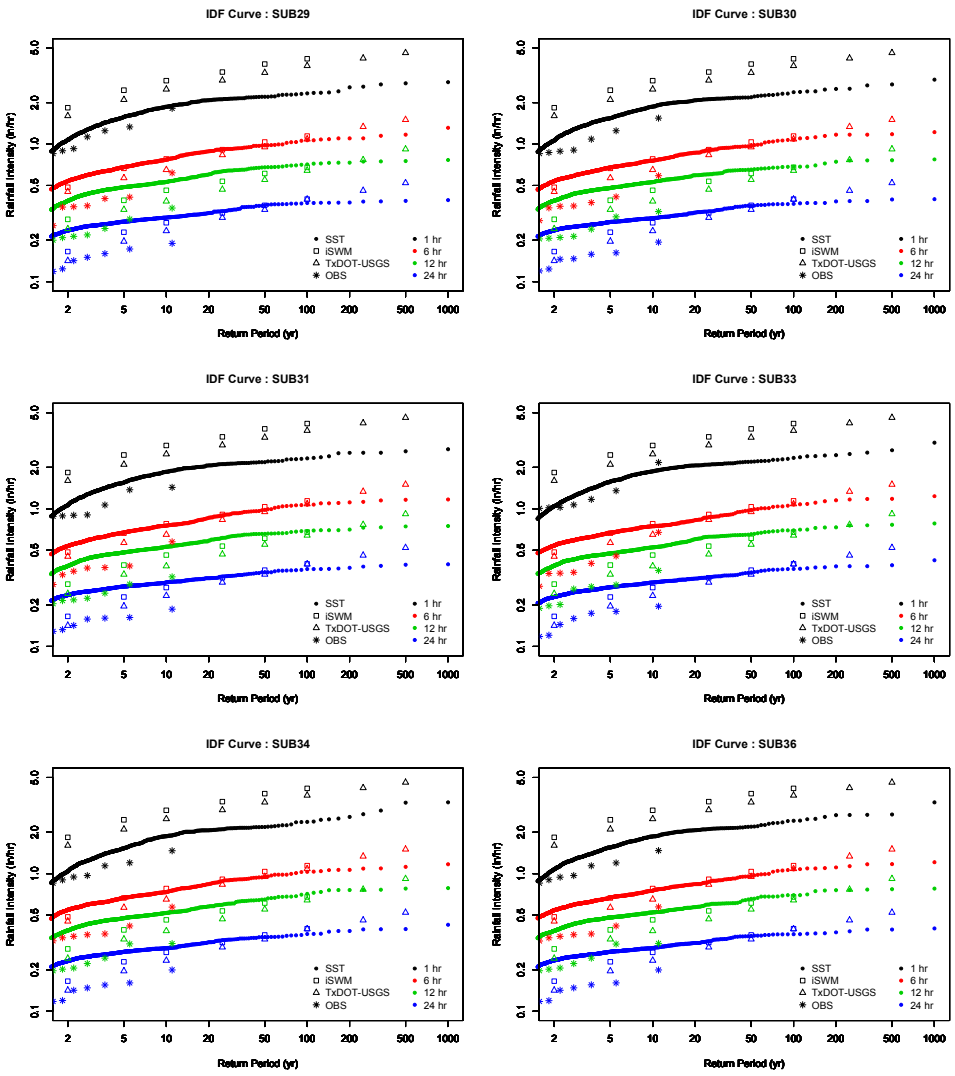

Figure 3-11 IDF curves based on observed values, iSWM, TxDOT-USGS and SST for Subbasins 29, 30, 31, 33, 34 and 36 in Group (I).

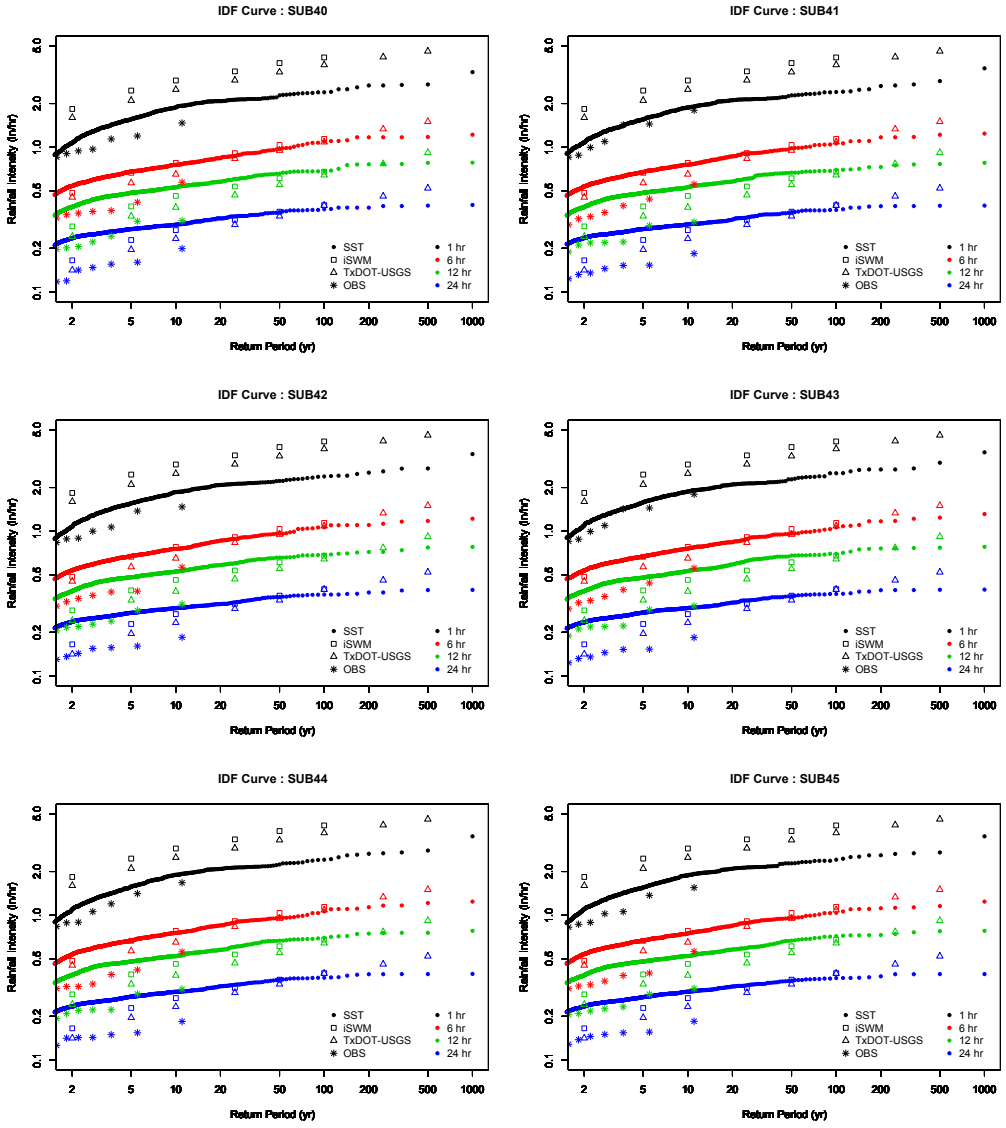

Figure 3-12 IDF curves based on observed values, iSWM, TxDOT-USGS and SST for Subbasins 40, 41, 42, 43, 44 and 45 in Group (I).

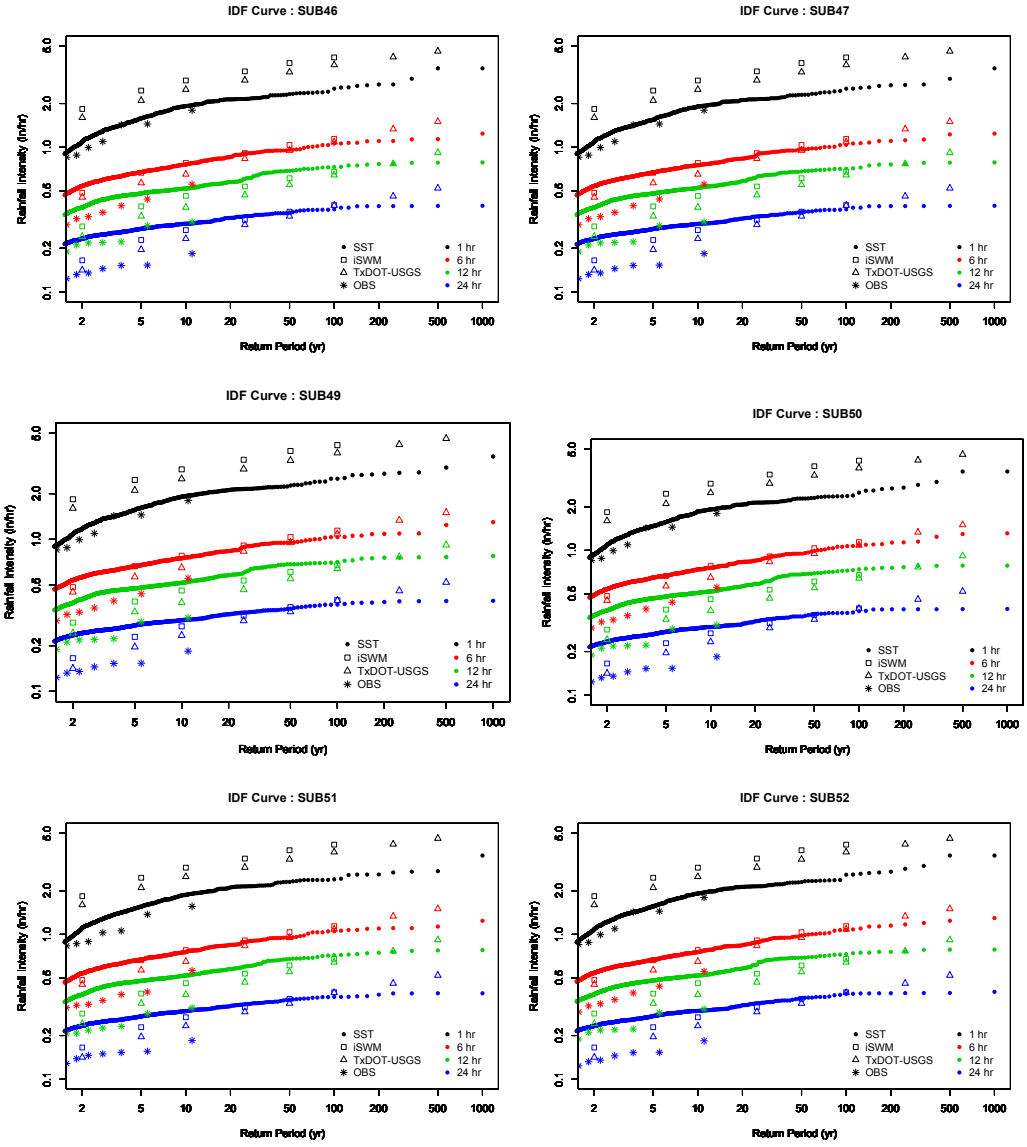

Figure 3-13 IDF curves based on observed values, iSWM, TxDOT-USGS and SST for Subbasins 46, 47, 49, 50, 51 and 52 in Group (I).

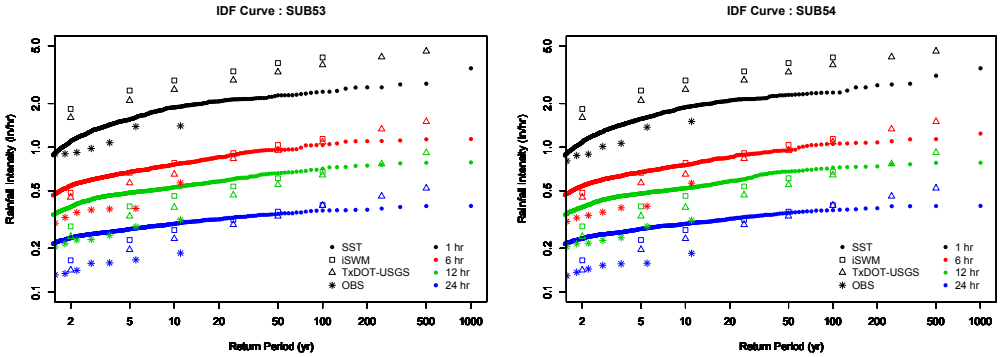

Figure 3-14 IDF curves based on observed values, iSWM, TxDOT-USGS and SST for Subbasins 53 and 54 in Group (I).

Figure 3-15 shows IDF curves based on observed, iSWM, TxDOT-USGS and SST for Group (II). In general, the same behavior as shown in Group (I) subbasins was observed. The main observations are: SST-based IDF curves are close to the observed IDF curves for rainfall duration of one hour but considerably lower than those of iSWM and TxDOT-USGS. While SST-based IDF cureves are considerably higher than those of the observed values from 6-, 12- and 24- hour rainfall durations, the SST-based IDF curves agree the best with those of the TxDOT-USGS and iSWM for 6-hour durations.

Figure 3-17 and Figure 3-18 show the comparisons among the SST-based IDF curves, the observed values, iSWM, and TxDOT-USGS for subbasins in Group (III). The results for Group (IV) are given in Figure 3-18. Similar observations were found among different IDF curves for Groups (III) and (IV).

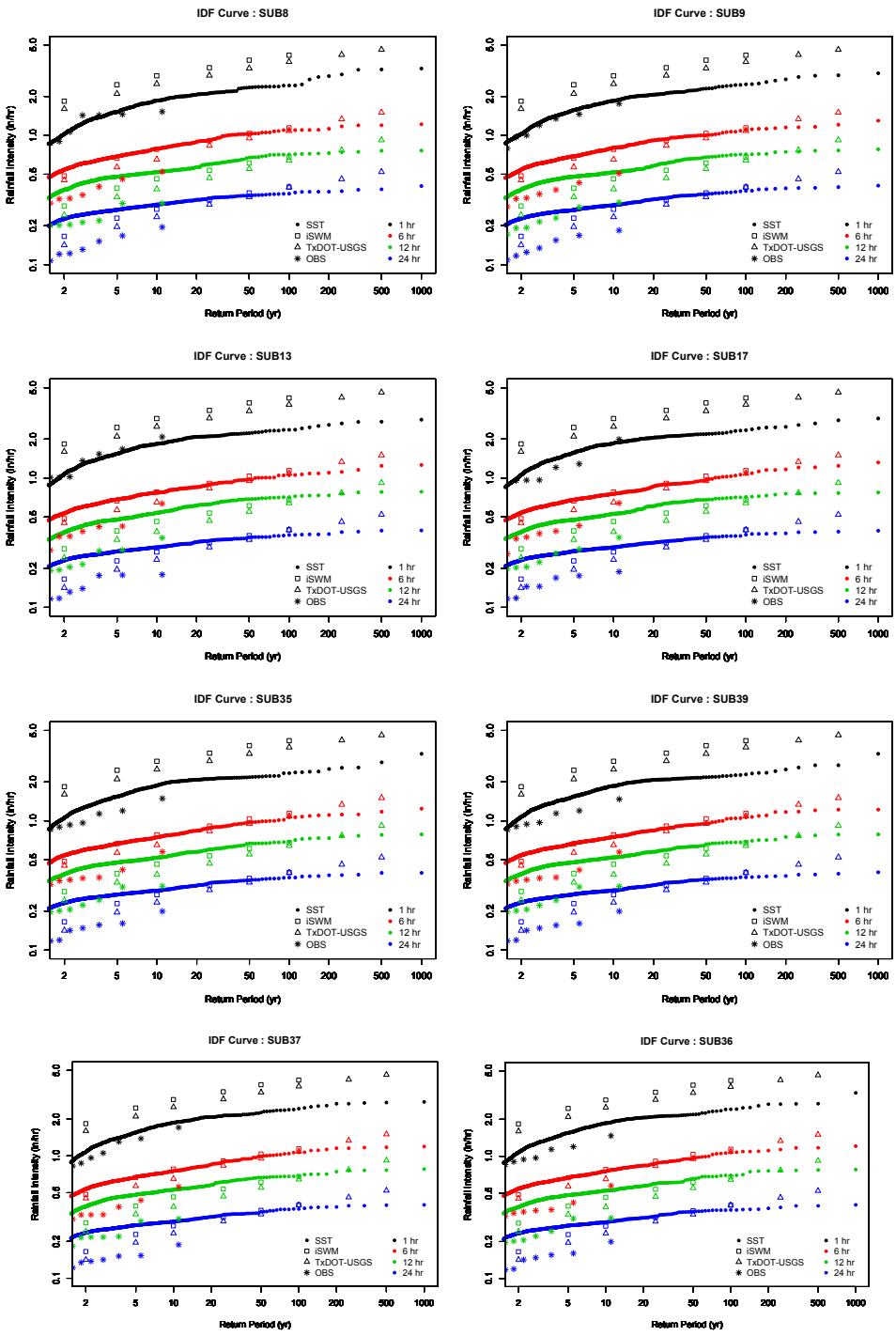

Figure 3-15 IDF curves based on observed values, iSWM, TxDOT-USGS and SST for Subbasins 8, 9, 13, 17, 35, 36, 37 and 39 in Group (II).

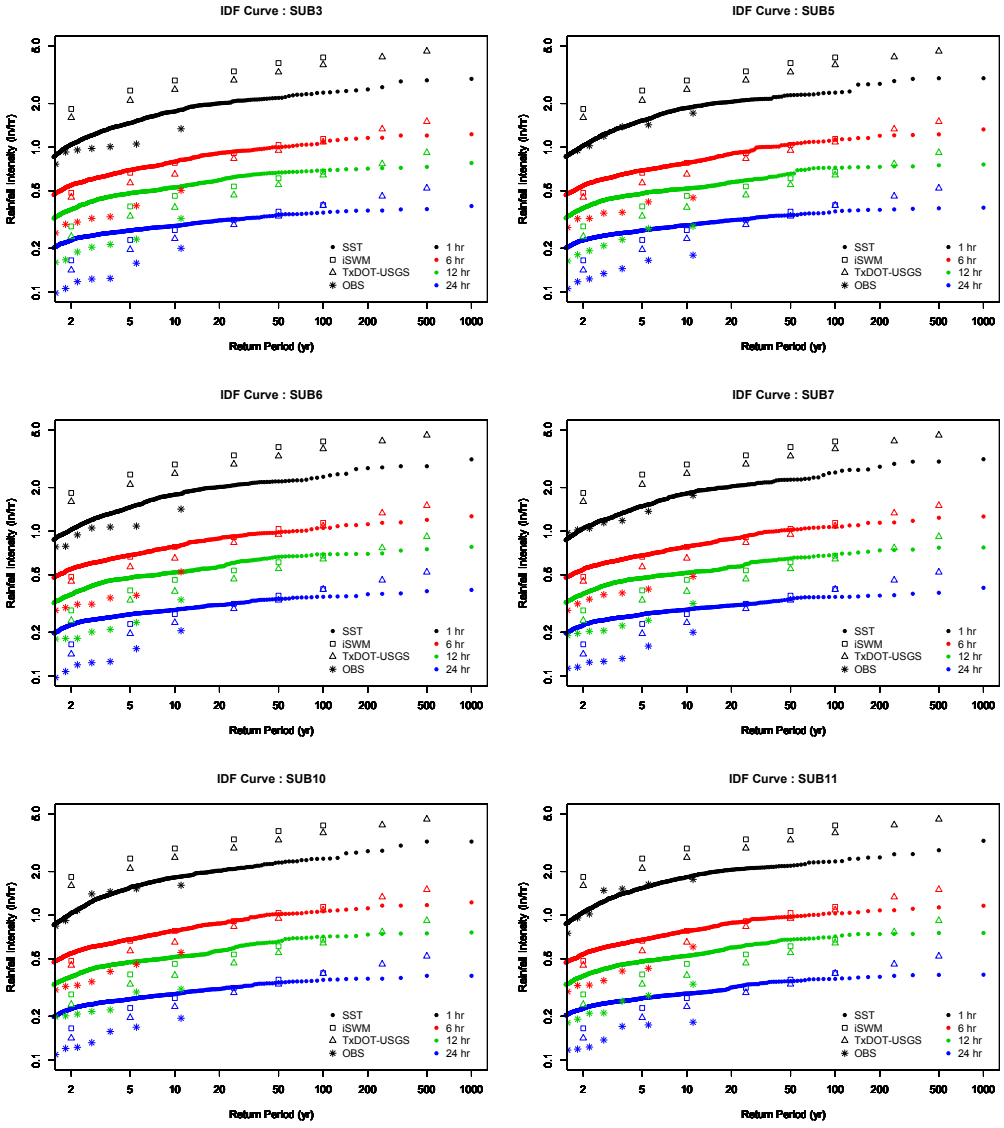

Figure 3-16 IDF curves based on observed values, iSWM, TxDOT-USGS and SST for Subbasins 3, 5, 6, 7, 10 and 11 in Group (III).

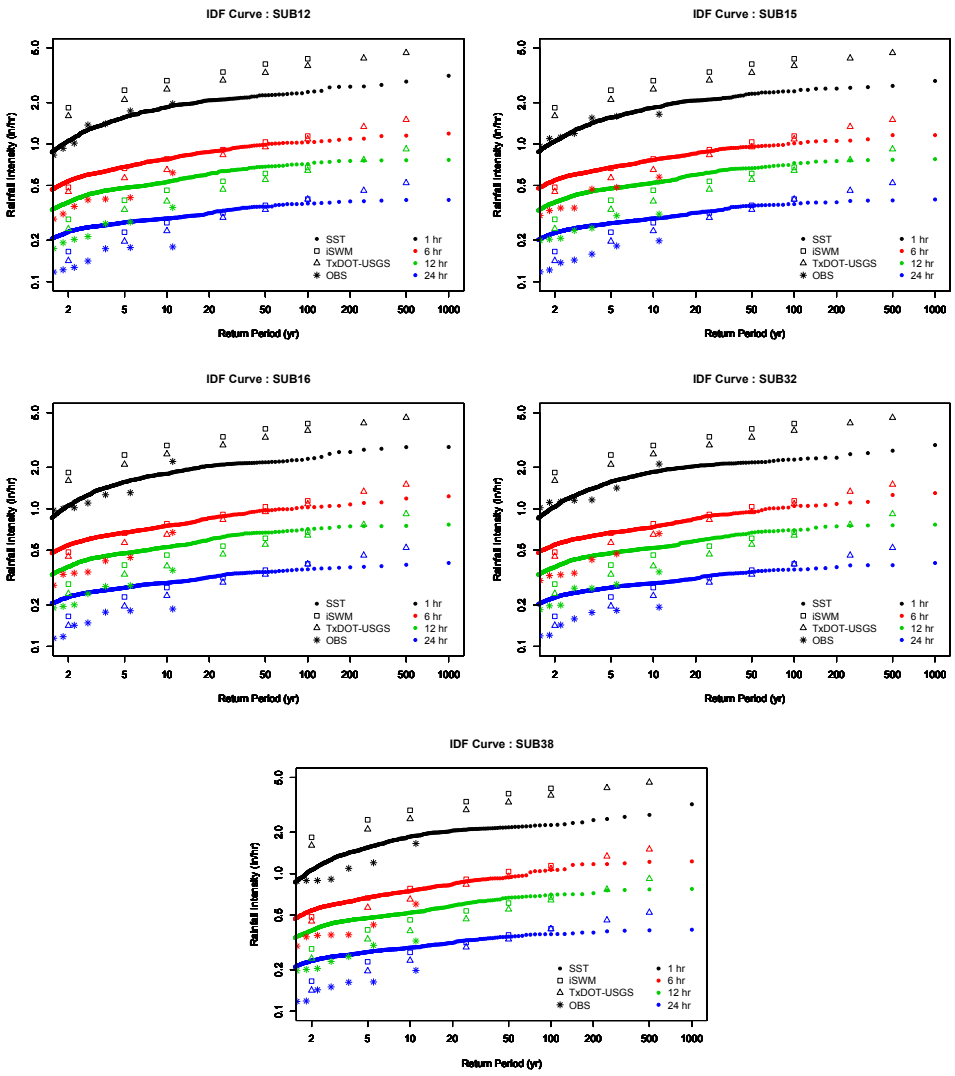

Figure 3-17 IDF curves based on observed values, iSWM, TxDOT-USGS and SST for Subbasins 12, 15, 16, 32 and 38 in Group (III).

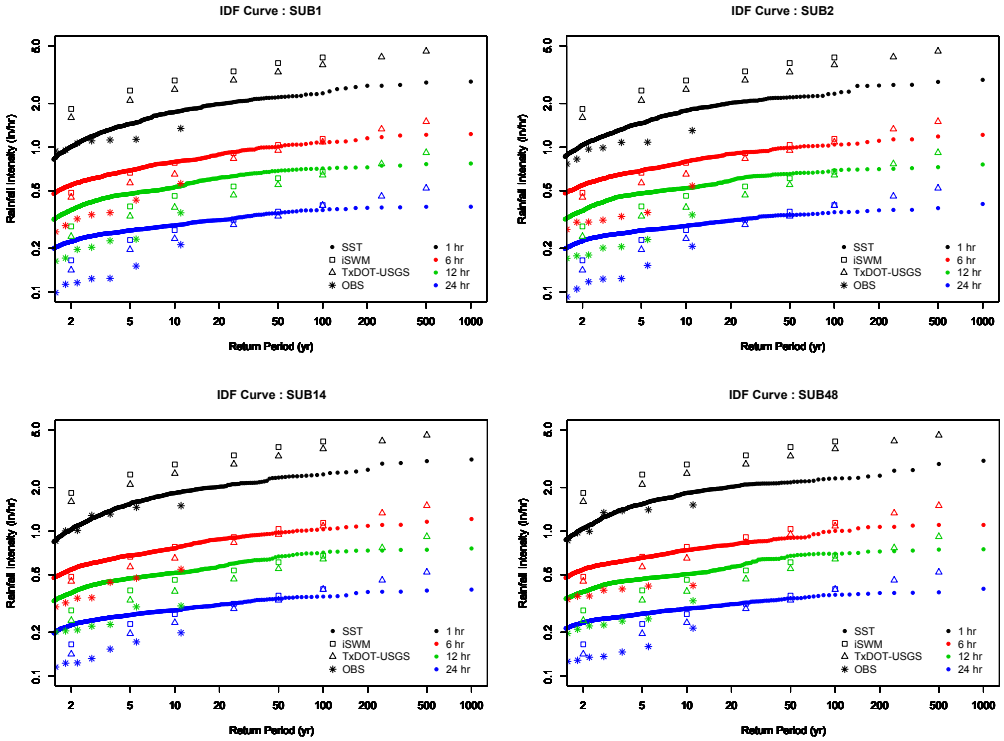

Figure 3-18 IDF curves based on observed, iSWM, TxDOT-USGS and SST for Subbasins 1, 2, 14, and 48 in group (IV).

Figure 3-9 to Figure 3-18 show the comparisons among different IDF curves for all the subbasins in the Mary's Creek River Basin. Based on the comparisons, it was found that the obtained IDF information from the SST approach is not sensitive to the size of subbasins. Some general findings from the rainfall frequency analysis are summarized below:

1. SST-based IDF curves are close to the observed values for one-hour durations up to 10-year return periods. This finding implies that the results of the SST approach are reasonable based on comparison against 10 years of available data. The SST approach enabled us to extend the rainfall frequency analysis based on the existing 10-year observed data to 1,000-year return periods without using any statistical extrapolation methods.

2. Figure 3-9 to Figure 3-18 show the SST-based IDF curves for the entire Mary's Creek River Basin in comparison with the observed values (using the Weibull plotting position formula), and the design rainfall information from iSWM as well as TxDOT/USGS. All subbasins behave similarly with respect to different IDF information: SST-based IDF curves are close to the observed IDF curves for rainfall durations of one-hour but considerably lower than those of iSWM and TxDOT-USGS; while SST-based IDF curves are considerably higher than those of the observed values from 6-, 12- and 24-hour rainfall durations, the SST-based IDF curves agree the best with those of the TxDOT-USGS and iSWM for 6-hour durations; the largest difference between the SST-based and observed IDF information is found for the 24-hour durations. The observed values for various durations (1, 6, 12, and 24 hours) can be found in **AppendixA**
3. It was found that the difference between SST-based and TxDOT-USGS as well as iSWM IDF curves is always larger for one-hour rainfall durations. We think that this may be due to underestimated MPE data for high intensity rainfall events. The underestimation of MPE is less influential for other rainfall durations (6, 12, and 24 hours). Ideally, there should be a conditional bias adjustment to MPE data; however, there were no rain gauges available to perform bias adjustment on MPE data. Since this is an on-going research project, improved methods will be applied in the near future.

3.4. Flood Frequency Analysis (FFA)

We used the SST approach to perform flood frequency analysis (FFA). This section is mainly to address two objectives: 1) to generate flood frequency curves for each subbasin and 2) to understand the relationship of rainfall and discharge frequencies from upstream to downstream of the Mary's Creek River Basin using a rainfall-runoff model. As introduced in Section 2.2, an available HEC-HMS model was used in the FFA with 250 hydrologic elements. Fifteen control points were selected out of the model as shown in Figure 3-19 to perform flood frequency analysis based on the results from the SST approach.

In addition, the available information from a USGS gauge (8047050) located in the Mary's Creek River Basin was used for FFA. The SST-based flood frequency developed for this location was compared with the observed data and design storms. For all other locations (14), FFA comparisons were only made based on design storms.

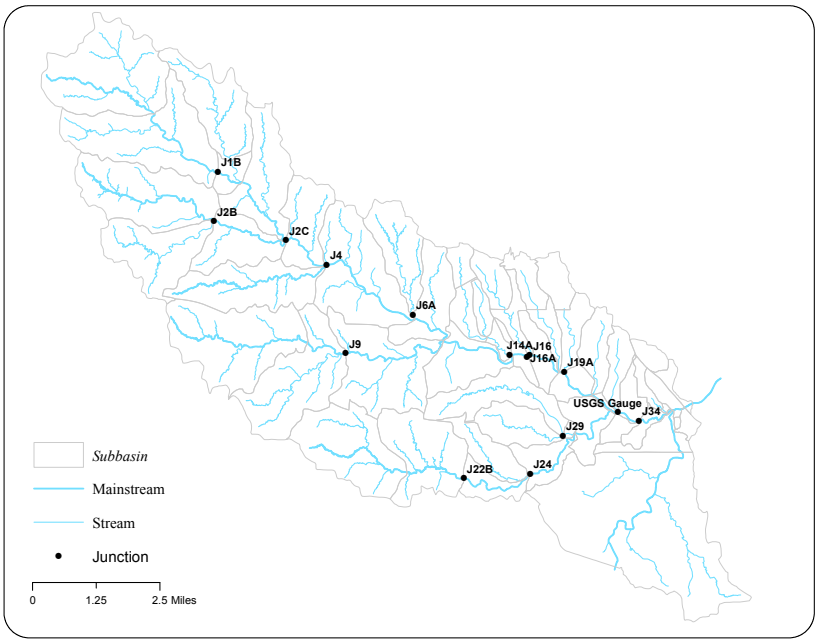

Figure 3-19 Locations of the selected control points and USGS gauge on the Mary's Creek River Basin

The SST procedure for flood frequency analysis is slightly different from rainfall frequency analysis as described in Section 3.3. In rainfall frequency analysis, after generating *k* (random value from Poisson distribution) storms, the *k* of corresponding MAP values were calculated. Then annual maximum values were chosen out of the *k* MAPs for each subbasin. However, in flood frequency analysis, the maximum peak flow is the selection criterion. On average, 5,000 realizations were needed to extend the flood frequency analysis for 1,000 years (if λ=5). Similar to rainfall frequency analysis, the number of flooding events is assumed to follow the Poisson distribution. The rate parameter (λ) of 5 was used in FFA, which means that the average number of flood occurrences is five per year. It is worth mentioning that the same 24-hour storms used in rainfall frequency analysis were also used in flood frequency analysis.

Figure 3-20 a and b show the simulated hydrographs from the HEC-HMS model for about 5,000 realizations at two control points: J1B and USGS gauge. J1B is a junction upstream of Mary's Creek while the USGS gauge is located downstream of the watershed. The resultant hydrographs (Figure 3-20) were used as a basis to perform FFA. Figure 3-20a shows that the peak flow varies from zero to ~ 8,700 cfs at J1B junction indicating that some of the storms did not produce any rainfall over the subbasins contributing to J1B with no runoff. Figure 3-20b shows that peak flow ranges from zero to ~29,000 at the USGS gauge location. Both figures imply that the response of the watershed is sensitive to the temporal and spatial variation of rainfall events.

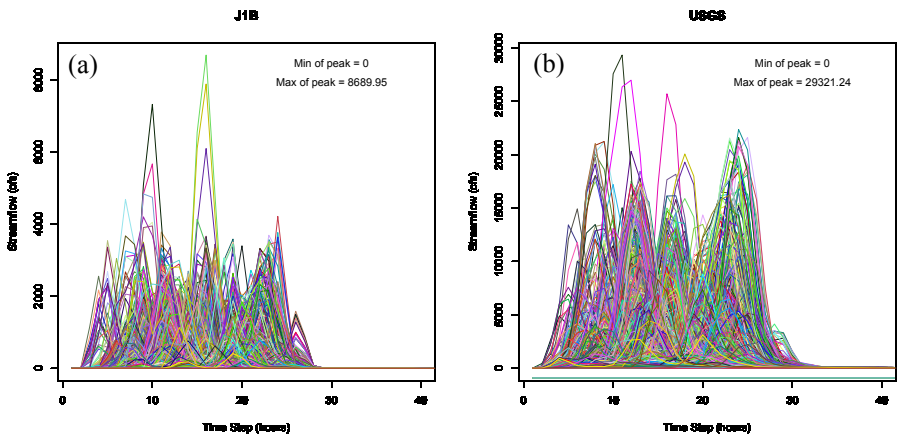

Figure 3-20 **a)** All simulated hydrographs were based on 5,000 realizations (~ 5,000 runs) from SST at an upstream junction (J1B) and **b)** at the USGS gauge location (downstream).

3.4.1. FFA at USGS gauge location

The USGS gauge at Benbrook (8047050) with 16 years of maximum daily peak flow information in Mary's Creek was used for FFA. The Weibull plotting position formula was applied to calculate return periods of the observed flow information. We adopted Log Pearson Type III (LP3) distribution to fit a function with the observed data at the USGS gauge (8047050). A bootstrap approach was used to estimate confidence intervals for our flood frequency model with a value of 90% (http://www.headwateranalytics.com/blog/flood-frequency-analysis-in-r). Figure 3-21 shows the fitted line to the 16 years of available annual maximum flow as well as the confidence interval.

The second source of information used to evaluate the SST-based frequency analysis was the design storms for Mary's Creek River Basin. There are seven design storms (2, 5, 10, 25, 50, 100 and 200 years) available from the HEC-HMS model for Mary's Creek River Basin, which were developed based on the IDF curves for Tarrant County. Corresponding peak values were calculated with respect to different design storms.

Figure 3-21 shows the SST-based flood frequency results in comparison with the design storm, observed flow values, and the Log-Pearson Type III fitted line at the USGS gauge location. Design storms fall in the confidence interval of 90% based on available observations, except from two years. Almost the same pattern is found for the SST-based frequency analysis. In general, the SST-based flood frequency results are overestimating for the high frequency events (below five years) and slightly underestimating for the low frequency events (above five years). This is similar to the results obtained from the rainfall frequency analysis (See Section 3.3). It is found that the discharge estimated by LP3 is significantly higher than those of design storms and SST. For example, as shown in Figure 3-21, the estimated discharge is about 100,000 cfs for the 100-year event, but is significantly higher than those of the design storm and SST-base frequency analysis.

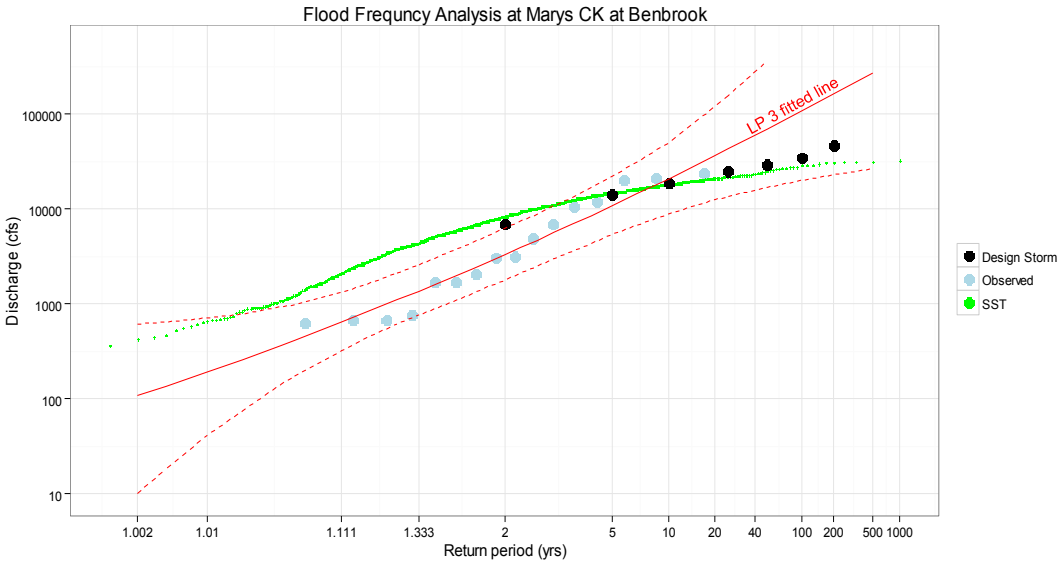

Figure 3-21 Results of the FFA at USGS gauge location for observed annual peak flow (blue dots), design storm (black dots) and SST (green). The solid red line is the fitted Log-Pearson III and the dashed red lines show the 90% confidence interval.

3.4.1. FFA Results at Other Junctions

A similar approach was applied to the other control locations in Mary's Creek River Basin. Since the observed discharge values are not available for those locations, we had to use design storm information to evaluate the SST-based flood frequency analysis. Three categories of subbasins were defined with respect to the sizes of the drainage contributing areas: low, medium and high. Table 3-5 lists all junctions in each category with their corresponding contributing areas. Figure 3-19 shows 15 selected control points for the FFA.

Table 3-5 Classifying the junctions based on drainage area

Contributing Area	*Junction Name*	*Drainage Area (mi^2)*
Low Drainage Area	J16A	0.27
	J14A	1.26
	J24	1.45
	J19A	1.86
Medium Drainage Area	J29	2.6
	J6A	4.34
	J22B	4.72
	J2B	4.82
	J9	6.19
	J1B	6.6
	J2C	17.08
	J4	20.61
High Drainage Area	J16	39
	USGS Gauge	51.88
	J34	52.51

Figure 3-22 shows the relationships of the SST-based flood frequency results and the design storms for all selected junctions in the category low drainage area. As illustrated, the design storm results for three of the upstream junctions are considerably higher than the SST-based flood

frequency curves. These junctions are located very close to the outlet of Mary's Creek River Basin. The high values of design storms can be attributed to the fact that HEC-HMS model will automatically locate the center of the synthetic design storm at a downstream location of the basin

The results for the categories of middle and high drainage areas are shown in Figure 3-23 and Figure 3-24, respectively. For basins with medium contributing areas, the SST results are higher than those of design storms for very short return periods (such as two years) which is consistent with the findings from the rainfall frequency analysis (See Section 3.3). For higher return periods, the SST-based frequency curves are lower than those of the design storms. For high drainage contributing areas, the SST-based flood frequency curves are similar to those of the design storms. The SST results agree with those of the design storms up to 100 years but are slightly lower than those of the design storms for return periods of higher than 100 years.

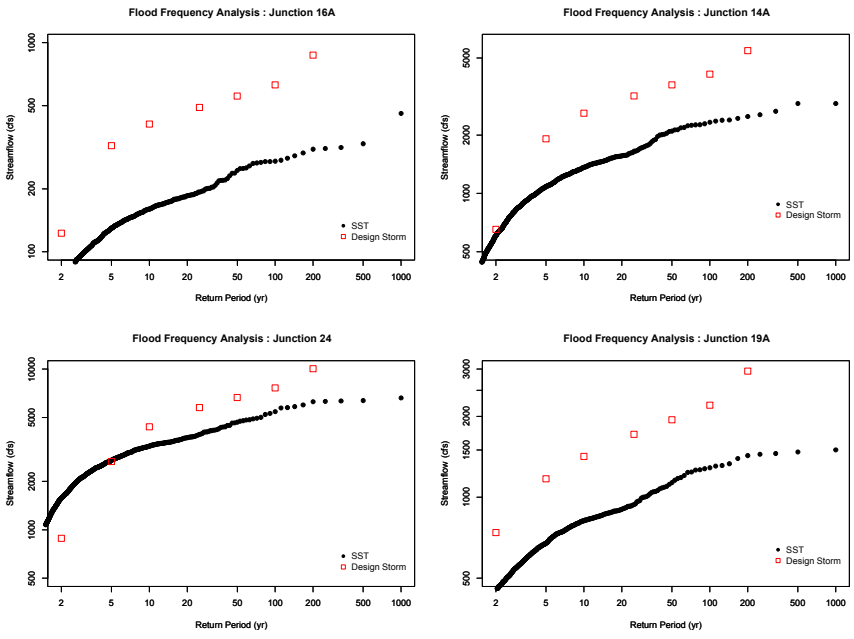

Figure 3-22 FFA results for the basins with low drainage areas

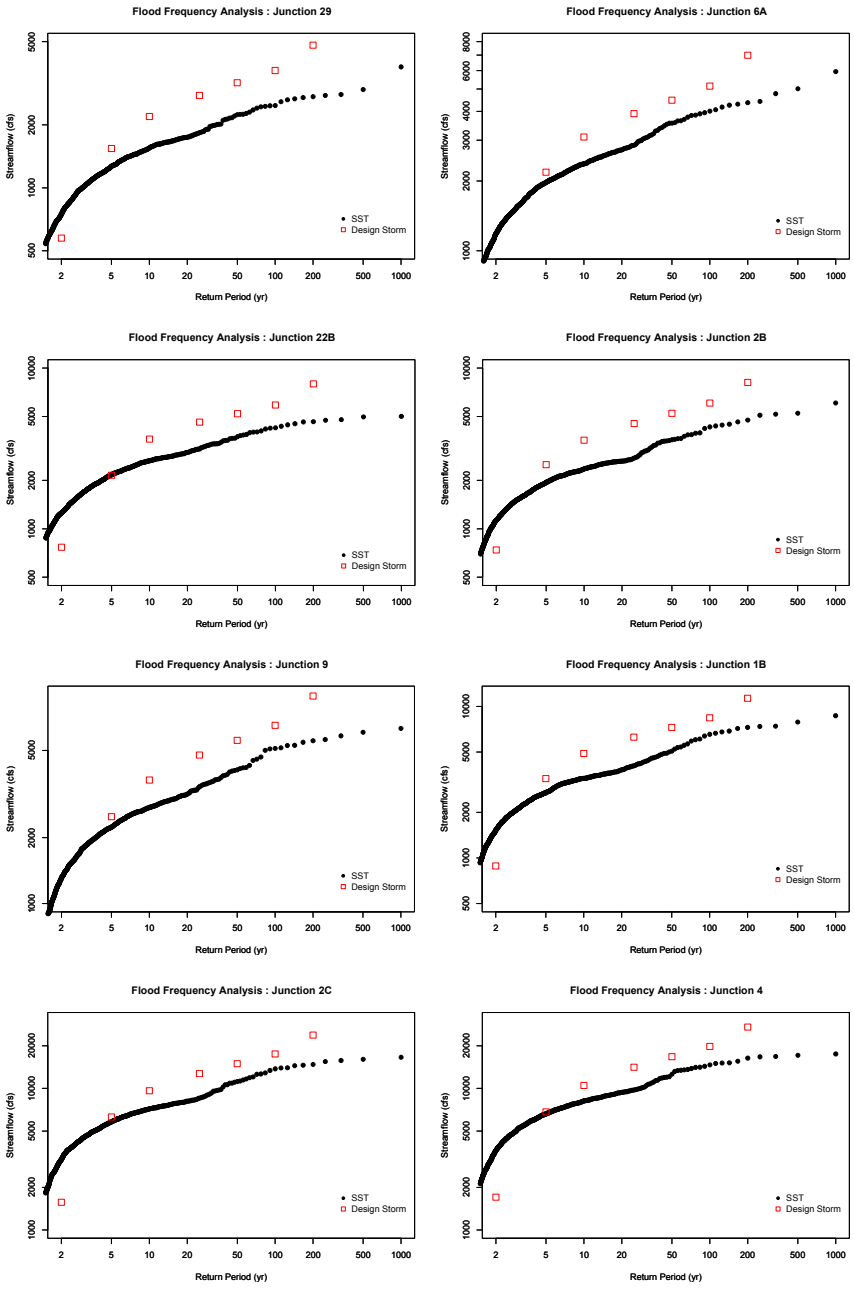

Figure 3-23 FFA results of the basins with medium drainage areas

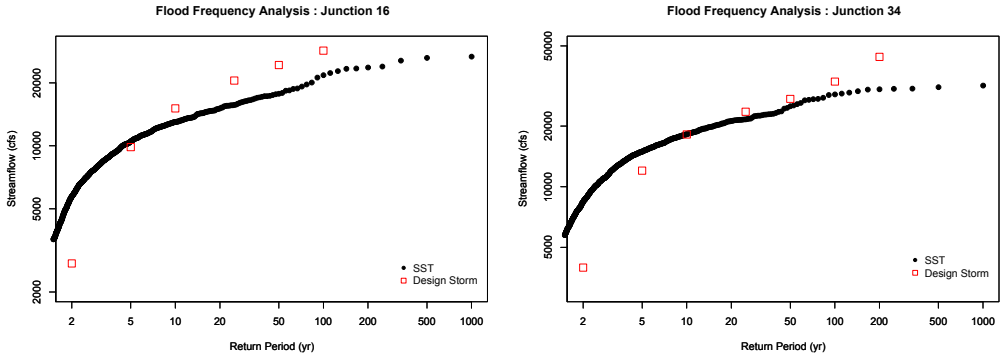

Figure 3-24 FFA results of the downstream basins with high drainage areas

3.5. Correlation between Rainfall and Flood Return Periods

It is a common practice in hydrologic modeling to assume that the design storms and resulting hydrographs share the same frequency (return period). However, this assumption has been questioned by many researchers (Adams and Howard 1986; Wright et al. 2014). Wright et al. (2014) showed that the rainfall with a T-year return period does not necessarily cause T-year flooding. In other words, there is no one-to-one relationship between rainfall frequency and flood frequency. Therefore, the conventional flood frequency analysis is subject to errors arising from this one-to-one relationship assumption. In this research, we also investigated the credibility of this assumption by calculating the Pearson correlation coefficient between the rainfall and the corresponding flood return period. Pearson correlation coefficient is described as the following

$$\rho_{r,f} = \frac{E[(r - \mu_r)(f - \mu_f)]}{\sigma_r \sigma_f} \tag{3-1}$$

where r and f are return periods of rainfall and the corresponding flood, respectively; μ_r and μ_f are the expected values of rainfall and flood return periods; σ_r and σ_f are the standard deviations of rainfall and flood return periods, respectively.

Figure 3-25 shows eight selected points from the watershed used to examine this relationship: three points from the headwater basins, three points from the midstream locations along the main channel; and two points at the downstream locations.

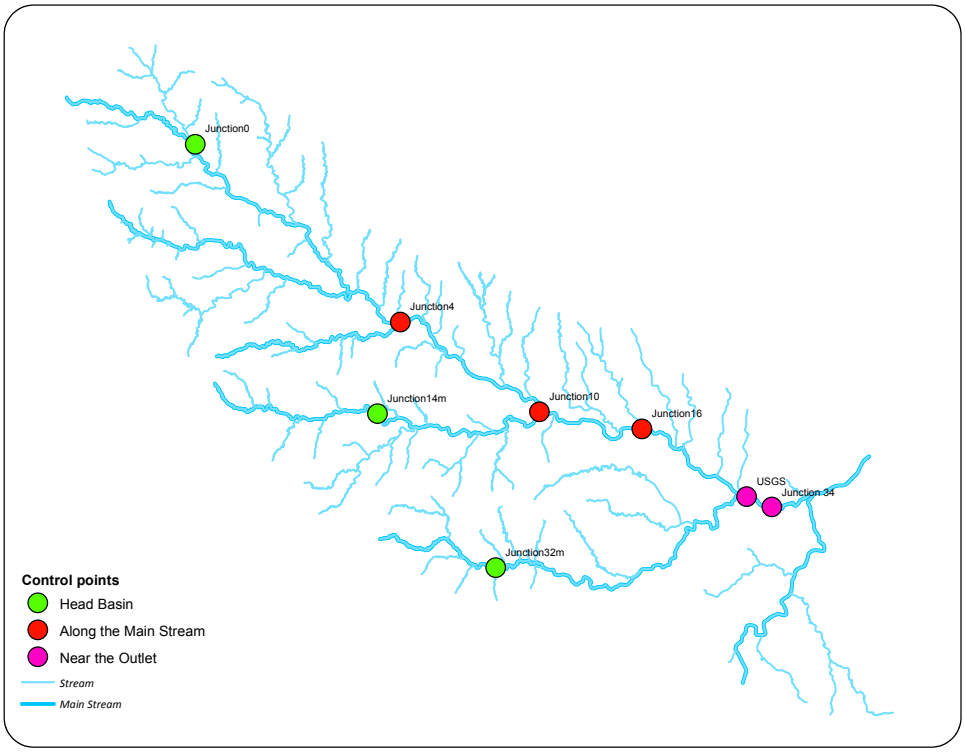

Figure 3-25 Locations of the selected points to study the relationship between rainfall and flood return periods.

Figure 3-26 shows the scatter plot of the rainfall and discharge return periods. The two downstream junctions (Junction 34 and USGS gauge (08047050) are apart by 0.5 mile. The scatter plots for these two locations are similar to each other as expected since they are located at the main stream with similar drainage areas. However, it was found that the Pearson correlation coefficients between the rainfall and discharge return periods for both of these locations is about

0.19. Such low correlation coefficients are due to the strong impact of mismatch between the return periods of rainfall and the corresponding floods at high return periods (especially 500 and 1,000).

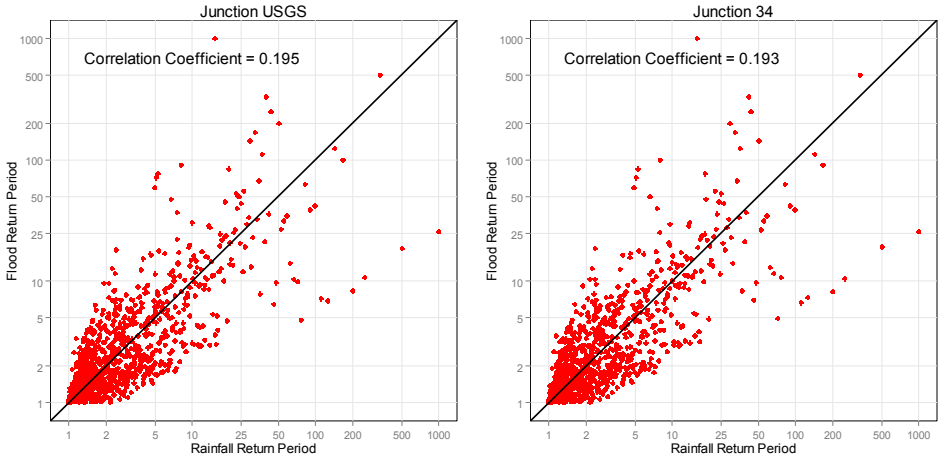

Figure 3-26 Scatter plots of return periods between rainfall and streamflow for the two downstream locations at the Mary's Creek Basin.

The Pearson correlation coefficient is given in each plot.

The same scatter plots for the junctions at the upstream and midstream locations are plotted in Figure 3-27 and Figure 3-28. As explained above, high return periods have a larger impact on correlation coefficients. Comparing all the junctions, we found that there is not a one-to-one relationship between rainfall and flood return periods for the study watershed. Also, we did not find any particular pattern by dividing the junctions to different categories of upstream, midstream and downstream.

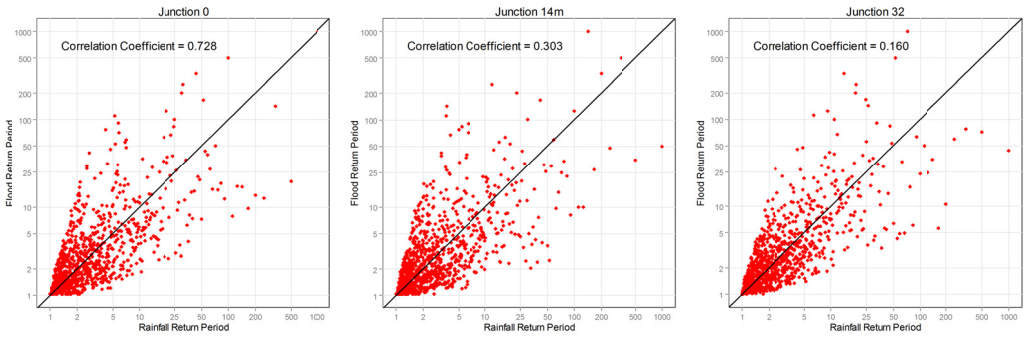

Figure 3-27 Scatter plots of the return period between rainfall and streamflow for three headwater basins.

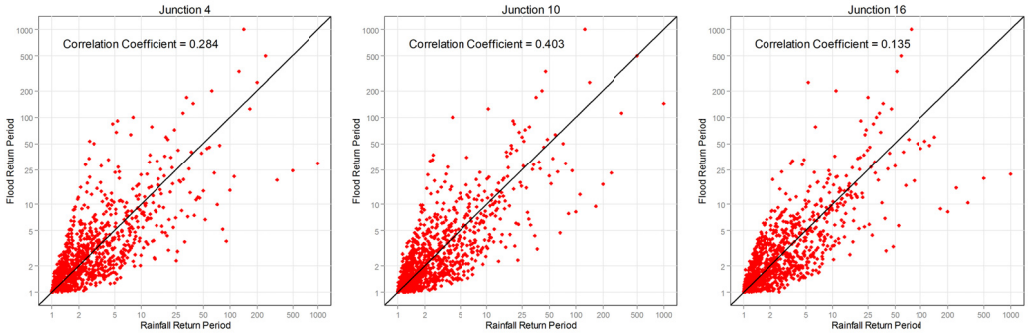

Figure 3-28 Scatter plots of the return period between rainfall and streamflow for three junctions in the midstream location.

Chapter 4

Conclusion and Recommendation for Operational Settings

In this study, stochastic storm transposition (SST) approach was used to perform rainfall and flood frequency analyses. Stochastic transposition of storms consists of transposing extraordinary storm data from one place to another within a meteorologically homogenous region, which also lengthens the data record enabling us to estimate rainfall and floods for higher return periods (beyond 100 years). This study presents a modified version of the SST approach along with the physically based rainfall-runoff model for flood frequency analysis. We improved the storm selection method in the standard SST approach through the deterministic transposition and used combined criteria such as highest MAP values and POE indices.

This is the first study to apply the SST in rainfall and flood frequency analysis for an urbanized watershed in Texas. The Mary's Creek River Basin was selected as the case study. The study was performed based on 10 years of radar-based rainfall (MPE) data obtained from NWS's West Gulf River Forecast Center (WGRFC).

A series of IDF curves were developed using the SST approach and compared against TxDOT/USGS as well as iSWM IDF curves. It was found that the SST-based IDF curves were close to the observed values for /one-hour durations, which implies that the results of the SST approach are reasonable based on our comparison against 10 years of available observed data. The SST approach enabled us to extend the rainfall frequency analysis based on the existing 10-year observed data to 1,000-year return periods without using any statistical extrapolation methods. It was also found that IDF curves from the SST are lower than TxDOT/USGS and iSWM IDF curves for one-hour rainfall durations which may be caused by underestimated MPE data for high intensity rainfall events. The underestimation of MPE is less influential for other rainfall durations (6, 12, and 24 hours). Ideally, there should be a conditional bias adjustment to

MPE data; however, there were no rain gauges available to perform bias adjustment on MPE data. Future research efforts will be invested to address this question. SST-based IDF curves were considerably higher than those of the observed values from 6-, 12- and 24-hour rainfall durations. The SST-based IDF curves agreed the best with those of the TxDOT/USGS and iSWM for 6-hour durations. For 12- and 24-hour rainfall durations, SST IDF curves were lower than TxDOT/USGS and iSWM for low return periods and larger for high return periods.

Only 24-hour rainfall events were used in flood frequency analyses. For the USGS streamflow gauge location, the comparisons were performed against 16 years of observed annual peak flow data as well as design storms developed for this region. For all other junctions, only design storms were used for comparisons. HEC-HMS was used to translate the 24-hour extreme events to hydrographs. Almost the same pattern like rainfall frequency analysis was found for SST-based frequency analysis. It is found that the SST-based flood frequency was overestimating the high frequency events (below five years) and slightly underestimating the low frequency events (above five years). This study proves the SST approach to be a promising capability for extending the frequency analysis from 10 years of data to more than 100 years.

In addition, the relationships between rainfall and flood return periods were investigated, and it was found that there is no one-to-one relationship between rainfall and flood return periods as typically used by practitioners for traditional frequency approaches. The results agreed with the study conducted by Wright et al. (2014).

In addition to all the findings, we have several recommendations for future studies as summarized below:

The coarse temporal and spatial resolution of the radar rainfall used in this research caused many challenges to this study. Using a higher resolution will improve the quality of the study in many aspects. Conditional bias adjustment of radar-based rainfall using rain gauge data will certainly improve the SST results particularly for one-hour rainfall durations.

The current SST method uses a uniform distribution to transpose the storms within the homogeneity zone. This can result in many unsuccessful transposition trials in which extreme events do not fall over a watershed of interest. In this study, a relatively smaller homogeneity zone was used to overcome this problem; however, this remedy reduced the number of extreme events needed to form a storm catalogue during the SST procedure. We believe that a multivariate PDF function is needed to take into account the depth and the location of the storm in the homogeneity zone.

Appendix A

Annual Maximum MAP for 54 subbasins

Table A.1. Annual maximum MAP values over each subbasin in Mary's Creek River Basin based on 10 years of radar data without any transposition.

		YEAR																			
		2005		2006		2007		2008		2009		2010		2011		2012		2013		2014	
SUB NO	duration	Max MAP	date	Max MAP	date	Max MAP	date	Max MAP	date	Max MAP	date	Max MAP	date	Max MAP	date	Max MAP	date	Max MAP	date	Max MAP	date
1	1	0.45	6/1/2005 6:00	0.72	11/6/2006 6:00	0.95	9/10/2007 16:00	1.35	8/18/2008 16:00	1.06	5/27/2009 00:00	1.11	9/2/2010 9:00	1.12	10/9/2011 5:00	0.73	3/19/2012 23:00	0.94	11/22/2013 2:00	1.13	5/12/2014 20:00
	6	0.71	6/1/2005 8:00	2.05	11/6/2006 10:00	2.12	4/25/2007	2.59	8/18/2008 19:00	1.72	10/9/2009 11:00	1.92	9/8/2010 10:00	3.37	10/9/2011 8:00	1.48	8/19/2012 2:00	1.32	1/9/2013 7:00	1.56	6/22/2014 16:00
	12	0.82	3/26/2005 21:00	2.06	11/6/2006 10:00	2.71	4/25/2007 3:00	2.78	8/18/2008 22:00	1.86	10/9/2009 14:00	2.36	9/8/2010 14:00	4.23	10/9/2011 11:00	2.44	3/20/2012 10:00	1.82	1/9/2013 13:00	1.96	6/22/2014 20:00
	24	0.97	3/27/2005 10:00	2.22	2/25/2006 21:00	2.71	4/25/2007 3:00	2.78	8/19/2008 9:00	2.96	10/22/2009 10:00	3.62	9/8/2010 12:00	5.09	10/9/2011 17:00	2.98	3/20/2012 14:00	2.37	1/9/2013 18:00	1.98	6/23/2014 12:00
2	1	0.69	7/15/2005	0.76	11/6/2006 6:00	0.99	3/31/2007 1:00	1.30	6/19/2008 13:00	0.83	6/3/2009 6:00	1.08	9/2/2010 9:00	0.97	10/9/2011 6:00	0.67	3/19/2012 23:00	0.77	11/22/2013 2:00	1.08	5/12/2014 20:00
	6	0.69	7/15/2005	2.12	11/6/2006 10:00	1.82	4/24/2007 23:00	1.99	8/18/2008 19:00	1.82	10/9/2009 11:00	1.88	9/8/2010 10:00	3.24	10/9/2011 8:00	1.43	8/19/2012 2:00	1.26	1/9/2013 7:00	1.62	6/22/2014 18:00
	12	0.78	3/26/2005 21:00	2.13	11/6/2006 10:00	2.16	4/25/2007 3:00	2.76	11/11/2008 10:00	1.98	10/9/2009 14:00	2.42	9/8/2010 14:00	4.09	10/9/2011 11:00	2.46	3/20/2012 10:00	1.73	1/9/2013 13:00	2.05	6/22/2014 20:00
	24	0.97	3/27/2005 11:00	2.16	2/25/2006 21:00	2.51	6/27/2007 12:00	2.82	11/11/2008 12:00	2.95	10/22/2009 10:00	3.66	9/8/2010 12:00	4.96	10/9/2011 17:00	2.97	3/20/2012 14:00	2.22	1/9/2013 18:00	2.05	6/23/2014 12:00
3	1	0.63	7/15/2005	0.73	5/5/2006 8:00	1.05	3/31/2007 1:00	1.34	6/19/2008 13:00	0.98	5/27/2009	0.96	9/2/2010 9:00	0.93	10/9/2011 6:00	0.76	7/21/2012	0.75	11/22/2013 2:00	1.01	5/12/2014 20:00
	6	0.68	6/1/2005 8:00	1.98	11/6/2006 10:00	1.82	3/31/2007 4:00	2.36	8/18/2008 19:00	1.76	10/9/2009 11:00	1.93	9/8/2010 10:00	3.02	10/9/2011 8:00	1.26	3/20/2012 4:00	1.32	1/9/2013 7:00	1.53	10/13/2014 11:00
	12	0.76	3/26/2005 21:00	2.00	11/6/2006 11:00	2.27	4/25/2007 3:00	2.77	11/11/2008 10:00	1.92	10/9/2009 14:00	2.56	9/8/2010 14:00	3.86	10/9/2011 11:00	2.44	3/20/2012 10:00	1.82	1/9/2013 13:00	1.87	6/22/2014 20:00
	24	0.98	3/27/2005 11:00	2.36	2/25/2006 21:00	2.54	6/27/2007 12:00	2.83	11/11/2008 12:00	2.98	10/22/2009 10:00	3.79	9/8/2010 12:00	4.81	10/9/2011 17:00	2.95	3/20/2012 14:00	2.36	1/9/2013 18:00	1.91	6/23/2014 12:00
4	1	0.63	7/15/2005	0.87	5/5/2006 8:00	1.19	3/31/2007 1:00	1.38	6/19/2008 13:00	1.01	6/3/2009 6:00	0.94	6/29/2010	0.88	10/9/2011 6:00	1.10	6/6/2012 20:00	0.63	2/10/2013 9:00	0.92	5/12/2014 20:00
	6	0.66	6/1/2005 8:00	2.09	11/6/2006 10:00	1.91	3/31/2007 4:00	2.30	11/11/2008 4:00	1.72	10/9/2009 11:00	1.91	9/8/2010 10:00	2.84	10/9/2011 8:00	1.28	3/20/2012 11:00	1.34	1/9/2013 7:00	1.58	10/13/2014 11:00
	12	0.77	3/26/2005 21:00	2.11	11/6/2006 11:00	2.28	6/27/2007 9:00	3.07	11/11/2008 10:00	1.90	10/9/2009 14:00	2.60	9/8/2010 14:00	3.65	10/9/2011 11:00	2.39	3/20/2012 10:00	1.83	1/9/2013 11:00	1.91	6/22/2014 20:00
	24	0.98	3/27/2005 11:00	2.34	2/25/2006 21:00	2.69	6/27/2007 21:00	3.13	11/11/2008 12:00	3.06	10/22/2009 10:00	3.82	9/8/2010 12:00	4.60	10/9/2011 17:00	2.89	3/20/2012 14:00	2.34	1/9/2013 18:00	1.92	6/23/2014 12:00
5	1	0.40	7/15/2005	1.02	5/5/2006 8:00	1.43	3/31/2007 1:00	1.38	6/19/2008 13:00	1.19	6/3/2009 6:00	0.75	5/14/2010 18:00	0.90	5/23/2011 16:00	1.72	6/6/2012 20:00	0.64	2/10/2013 9:00	0.95	6/24/2014 22:00
	6	0.64	6/1/2005 8:00	2.13	11/6/2006 10:00	2.10	3/31/2007 4:00	2.68	11/11/2008 5:00	1.59	10/9/2009 11:00	1.93	9/8/2010 10:00	2.51	10/9/2011 8:00	1.92	6/7/2012 1:00	1.45	1/9/2013 7:00	1.67	10/13/2014 11:00
	12	0.77	3/26/2005 21:00	2.17	11/6/2006 11:00	2.50	6/27/2007 9:00	3.42	11/11/2008 10:00	1.96	10/22/2009 9:00	2.75	9/8/2010 14:00	3.29	10/9/2011 11:00	2.31	3/20/2012 10:00	1.96	1/9/2013 11:00	1.86	6/22/2014 20:00
	24	1.00	3/27/2005 11:00	2.53	2/25/2006 21:00	2.95	6/27/2007 21:00	3.47	11/11/2008 12:00	3.22	10/22/2009 10:00	3.97	9/8/2010 12:00	4.31	10/9/2011 17:00	2.82	3/20/2012 14:00	2.51	1/9/2013 23:00	1.87	6/23/2014 12:00
6	1	0.68	7/15/2005	0.79	11/6/2006 6:00	1.08	3/31/2007 1:00	1.42	6/19/2008 13:00	0.78	9/12/2009 2:00	1.05	9/2/2010 9:00	0.94	10/9/2011 6:00	0.69	3/19/2012 23:00	0.71	11/22/2013 2:00	1.07	5/12/2014 20:00
	6	0.68	7/15/2005	2.16	11/6/2006 10:00	1.87	3/31/2007 4:00	2.07	11/11/2008 4:00	1.78	10/9/2009 11:00	1.88	9/8/2010 10:00	3.15	10/9/2011 8:00	1.50	8/19/2012 2:00	1.35	1/9/2013 7:00	1.70	6/22/2014 18:00
	12	0.77	3/26/2005 21:00	2.18	11/6/2006 11:00	2.18	6/27/2007 9:00	2.81	11/11/2008 10:00	1.95	10/9/2009 14:00	2.42	9/8/2010 14:00	4.03	10/9/2011 11:00	2.51	3/20/2012 10:00	1.83	1/9/2013 11:00	2.16	6/22/2014 20:00
	24	0.98	3/27/2005 11:00	2.20	2/25/2006 21:00	2.57	5/26/2007 22:00	2.87	11/11/2008 14:00	2.96	10/22/2009 10:00	3.70	9/8/2010 12:00	4.93	10/9/2011 17:00	3.02	3/20/2012 14:00	2.34	1/9/2013 18:00	2.20	6/23/2014 12:00
7	1	0.67	7/15/2005	0.85	11/6/2006 6:00	1.37	3/31/2007 1:00	1.77	6/19/2008 13:00	1.18	9/22/2009 1:00	0.97	9/2/2010 9:00	1.05	5/23/2011 16:00	1.14	6/6/2012 20:00	0.67	2/10/2013 9:00	1.02	5/12/2014 20:00
	6	0.67	7/15/2005	2.24	11/6/2006 10:00	2.18	7/24/2007 2:00	2.39	11/11/2008 3:00	1.70	9/12/2009 6:00	1.89	9/8/2010 10:00	2.92	10/9/2011 7:00	1.68	8/19/2012 2:00	1.62	1/9/2013 7:00	2.04	6/22/2014 19:00
	12	0.75	3/26/2005 21:00	2.28	11/6/2006 11:00	2.36	6/27/2007 9:00	2.91	11/11/2008 10:00	1.88	9/12/2009 12:00	2.44	9/8/2010 14:00	3.80	10/9/2011 11:00	2.67	3/20/2012 10:00	2.20	1/9/2013 11:00	2.47	6/22/2014 20:00

	24	1.01	3/27/2005 11:00	2.34	2/25/2006 21:00	2.76	5/26/2007 22:00	2.98	11/11/2008 14:00	3.03	10/22/2009 10:00	3.86	9/8/2010 12:00	4.80	10/9/2011 17:00	3.17	3/20/2012 14:00	2.71	1/9/2013 23:00	2.61	6/23/2014 12:00
8	1	0.52	7/15/2005	0.90	11/6/2006 6:00	1.43	3/31/2007 1:00	1.45	6/19/2008 13:00	1.43	9/22/2009 1:00	0.78	5/14/2010 18:00	1.06	5/23/2011 16:00	1.52	6/6/2012 20:00	0.72	2/10/2013 9:00	0.87	5/12/2014 20:00
	6	0.61	6/1/2005 8:00	2.40	11/6/2006 10:00	2.07	3/31/2007 4:00	3.14	11/11/2008 4:00	1.79	9/12/2009 6:00	1.93	9/8/2010 10:00	2.75	10/9/2011 8:00	1.69	6/7/2012 1:00	1.53	1/9/2013 7:00	1.95	6/22/2014 19:00
	12	0.76	3/26/2005 21:00	2.44	11/6/2006 11:00	2.55	6/27/2007 9:00	3.56	11/11/2008 10:00	1.98	9/12/2009 12:00	2.63	9/8/2010 14:00	3.57	10/9/2011 11:00	2.42	3/20/2012 10:00	2.06	1/9/2013 11:00	2.40	6/22/2014 20:00
	24	1.05	3/27/2005	2.56	2/25/2006	2.89	6/27/2007	3.63	11/11/2008	3.14	10/22/2009	4.01	9/8/2010	4.67	10/9/2011	2.92	3/20/2012	2.55	1/9/2013	2.54	6/23/2014

			11:00		21:00		21:00		14:00		10:00		12:00		17:00		14:00		23:00		12:00	
9	1	0.40	7/15/2005	1.00	5/5/2006 8:00	1.46	6/30/2007 7:00	1.35	6/19/2008 13:00	1.20	6/3/2009 6:00	0.76	5/14/2010 18:00	0.97	5/23/2011 16:00	1.76	6/6/2012 20:00	0.68	2/10/2013 9:00	0.79	5/12/2014 20:00	
	6	0.63	6/1/2005 8:00	2.27	11/6/2006 10:00	2.11	3/31/2007 4:00	3.05	11/11/2008 5:00	1.61	9/12/2009 6:00	1.94	9/8/2010 10:00	2.58	10/9/2011 8:00	1.96	6/7/2012 1:00	1.47	1/9/2013 7:00	1.68	10/13/2014 11:00	
	12	0.77	3/26/2005 21:00	2.31	11/6/2006 11:00	2.57	6/27/2007 9:00	3.63	11/11/2008 10:00	1.97	10/22/2009 9:00	2.75	9/8/2010 14:00	3.33	10/9/2011 11:00	2.30	3/20/2012 10:00	1.98	1/9/2013 11:00	2.06	6/22/2014 20:00	
	24	1.03	3/27/2005 11:00	2.60	2/25/2006 21:00	2.99	6/27/2007 21:00	3.70	11/11/2008 12:00	3.22	10/22/2009 10:00	4.03	9/8/2010 12:00	4.41	10/9/2011 17:00	2.81	3/20/2012 14:00	2.51	1/9/2013 23:00	2.12	6/23/2014 12:00	
10	1	0.49	7/15/2005	0.92	11/6/2006 6:00	1.45	3/31/2007 1:00	1.40	6/19/2008 13:00	1.52	9/22/2009 1:00	0.78	5/14/2010 18:00	1.08	5/23/2011 16:00	1.61	6/6/2012 20:00	0.73	2/10/2013 9:00	0.84	5/12/2014 20:00	
	6	0.62	3/27/2005 14:00	2.45	11/6/2006 10:00	2.08	3/31/2007 4:00	3.32	11/11/2008 4:00	1.83	9/12/2009 6:00	1.93	9/8/2010 10:00	2.74	10/9/2011 8:00	1.78	6/7/2012 1:00	1.53	1/9/2013 7:00	1.97	6/22/2014 19:00	
	12	0.76	3/26/2005 21:00	2.49	11/6/2006 11:00	2.59	6/27/2007 9:00	3.70	11/11/2008 10:00	2.01	9/12/2009 12:00	2.66	9/8/2010 14:00	3.53	10/9/2011 11:00	2.38	3/20/2012 10:00	2.04	1/9/2013 11:00	2.42	6/22/2014 20:00	
	24	1.06	3/27/2005 11:00	2.61	2/25/2006 21:00	2.93	6/27/2007 21:00	3.77	11/11/2008 14:00	3.16	10/22/2009 10:00	4.04	9/8/2010 12:00	4.66	10/9/2011 17:00	2.88	3/20/2012 14:00	2.58	9/21/2013	2.57	6/23/2014 13:00	
11	1	0.75	8/16/2005 1:00	0.96	11/6/2006 6:00	1.63	6/30/2007 7:00	1.77	11/11/2008 3:00	1.48	9/22/2009 1:00	0.73	5/14/2010 18:00	1.02	5/23/2011 16:00	1.52	6/6/2012 20:00	0.72	2/10/2013 9:00	0.66	6/22/2014 15:00	
	6	0.90	8/16/2005 3:00	2.47	11/6/2006 10:00	2.12	6/30/2007 9:00	3.62	11/11/2008 5:00	1.96	9/12/2009 6:00	1.98	9/8/2010 11:00	2.58	10/9/2011 8:00	1.78	6/7/2012 1:00	1.45	1/9/2013 7:00	1.67	6/22/2014 19:00	
	12	0.91	8/16/2005 10:00	2.52	11/6/2006 11:00	2.53	6/27/2007 9:00	4.01	11/11/2008 10:00	2.16	9/12/2009 12:00	3.06	9/8/2010 14:00	3.34	10/9/2011 14:00	2.29	3/20/2012 10:00	1.94	1/9/2013 11:00	2.10	6/22/2014 20:00	
	24	1.09	3/27/2005 11:00	2.95	2/25/2006 21:00	2.85	6/27/2007 21:00	4.09	11/11/2008 13:00	3.30	10/22/2009 10:00	4.19	9/8/2010 12:00	4.37	10/9/2011 17:00	2.81	3/20/2012 14:00	2.59	9/21/2013	2.28	6/23/2014 12:00	
12	1	0.75	8/16/2005 1:00	0.93	5/5/2006 8:00	1.74	6/30/2007 7:00	1.96	11/11/2008 3:00	1.40	9/22/2009 1:00	0.78	9/8/2010 11:00	1.01	5/23/2011 16:00	1.37	6/6/2012 20:00	0.70	2/10/2013 9:00	0.83	9/6/2014 22:00	
	6	0.97	8/16/2005 3:00	2.35	11/6/2006 10:00	2.45	6/30/2007 9:00	3.70	11/11/2008 5:00	1.86	9/12/2009 6:00	2.11	9/8/2010 11:00	2.39	10/9/2011 8:00	1.67	6/7/2012 1:00	1.45	1/9/2013 7:00	1.71	10/13/2014 11:00	
	12	0.97	8/16/2005 10:00	2.43	11/6/2006 11:00	2.55	6/30/2007 9:00	4.15	11/11/2008 10:00	2.09	9/12/2009 12:00	3.24	9/8/2010 14:00	3.16	10/9/2011 14:00	2.30	3/20/2012 10:00	1.99	1/9/2013 11:00	1.89	6/22/2014 20:00	
	24	1.06	3/27/2005 11:00	3.04	2/25/2006 21:00	2.92	6/27/2007 12:00	4.24	11/11/2008 13:00	3.38	10/22/2009 10:00	4.29	9/8/2010 12:00	4.16	10/9/2011 17:00	2.82	3/20/2012 14:00	2.57	9/21/2013 1:00	2.07	6/23/2014 12:00	
13	1	1.02	8/16/2005 1:00	1.01	11/6/2006 6:00	1.68	6/30/2007 7:00	2.08	11/11/2008 3:00	1.54	9/22/2009 1:00	0.83	6/28/2010 23:00	1.01	5/23/2011 16:00	1.36	6/6/2012 20:00	0.72	2/10/2013 9:00	0.94	9/6/2014 22:00	
	6	1.22	8/16/2005 3:00	2.53	11/6/2006 10:00	2.32	6/30/2007 9:00	3.80	11/11/2008 5:00	2.13	9/12/2009 6:00	2.11	9/8/2010 11:00	2.55	10/9/2011 8:00	1.66	6/7/2012 1:00	1.42	1/9/2013 7:00	1.64	10/13/2014 11:00	
	12	1.23	8/16/2005 10:00	2.58	11/6/2006 11:00	2.46	6/27/2007 9:00	4.13	11/11/2008 11:00	2.33	9/12/2009 12:00	3.27	9/8/2010 14:00	3.32	10/9/2011 14:00	2.30	3/20/2012 10:00	1.91	1/9/2013 11:00	2.02	6/22/2014 20:00	
	24	1.23	8/16/2005 10:00	3.15	2/25/2006 21:00	2.79	6/27/2007 12:00	4.22	11/11/2008 13:00	3.35	10/22/2009 10:00	4.26	9/8/2010 14:00	4.29	10/9/2011 17:00	2.81	3/20/2012 14:00	2.60	9/21/2013 1:00	2.24	6/23/2014 12:00	
14	1	0.40	4/11/2005	1.01	11/6/2006 6:00	1.46	3/29/2007 23:00	1.28	11/11/2008 3:00	1.50	9/22/2009 1:00	0.79	9/7/2010 21:00	1.00	5/23/2011 16:00	1.31	6/6/2012 20:00	0.80	5/16/2013 2:00	0.85	5/12/2014 20:00	
	6	0.65	3/27/2005 14:00	2.66	11/6/2006 11:00	2.08	3/31/2007 4:00	3.28	11/11/2008 4:00	1.80	9/12/2009 6:00	1.92	9/8/2010 10:00	2.84	10/9/2011 7:00	1.49	6/7/2012 1:00	1.60	1/9/2013 7:00	2.06	6/22/2014 19:00	
	12	0.78	3/26/2005 21:00	2.72	11/6/2006 11:00	2.45	6/27/2007 9:00	3.60	11/11/2008 10:00	1.98	9/12/2009 12:00	2.65	9/8/2010 14:00	3.65	10/9/2011 11:00	2.42	3/20/2012 10:00	2.16	1/9/2013 11:00	2.49	6/22/2014 20:00	
	24	1.12	3/27/2005 11:00	2.96	2/25/2006 21:00	2.76	6/27/2007 21:00	3.68	11/11/2008 14:00	3.16	10/22/2009 10:00	4.13	9/8/2010 11:00	4.77	10/9/2011 17:00	2.94	3/20/2012 14:00	2.67	1/9/2013 23:00	2.67	6/23/2014 12:00	
15	1	0.43	5/14/2005 7:00	1.12	11/6/2006 6:00	1.65	3/29/2007 23:00	1.59	11/11/2008 3:00	1.55	9/22/2009 1:00	0.96	6/28/2010 23:00	0.94	10/9/2011 6:00	1.19	6/6/2012 20:00	1.10	5/16/2013 2:00	0.78	5/12/2014 20:00	
	6	0.71	3/27/2005 14:00	2.90	11/6/2006 11:00	2.05	6/27/2007 2:00	3.45	11/11/2008 5:00	1.81	9/12/2009 6:00	1.97	9/8/2010 10:00	2.82	10/9/2011 7:00	1.42	6/7/2012 1:00	1.59	1/9/2013 7:00	2.06	6/22/2014 19:00	
	12	0.80	3/26/2005 21:00	2.94	11/6/2006 11:00	2.44	6/27/2007 9:00	3.71	11/11/2008 10:00	2.00	9/12/2009 12:00	2.82	9/8/2010 14:00	3.61	10/9/2011 12:00	2.38	3/20/2012 10:00	2.18	1/9/2013 11:00	2.48	6/22/2014 20:00	
	24	1.19	3/27/2005 11:00	3.44	2/25/2006 21:00	2.71	6/27/2007 21:00	3.80	11/11/2008 13:00	3.29	10/22/2009 10:00	4.36	9/8/2010 11:00	4.75	10/9/2011 17:00	2.91	3/20/2012 14:00	2.82	9/21/2013	2.67	6/23/2014 12:00	
16	1	0.75	8/16/2005 1:00	1.00	11/6/2006 6:00	1.31	3/31/2007 1:00	2.21	11/11/2008 3:00	1.26	9/22/2009 1:00	1.02	6/28/2010 23:00	0.98	4/11/2011 7:00	1.10	6/6/2012 20:00	0.94	5/16/2013 2:00	0.74	9/6/2014 22:00	
	6	0.87	8/16/2005 3:00	2.66	11/6/2006 11:00	2.00	6/27/2007 2:00	4.04	11/11/2008 5:00	2.08	9/12/2009 6:00	2.04	9/8/2010 11:00	2.51	10/9/2011 8:00	1.46	6/7/2012 1:00	1.42	1/9/2013 7:00	1.67	6/22/2014 19:00	
	12	0.87	8/16/2005 10:00	2.89	2/25/2006 13:00	2.40	6/27/2007 9:00	4.29	11/11/2008 12:00	2.28	9/12/2009 12:00	3.27	9/8/2010 14:00	3.32	10/9/2011 14:00	2.34	3/20/2012 11:00	1.96	9/20/2013 12:00	2.08	6/22/2014 20:00	
	24	1.16	3/27/2005 11:00	3.55	2/25/2006 21:00	2.67	6/27/2007 21:00	4.36	11/11/2008 13:00	3.41	10/22/2009 10:00	4.49	9/8/2010 11:00	4.25	10/9/2011 17:00	2.82	3/20/2012 14:00	2.75	9/21/2013	2.28	6/23/2014 12:00	

17	1	0.96	8/16/2005 1:00	0.97	11/6/2006 6:00	1.29	3/31/2007 1:00	2.00	11/11/2008 3:00	1.21	9/22/2009 1:00	0.81	9/8/2010 11:00	0.90	4/11/2011 7:00	0.95	6/6/2012 20:00	0.68	11/22/2013 3:00	0.85	9/6/2014 22:00
	6	1.15	8/16/2005 3:00	2.57	11/6/2006 11:00	2.04	6/27/2007 2:00	3.84	11/11/2008 6:00	2.23	9/12/2009 6:00	2.09	9/8/2010 11:00	2.33	10/9/2011 8:00	1.44	6/7/2012 1:00	1.41	1/9/2013 7:00	1.55	10/13/2014 11:00
	12	1.17	8/16/2005 10:00	2.69	2/25/2006 13:00	2.47	6/27/2007 9:00	4.17	11/11/2008 12:00	2.44	9/12/2009 12:00	3.38	9/8/2010 14:00	3.13	10/9/2011 14:00	2.37	3/20/2012 11:00	1.95	9/20/2013 13:00	1.83	6/22/2014 20:00
	24	1.17	8/16/2005 10:00	3.47	2/25/2006 21:00	2.80	6/27/2007 21:00	4.21	11/11/2008 13:00	3.48	10/22/2009 10:00	4.52	9/8/2010 14:00	4.06	10/9/2011 17:00	2.83	3/20/2012 14:00	2.67	9/21/2013	2.07	6/23/2014 12:00
18	1	1.01	8/16/2005 1:00	1.00	11/6/2006 6:00	1.66	6/30/2007 7:00	2.07	11/11/2008 3:00	1.52	9/22/2009 1:00	0.82	6/28/2010 23:00	1.01	5/23/2011 16:00	1.35	6/6/2012 20:00	0.72	2/10/2013 9:00	0.93	9/6/2014 22:00
	6	1.20	8/16/2005 3:00	2.51	11/6/2006 10:00	2.31	6/30/2007 9:00	3.79	11/11/2008 5:00	2.11	9/12/2009 6:00	2.11	9/8/2010 11:00	2.53	10/9/2011 8:00	1.65	6/7/2012 1:00	1.42	1/9/2013 7:00	1.65	10/13/2014 11:00
	12	1.22	8/16/2005 10:00	2.57	11/6/2006 11:00	2.47	6/27/2007 9:00	4.13	11/11/2008 11:00	2.32	9/12/2009 12:00	3.27	9/8/2010 14:00	3.30	10/9/2011 14:00	2.30	3/20/2012 10:00	1.91	1/9/2013 11:00	2.00	6/22/2014 20:00
	24	1.22	8/16/2005 10:00	3.15	2/25/2006 21:00	2.80	6/27/2007 12:00	4.22	11/11/2008 13:00	3.35	10/22/2009 10:00	4.27	9/8/2010 14:00	4.27	10/9/2011 17:00	2.81	3/20/2012 14:00	2.60	9/21/2013 1:00	2.22	6/23/2014 12:00
19	1	1.12	8/16/2005 1:00	0.98	11/6/2006 6:00	1.25	3/31/2007 1:00	1.97	11/11/2008 3:00	1.38	9/22/2009 1:00	0.82	9/8/2010 11:00	0.95	5/23/2011 16:00	1.10	6/6/2012 20:00	0.70	2/10/2013 9:00	0.92	9/6/2014 22:00
	6	1.34	8/16/2005 3:00	2.51	11/6/2006 11:00	2.02	6/27/2007 2:00	3.75	11/11/2008 6:00	2.25	9/12/2009 6:00	2.11	9/8/2010 11:00	2.38	10/9/2011 8:00	1.50	6/7/2012 1:00	1.41	1/9/2013 7:00	1.60	10/13/2014 11:00
	12	1.36	8/16/2005 10:00	2.56	11/6/2006 11:00	2.50	6/27/2007 9:00	4.12	11/11/2008 12:00	2.46	9/12/2009 12:00	3.33	9/8/2010 14:00	3.16	10/9/2011 14:00	2.32	3/20/2012 11:00	1.89	1/9/2013 11:00	1.83	6/22/2014 20:00
	24	1.36	8/16/2005 10:00	3.26	2/25/2006 21:00	2.83	6/27/2007 12:00	4.19	11/11/2008 13:00	3.45	10/22/2009 10:00	4.38	9/8/2010 14:00	4.11	10/9/2011 17:00	2.82	3/20/2012 14:00	2.59	9/21/2013 1:00	2.09	6/23/2014 12:00
20	1	1.25	8/16/2005 1:00	0.93	11/6/2006 6:00	1.33	3/31/2007 1:00	1.81	11/11/2008 3:00	1.14	9/22/2009 1:00	0.86	9/8/2010 11:00	0.85	5/23/2011 16:00	0.77	10/14/2012 7:00	0.68	11/22/2013 3:00	0.90	9/6/2014 22:00
	6	1.53	8/16/2005 3:00	2.48	11/6/2006 11:00	2.09	6/27/2007 2:00	3.70	11/11/2008 6:00	2.43	9/12/2009 6:00	2.10	9/8/2010 11:00	2.12	10/9/2011 8:00	1.30	3/20/2012 11:00	1.40	1/9/2013 7:00	1.53	10/13/2014 11:00
	12	1.57	8/16/2005 10:00	2.52	11/6/2006 11:00	2.56	6/27/2007 9:00	4.10	11/11/2008 12:00	2.64	9/12/2009 12:00	3.43	9/8/2010 14:00	2.91	10/9/2011 14:00	2.40	3/20/2012 11:00	1.94	9/20/2013 13:00	1.54	10/13/2014 13:00
	24	1.57	8/16/2005 10:00	3.41	2/25/2006 21:00	2.97	6/27/2007 21:00	4.13	11/11/2008 13:00	3.60	10/22/2009 10:00	4.57	9/8/2010 14:00	3.82	10/9/2011 17:00	2.84	3/20/2012 14:00	2.58	9/21/2013 1:00	1.84	6/23/2014 12:00
21	1	1.25	8/16/2005 1:00	0.93	11/6/2006 6:00	1.33	3/31/2007 1:00	1.81	11/11/2008 3:00	1.14	9/22/2009 1:00	0.86	9/8/2010 11:00	0.85	5/23/2011 16:00	0.77	10/14/2012 7:00	0.68	11/22/2013 3:00	0.90	9/6/2014 22:00
	6	1.53	8/16/2005 3:00	2.48	11/6/2006 11:00	2.09	6/27/2007 2:00	3.70	11/11/2008 6:00	2.43	9/12/2009 6:00	2.10	9/8/2010 11:00	2.12	10/9/2011 8:00	1.30	3/20/2012 11:00	1.40	1/9/2013 7:00	1.53	10/13/2014 11:00
	12	1.57	8/16/2005 10:00	2.52	11/6/2006 11:00	2.56	6/27/2007 9:00	4.10	11/11/2008 12:00	2.64	9/12/2009 12:00	3.43	9/8/2010 14:00	2.91	10/9/2011 14:00	2.40	3/20/2012 11:00	1.94	9/20/2013 13:00	1.54	10/13/2014 13:00
	24	1.57	8/16/2005 10:00	3.41	2/25/2006 21:00	2.97	6/27/2007 21:00	4.13	11/11/2008 13:00	3.60	10/22/2009 10:00	4.57	9/8/2010 14:00	3.82	10/9/2011 17:00	2.84	3/20/2012 14:00	2.58	9/21/2013 1:00	1.84	6/23/2014 12:00
22	1	1.22	8/16/2005 1:00	0.93	11/6/2006 6:00	1.32	3/31/2007 1:00	1.79	11/11/2008 3:00	1.12	9/22/2009 1:00	0.86	9/8/2010 11:00	0.85	5/23/2011 16:00	0.76	10/14/2012 7:00	0.69	11/22/2013 3:00	0.90	9/6/2014 22:00
	6	1.50	8/16/2005 3:00	2.48	11/6/2006 11:00	2.09	6/27/2007 2:00	3.68	11/11/2008 6:00	2.42	9/12/2009 6:00	2.11	9/8/2010 11:00	2.12	10/9/2011 8:00	1.30	3/20/2012 11:00	1.41	1/9/2013 7:00	1.52	10/13/2014 11:00
	12	1.53	8/16/2005 10:00	2.52	11/6/2006 11:00	2.55	6/27/2007 9:00	4.08	11/11/2008 12:00	2.63	9/12/2009 12:00	3.44	9/8/2010 14:00	2.91	10/9/2011 14:00	2.40	3/20/2012 11:00	1.95	9/20/2013 13:00	1.54	6/22/2014 20:00
	24	1.53	8/16/2005 10:00	3.42	2/25/2006 21:00	2.96	6/27/2007 21:00	4.11	11/11/2008 13:00	3.59	10/22/2009 10:00	4.58	9/8/2010 14:00	3.82	10/9/2011 17:00	2.84	3/20/2012 14:00	2.59	9/21/2013 1:00	1.84	6/23/2014 12:00
23	1	1.25	8/16/2005 1:00	0.93	11/6/2006 6:00	1.33	3/31/2007 1:00	1.81	11/11/2008 3:00	1.14	9/22/2009 1:00	0.86	9/8/2010 11:00	0.85	5/23/2011 16:00	0.77	10/14/2012 7:00	0.68	11/22/2013 3:00	0.90	9/6/2014 22:00
	6	1.53	8/16/2005 3:00	2.48	11/6/2006 11:00	2.09	6/27/2007 2:00	3.70	11/11/2008 6:00	2.43	9/12/2009 6:00	2.10	9/8/2010 11:00	2.12	10/9/2011 8:00	1.30	3/20/2012 11:00	1.40	1/9/2013 7:00	1.53	10/13/2014 11:00
	12	1.57	8/16/2005 10:00	2.52	11/6/2006 11:00	2.56	6/27/2007 9:00	4.10	11/11/2008 12:00	2.64	9/12/2009 12:00	3.43	9/8/2010 14:00	2.91	10/9/2011 14:00	2.40	3/20/2012 11:00	1.94	9/20/2013 13:00	1.54	10/13/2014 13:00
	24	1.57	8/16/2005 10:00	3.41	2/25/2006 21:00	2.97	6/27/2007 21:00	4.13	11/11/2008 13:00	3.60	10/22/2009 10:00	4.57	9/8/2010 14:00	3.82	10/9/2011 17:00	2.84	3/20/2012 14:00	2.58	9/21/2013 1:00	1.84	6/23/2014 12:00
24	1	1.24	8/16/2005 1:00	0.93	11/6/2006 6:00	1.32	3/31/2007 1:00	1.82	11/11/2008 3:00	1.15	9/22/2009 1:00	0.85	9/8/2010 11:00	0.86	5/23/2011 16:00	0.76	10/14/2012 7:00	0.68	11/22/2013 3:00	0.91	9/6/2014 22:00
	6	1.52	8/16/2005 3:00	2.48	11/6/2006 11:00	2.08	6/27/2007 2:00	3.70	11/11/2008 6:00	2.41	9/12/2009 6:00	2.11	9/8/2010 11:00	2.14	10/9/2011 8:00	1.30	3/20/2012 11:00	1.40	1/9/2013 7:00	1.53	10/13/2014 11:00
	12	1.55	8/16/2005 10:00	2.52	11/6/2006 11:00	2.56	6/27/2007 9:00	4.10	11/11/2008 12:00	2.63	9/12/2009 12:00	3.42	9/8/2010 14:00	2.93	10/9/2011 14:00	2.39	3/20/2012 11:00	1.93	9/20/2013 13:00	1.56	6/22/2014 20:00
	24	1.55	8/16/2005 10:00	3.40	2/25/2006 21:00	2.96	6/27/2007 21:00	4.13	11/11/2008 13:00	3.59	10/22/2009 10:00	4.55	9/8/2010 14:00	3.84	10/9/2011 17:00	2.84	3/20/2012 14:00	2.58	9/21/2013 1:00	1.86	6/23/2014 12:00
25	1	1.20	8/16/2005 1:00	0.92	11/6/2006 6:00	1.32	3/31/2007 1:00	1.78	11/11/2008 3:00	1.12	9/22/2009 1:00	0.86	9/8/2010 11:00	0.85	5/23/2011 16:00	0.76	10/14/2012 7:00	0.69	11/22/2013 3:00	0.90	9/6/2014 22:00

	6	1.47	8/16/2005 3:00	2.48	11/6/2006 11:00	2.09	6/27/2007 2:00	3.68	11/11/2008 6:00	2.41	9/12/2009 6:00	2.11	9/8/2010 11:00	2.12	10/9/2011 8:00	1.30	6/7/2012 1:00	1.41	1/9/2013 7:00	1.52	10/13/2014 11:00
	12	1.50	8/16/2005 10:00	2.52	11/6/2006 11:00	2.55	6/27/2007 9:00	4.07	11/11/2008 12:00	2.62	9/12/2009 12:00	3.45	9/8/2010 14:00	2.91	10/9/2011 14:00	2.40	3/20/2012 11:00	1.95	9/20/2013 13:00	1.54	6/22/2014 20:00
	24	1.50	8/16/2005 10:00	3.42	2/25/2006 21:00	2.96	6/27/2007 21:00	4.10	11/11/2008 13:00	3.59	10/22/2009 10:00	4.58	9/8/2010 14:00	3.82	10/9/2011 17:00	2.83	3/20/2012 14:00	2.60	9/21/2013 1:00	1.84	6/23/2014 12:00
26	1	1.25	8/16/2005 1:00	0.93	11/6/2006 6:00	1.33	3/31/2007 1:00	1.81	11/11/2008 3:00	1.14	9/22/2009 1:00	0.86	9/8/2010 11:00	0.85	5/23/2011 16:00	0.77	10/14/2012 7:00	0.68	11/22/2013 3:00	0.90	9/6/2014 22:00
	6	1.53	8/16/2005 3:00	2.48	11/6/2006 11:00	2.09	6/27/2007 2:00	3.70	11/11/2008 6:00	2.43	9/12/2009 6:00	2.10	9/8/2010 11:00	2.12	10/9/2011 8:00	1.30	3/20/2012 11:00	1.40	1/9/2013 7:00	1.53	10/13/2014 11:00
	12	1.57	8/16/2005 10:00	2.52	11/6/2006 11:00	2.56	6/27/2007 9:00	4.10	11/11/2008 12:00	2.64	9/12/2009 12:00	3.43	9/8/2010 14:00	2.91	10/9/2011 14:00	2.40	3/20/2012 11:00	1.94	9/20/2013 13:00	1.54	10/13/2014 13:00
	24	1.57	8/16/2005 10:00	3.41	2/25/2006 21:00	2.97	6/27/2007 21:00	4.13	11/11/2008 13:00	3.60	10/22/2009 10:00	4.57	9/8/2010 14:00	3.82	10/9/2011 17:00	2.84	3/20/2012 14:00	2.58	9/21/2013 1:00	1.84	6/23/2014 12:00
27	1	1.25	8/16/2005 1:00	0.93	11/6/2006 6:00	1.33	3/31/2007 1:00	1.81	11/11/2008 3:00	1.14	9/22/2009 1:00	0.86	9/8/2010 11:00	0.85	5/23/2011 16:00	0.77	10/14/2012 7:00	0.68	11/22/2013 3:00	0.90	9/6/2014 22:00
	6	1.53	8/16/2005 3:00	2.48	11/6/2006 11:00	2.09	6/27/2007 2:00	3.70	11/11/2008 6:00	2.43	9/12/2009 6:00	2.10	9/8/2010 11:00	2.12	10/9/2011 8:00	1.30	3/20/2012 11:00	1.40	1/9/2013 7:00	1.53	10/13/2014 11:00
	12	1.57	8/16/2005 10:00	2.52	11/6/2006 11:00	2.56	6/27/2007 9:00	4.10	11/11/2008 12:00	2.64	9/12/2009 12:00	3.43	9/8/2010 14:00	2.91	10/9/2011 14:00	2.40	3/20/2012 11:00	1.94	9/20/2013 13:00	1.54	10/13/2014 13:00
	24	1.57	8/16/2005 10:00	3.41	2/25/2006 21:00	2.97	6/27/2007 21:00	4.13	11/11/2008 13:00	3.60	10/22/2009 10:00	4.57	9/8/2010 14:00	3.82	10/9/2011 17:00	2.84	3/20/2012 14:00	2.58	9/21/2013 1:00	1.84	6/23/2014 12:00
28	1	1.25	8/16/2005 1:00	0.93	11/6/2006 6:00	1.33	3/31/2007 1:00	1.81	11/11/2008 3:00	1.14	9/22/2009 1:00	0.86	9/8/2010 11:00	0.85	5/23/2011 16:00	0.77	10/14/2012 7:00	0.68	11/22/2013 3:00	0.90	9/6/2014 22:00
	6	1.53	8/16/2005 3:00	2.48	11/6/2006 11:00	2.09	6/27/2007 2:00	3.70	11/11/2008 6:00	2.43	9/12/2009 6:00	2.10	9/8/2010 11:00	2.12	10/9/2011 8:00	1.30	3/20/2012 11:00	1.40	1/9/2013 7:00	1.53	10/13/2014 11:00
	12	1.57	8/16/2005 10:00	2.52	11/6/2006 11:00	2.56	6/27/2007 9:00	4.10	11/11/2008 12:00	2.64	9/12/2009 12:00	3.43	9/8/2010 14:00	2.91	10/9/2011 14:00	2.40	3/20/2012 11:00	1.94	9/20/2013 13:00	1.54	10/13/2014 13:00
	24	1.57	8/16/2005 10:00	3.41	2/25/2006 21:00	2.97	6/27/2007 21:00	4.13	11/11/2008 13:00	3.60	10/22/2009 10:00	4.57	9/8/2010 14:00	3.82	10/9/2011 17:00	2.84	3/20/2012 14:00	2.58	9/21/2013 1:00	1.84	6/23/2014 12:00
29	1	1.25	8/16/2005 1:00	0.93	11/6/2006 6:00	1.33	3/31/2007 1:00	1.81	11/11/2008 3:00	1.13	9/22/2009 1:00	0.85	9/8/2010 11:00	0.85	5/23/2011 16:00	0.77	10/14/2012 7:00	0.68	11/22/2013 3:00	0.89	9/6/2014 22:00
	6	1.53	8/16/2005 3:00	2.46	11/6/2006 11:00	2.09	6/27/2007 2:00	3.70	11/11/2008 6:00	2.41	9/12/2009 6:00	2.10	9/8/2010 11:00	2.13	10/9/2011 8:00	1.30	3/20/2012 11:00	1.41	1/9/2013 7:00	1.53	10/13/2014 11:00
	12	1.56	8/16/2005 10:00	2.50	11/6/2006 11:00	2.56	6/27/2007 9:00	4.11	11/11/2008 12:00	2.62	9/12/2009 12:00	3.42	9/8/2010 14:00	2.92	10/9/2011 14:00	2.40	3/20/2012 11:00	1.93	9/20/2013 13:00	1.54	10/13/2014 14:00
	24	1.56	8/16/2005 10:00	3.41	2/25/2006 21:00	2.97	6/27/2007 21:00	4.14	11/11/2008 13:00	3.60	10/22/2009 10:00	4.55	9/8/2010 14:00	3.83	10/9/2011 18:00	2.84	3/20/2012 14:00	2.57	9/21/2013 1:00	1.83	6/23/2014 12:00
30	1	0.85	8/16/2005 1:00	0.89	11/6/2006 6:00	1.25	3/31/2007 1:00	1.54	11/11/2008 3:00	1.08	9/12/2009 1:00	0.90	9/8/2010 11:00	0.84	4/11/2011 7:00	0.79	6/6/2012 20:00	0.76	11/22/2013 3:00	0.87	9/6/2014 22:00
	6	1.05	8/16/2005 6:00	2.48	11/6/2006 11:00	2.13	6/27/2007 2:00	3.53	11/11/2008 6:00	2.25	9/12/2009 6:00	2.11	9/8/2010 11:00	2.06	10/9/2011 8:00	1.66	6/7/2012 1:00	1.46	1/9/2013 7:00	1.48	9/7/2014 1:00
	12	1.07	8/16/2005 10:00	2.56	2/25/2006 13:00	2.51	6/27/2007 9:00	3.87	11/11/2008 12:00	2.45	9/12/2009 12:00	3.54	9/8/2010 14:00	2.89	10/9/2011 14:00	2.48	3/20/2012 11:00	2.05	9/20/2013 13:00	1.51	6/22/2014 20:00
	24	1.07	8/16/2005 10:00	3.49	2/25/2006 21:00	2.96	6/27/2007 21:00	3.88	11/11/2008 13:00	3.52	10/22/2009 10:00	4.64	9/8/2010 14:00	3.79	10/9/2011 18:00	2.87	3/20/2012 14:00	2.72	9/21/2013	1.73	6/23/2014 12:00
31	1	0.87	8/16/2005 1:00	0.90	11/6/2006 6:00	1.37	3/31/2007 1:00	1.43	11/11/2008 3:00	1.07	9/12/2009 1:00	0.78	9/2/2010 10:00	0.88	4/11/2011 7:00	0.89	6/6/2012 21:00	0.71	11/22/2013 3:00	0.90	9/6/2014 22:00
	6	1.13	8/16/2005 6:00	2.31	11/6/2006 11:00	2.23	6/27/2007 3:00	3.46	11/11/2008 6:00	2.24	9/12/2009 6:00	1.99	9/8/2010 11:00	2.11	10/9/2011 8:00	1.69	6/7/2012 1:00	1.58	1/9/2013 7:00	1.53	9/7/2014 2:00
	12	1.16	8/16/2005 10:00	2.45	2/25/2006 11:00	2.58	6/27/2007 9:00	3.85	11/11/2008 12:00	2.61	10/22/2009 9:00	3.40	9/8/2010 14:00	2.92	10/9/2011 14:00	2.68	3/20/2012 11:00	2.09	1/9/2013 10:00	1.55	9/7/2014 6:00
	24	1.34	1/3/2005 23:00	3.40	2/25/2006 21:00	3.18	6/27/2007 21:00	3.85	11/11/2008 13:00	3.89	10/22/2009 10:00	4.47	9/8/2010 14:00	3.79	10/9/2011 18:00	3.08	3/20/2012 14:00	2.66	1/9/2013 16:00	1.55	9/7/2014 6:00
32	1	0.51	8/16/2005 1:00	1.11	2/25/2006 11:00	1.42	3/31/2007 1:00	2.12	11/11/2008 3:00	1.15	9/22/2009 1:00	1.12	6/28/2010 23:00	1.02	4/11/2011 7:00	0.95	6/6/2012 20:00	1.16	5/16/2013 2:00	0.70	10/13/2014 8:00
	6	0.79	3/27/2005 14:00	2.82	11/6/2006 11:00	2.04	6/27/2007 2:00	3.96	11/11/2008 5:00	1.99	9/12/2009 6:00	1.96	9/8/2010 11:00	2.56	10/9/2011 7:00	1.36	3/20/2012 11:00	1.46	1/9/2013 7:00	1.81	6/22/2014 19:00
	12	0.82	3/27/2005 15:00	3.18	2/25/2006 13:00	2.37	6/27/2007 9:00	4.17	11/11/2008 12:00	2.18	9/12/2009 12:00	3.18	9/8/2010 14:00	3.38	10/9/2011 14:00	2.39	3/20/2012 11:00	2.10	9/20/2013 12:00	2.22	6/22/2014 20:00
	24	1.21	3/27/2005 11:00	3.80	2/25/2006 21:00	2.62	6/27/2007 21:00	4.23	11/11/2008 14:00	3.43	10/22/2009 10:00	4.62	9/8/2010 11:00	4.38	10/9/2011 17:00	2.86	3/20/2012 14:00	2.89	9/21/2013	2.42	6/23/2014 12:00
33	1	0.57	8/16/2005 1:00	1.17	2/25/2006 11:00	1.35	3/31/2007 1:00	2.17	11/11/2008 3:00	1.01	9/22/2009 1:00	1.03	6/28/2010 23:00	1.02	4/11/2011 7:00	0.90	6/6/2012 20:00	1.07	5/16/2013 2:00	0.68	9/6/2014 22:00
	6	0.78	3/27/2005	2.72	11/6/2006	2.04	6/27/2007	4.05	11/11/2008	2.07	9/12/2009	2.03	9/8/2010	2.41	10/9/2011	1.42	6/7/2012	1.41	1/9/2013	1.64	6/22/2014

			14:00		11:00		2:00		6:00		6:00		11:00		8:00		1:00		7:00		19:00
	12	0.80	3/27/2005 15:00	3.13	2/25/2006 13:00	2.37	6/27/2007 9:00	4.28	11/11/2008 12:00	2.27	9/12/2009 12:00	3.36	9/8/2010 14:00	3.26	10/9/2011 14:00	2.42	3/20/2012 11:00	2.11	9/20/2013 12:00	2.05	6/22/2014 20:00
	24	1.17	3/27/2005 11:00	3.82	2/25/2006 21:00	2.64	6/27/2007 21:00	4.30	11/11/2008 14:00	3.46	10/22/2009 10:00	4.69	9/8/2010 14:00	4.18	10/9/2011 17:00	2.83	3/20/2012 14:00	2.89	9/21/2013	2.24	6/23/2014 12:00
34	1	0.55	8/16/2005 1:00	0.84	11/6/2006 6:00	1.20	6/26/2007 23:00	1.47	11/11/2008 3:00	1.14	9/12/2009 1:00	0.97	9/8/2010 11:00	0.85	4/11/2011 7:00	0.94	6/6/2012 21:00	0.84	11/22/2013 3:00	0.90	9/6/2014 22:00
	6	0.77	6/1/2005 8:00	2.50	11/6/2006 11:00	2.10	6/27/2007 3:00	3.43	11/11/2008 6:00	2.16	9/12/2009 6:00	2.19	9/8/2010 11:00	2.05	10/9/2011 8:00	1.95	6/7/2012 1:00	1.44	1/9/2013 7:00	1.66	9/7/2014 1:00
	12	0.77	6/1/2005 8:00	2.66	2/25/2006 13:00	2.42	6/27/2007 9:00	3.72	11/11/2008 12:00	2.36	9/12/2009 12:00	3.70	9/8/2010 14:00	2.92	10/9/2011 14:00	2.47	3/20/2012 11:00	2.16	9/20/2013 13:00	1.68	9/7/2014 6:00
	24	1.07	1/3/2005 23:00	3.54	2/25/2006 21:00	2.82	6/27/2007 21:00	3.72	11/11/2008 13:00	3.40	10/22/2009 10:00	4.79	9/8/2010 14:00	3.85	10/9/2011 17:00	2.82	3/20/2012 14:00	2.87	9/21/2013	1.82	6/23/2014 12:00
35	1	0.55	8/16/2005 1:00	0.85	11/6/2006 6:00	1.20	6/26/2007 23:00	1.49	11/11/2008 3:00	1.13	9/12/2009 1:00	0.96	9/8/2010 11:00	0.86	4/11/2011 7:00	0.93	6/6/2012 21:00	0.83	11/22/2013 3:00	0.90	9/6/2014 22:00
	6	0.77	6/1/2005 8:00	2.50	11/6/2006 11:00	2.10	6/27/2007 3:00	3.45	11/11/2008 6:00	2.16	9/12/2009 6:00	2.18	9/8/2010 11:00	2.06	10/9/2011 8:00	1.93	6/7/2012 1:00	1.44	1/9/2013 7:00	1.66	9/7/2014 1:00
	12	0.77	6/1/2005 8:00	2.67	2/25/2006 13:00	2.42	6/27/2007 9:00	3.74	11/11/2008 12:00	2.36	9/12/2009 12:00	3.69	9/8/2010 14:00	2.92	10/9/2011 14:00	2.47	3/20/2012 11:00	2.15	9/20/2013 13:00	1.68	9/7/2014 6:00
	24	1.06	1/3/2005 23:00	3.55	2/25/2006 21:00	2.81	6/27/2007 21:00	3.75	11/11/2008 13:00	3.40	10/22/2009 10:00	4.78	9/8/2010 14:00	3.85	10/9/2011 17:00	2.82	3/20/2012 14:00	2.86	9/21/2013	1.82	6/23/2014 12:00
36	1	0.55	8/16/2005 1:00	0.84	11/6/2006 6:00	1.20	6/26/2007 23:00	1.47	11/11/2008 3:00	1.14	9/12/2009 1:00	0.97	9/8/2010 11:00	0.85	4/11/2011 7:00	0.94	6/6/2012 21:00	0.84	11/22/2013 3:00	0.90	9/6/2014 22:00
	6	0.77	6/1/2005 8:00	2.50	11/6/2006 11:00	2.10	6/27/2007 3:00	3.44	11/11/2008 6:00	2.16	9/12/2009 6:00	2.19	9/8/2010 11:00	2.05	10/9/2011 8:00	1.94	6/7/2012 1:00	1.44	1/9/2013 7:00	1.66	9/7/2014 1:00
	12	0.77	6/1/2005 8:00	2.66	2/25/2006 13:00	2.42	6/27/2007 9:00	3.73	11/11/2008 12:00	2.36	9/12/2009 12:00	3.70	9/8/2010 14:00	2.91	10/9/2011 14:00	2.47	3/20/2012 11:00	2.15	9/20/2013 13:00	1.69	9/7/2014 6:00
	24	1.07	1/3/2005 23:00	3.54	2/25/2006 21:00	2.82	6/27/2007 21:00	3.73	11/11/2008 13:00	3.40	10/22/2009 10:00	4.78	9/8/2010 14:00	3.85	10/9/2011 17:00	2.82	3/20/2012 14:00	2.86	9/21/2013	1.81	6/23/2014 12:00
37	1	0.62	8/16/2005 1:00	0.87	11/6/2006 6:00	1.38	6/26/2007 23:00	1.71	11/11/2008 2:00	1.31	8/1/2009 2:00	0.96	9/8/2010 11:00	0.82	4/11/2011 7:00	1.05	6/6/2012 21:00	0.82	11/22/2013 3:00	0.64	10/13/2014 8:00
	6	1.22	1/3/2005 16:00	2.60	11/6/2006 11:00	2.29	6/27/2007 3:00	3.36	11/11/2008 6:00	1.98	9/12/2009 6:00	1.98	9/8/2010 11:00	1.83	10/9/2011 8:00	1.98	6/7/2012 1:00	1.62	1/9/2013 7:00	1.24	10/13/2014 11:00
	12	1.24	1/3/2005 19:00	2.60	11/6/2006 11:00	2.60	6/27/2007 9:00	3.68	11/11/2008 12:00	2.15	9/12/2009 12:00	3.51	9/8/2010 14:00	2.63	10/9/2011 14:00	2.58	3/20/2012 11:00	2.20	9/20/2013 13:00	1.26	10/13/2014 14:00
	24	1.65	1/3/2005 23:00	3.64	2/25/2006 21:00	3.30	6/27/2007 21:00	3.68	11/11/2008 13:00	3.23	10/22/2009 10:00	4.51	9/8/2010 14:00	3.40	10/9/2011 17:00	2.92	3/20/2012 14:00	2.87	9/21/2013 1:00	1.30	6/23/2014 12:00
38	1	0.59	8/16/2005 1:00	0.88	11/6/2006 6:00	1.20	6/26/2007 23:00	1.65	11/11/2008 3:00	1.09	9/12/2009 1:00	0.91	9/8/2010 11:00	0.89	4/11/2011 7:00	0.89	6/6/2012 20:00	0.80	11/22/2013 3:00	0.85	9/6/2014 22:00
	6	0.74	6/1/2005 8:00	2.55	11/6/2006 11:00	2.08	6/27/2007 2:00	3.60	11/11/2008 6:00	2.16	9/12/2009 6:00	2.15	9/8/2010 11:00	2.13	10/9/2011 8:00	1.78	6/7/2012 1:00	1.44	1/9/2013 7:00	1.61	9/7/2014 1:00
	12	0.74	6/1/2005 8:00	2.76	2/25/2006 13:00	2.41	6/27/2007 9:00	3.89	11/11/2008 12:00	2.36	9/12/2009 12:00	3.61	9/8/2010 14:00	2.99	10/9/2011 14:00	2.45	3/20/2012 11:00	2.12	9/20/2013 13:00	1.72	6/22/2014 20:00
	24	1.02	3/27/2005 11:00	3.60	2/25/2006 21:00	2.79	6/27/2007 21:00	3.89	11/11/2008 13:00	3.43	10/22/2009 10:00	4.75	9/8/2010 14:00	3.91	10/9/2011 17:00	2.82	3/20/2012 14:00	2.85	9/21/2013	1.90	6/23/2014 12:00
39	1	0.55	8/16/2005 1:00	0.84	11/6/2006 6:00	1.20	6/26/2007 23:00	1.47	11/11/2008 3:00	1.14	9/12/2009 1:00	0.97	9/8/2010 11:00	0.85	4/11/2011 7:00	0.94	6/6/2012 21:00	0.84	11/22/2013 3:00	0.90	9/6/2014 22:00
	6	0.77	6/1/2005 8:00	2.50	11/6/2006 11:00	2.10	6/27/2007 3:00	3.44	11/11/2008 6:00	2.16	9/12/2009 6:00	2.19	9/8/2010 11:00	2.05	10/9/2011 8:00	1.94	6/7/2012 1:00	1.44	1/9/2013 7:00	1.66	9/7/2014 1:00
	12	0.77	6/1/2005 8:00	2.66	2/25/2006 13:00	2.42	6/27/2007 9:00	3.73	11/11/2008 12:00	2.36	9/12/2009 12:00	3.70	9/8/2010 14:00	2.91	10/9/2011 14:00	2.47	3/20/2012 11:00	2.15	9/20/2013 13:00	1.69	9/7/2014 6:00
	24	1.07	1/3/2005 23:00	3.54	2/25/2006 21:00	2.82	6/27/2007 21:00	3.73	11/11/2008 13:00	3.40	10/22/2009 10:00	4.78	9/8/2010 14:00	3.85	10/9/2011 17:00	2.82	3/20/2012 14:00	2.86	9/21/2013	1.81	6/23/2014 12:00
40	1	0.55	8/16/2005 1:00	0.84	11/6/2006 6:00	1.20	6/26/2007 23:00	1.47	11/11/2008 3:00	1.14	9/12/2009 1:00	0.97	9/8/2010 11:00	0.85	4/11/2011 7:00	0.94	6/6/2012 21:00	0.84	11/22/2013 3:00	0.90	9/6/2014 22:00
	6	0.77	6/1/2005 8:00	2.50	11/6/2006 11:00	2.10	6/27/2007 3:00	3.44	11/11/2008 6:00	2.16	9/12/2009 6:00	2.19	9/8/2010 11:00	2.05	10/9/2011 8:00	1.94	6/7/2012 1:00	1.44	1/9/2013 7:00	1.66	9/7/2014 1:00
	12	0.77	6/1/2005 8:00	2.66	2/25/2006 13:00	2.42	6/27/2007 9:00	3.73	11/11/2008 12:00	2.36	9/12/2009 12:00	3.70	9/8/2010 14:00	2.91	10/9/2011 14:00	2.47	3/20/2012 11:00	2.15	9/20/2013 13:00	1.69	9/7/2014 6:00
	24	1.07	1/3/2005 23:00	3.54	2/25/2006 21:00	2.82	6/27/2007 21:00	3.73	11/11/2008 13:00	3.40	10/22/2009 10:00	4.78	9/8/2010 14:00	3.85	10/9/2011 17:00	2.82	3/20/2012 14:00	2.86	9/21/2013	1.81	6/23/2014 12:00
41	1	0.68	6/5/2005 12:00	0.88	11/6/2006 6:00	1.45	6/26/2007 23:00	1.80	11/11/2008 2:00	1.43	8/1/2009 2:00	1.00	7/9/2010 22:00	0.80	4/11/2011 7:00	1.09	6/6/2012 21:00	0.85	5/16/2013 5:00	0.62	10/13/2014 8:00
	6	1.40	1/3/2005 16:00	2.63	11/6/2006 11:00	2.36	6/27/2007 2:00	3.33	11/11/2008 6:00	2.12	5/3/2009	1.92	9/8/2010 14:00	1.75	10/9/2011 8:00	1.99	6/7/2012 1:00	1.68	1/9/2013 7:00	1.19	10/13/2014 11:00
	12	1.41	1/3/2005	2.63	11/6/2006	2.66	6/27/2007	3.66	11/11/2008	2.27	5/3/2009	3.45	9/8/2010	2.53	10/9/2011	2.62	3/20/2012	2.27	1/9/2013	1.21	5/13/2014

			19:00		11:00		9:00		12:00		3:00		14:00		14:00		11:00		11:00		6:00
	24	1.85	1/3/2005 23:00	3.67	2/25/2006 21:00	3.48	6/27/2007 21:00	3.66	11/11/2008 12:00	3.17	10/22/2009 10:00	4.41	9/8/2010 14:00	3.24	10/9/2011 17:00	2.96	3/20/2012 14:00	2.89	9/21/2013 1:00	1.21	5/13/2014 6:00
42	1	0.76	8/16/2005 1:00	0.89	11/6/2006 6:00	1.38	3/31/2007 1:00	1.47	11/11/2008 2:00	1.07	9/12/2009 1:00	0.78	9/8/2010 11:00	0.88	4/11/2011 7:00	1.00	6/6/2012 21:00	0.73	11/22/2013 3:00	0.83	9/6/2014 22:00
	6	1.10	1/3/2005 16:00	2.31	11/6/2006 11:00	2.28	6/27/2007 3:00	3.39	11/11/2008 6:00	2.16	9/12/2009 6:00	1.95	9/8/2010 11:00	2.06	10/9/2011 8:00	1.82	6/7/2012 1:00	1.63	1/9/2013 7:00	1.48	9/7/2014 2:00
	12	1.11	1/3/2005 23:00	2.46	2/25/2006 11:00	2.60	6/27/2007 9:00	3.76	11/11/2008 12:00	2.63	10/22/2009 9:00	3.40	9/8/2010 14:00	2.87	10/9/2011 15:00	2.74	3/20/2012 11:00	2.16	1/9/2013 11:00	1.51	9/7/2014 6:00
	24	1.56	1/3/2005 23:00	3.44	2/25/2006 21:00	3.26	6/27/2007 21:00	3.76	11/11/2008 12:00	3.86	10/22/2009 10:00	4.44	9/8/2010 14:00	3.71	10/9/2011 18:00	3.12	3/20/2012 14:00	2.75	1/9/2013 16:00	1.51	9/7/2014 6:00
43	1	0.68	6/5/2005 12:00	0.88	11/6/2006 6:00	1.45	6/26/2007 23:00	1.80	11/11/2008 2:00	1.43	8/1/2009 2:00	1.00	7/9/2010 22:00	0.80	4/11/2011 7:00	1.09	6/6/2012 21:00	0.85	5/16/2013 5:00	0.62	10/13/2014 8:00
	6	1.40	1/3/2005 16:00	2.63	11/6/2006 11:00	2.36	6/27/2007 2:00	3.33	11/11/2008 6:00	2.12	5/3/2009	1.92	9/8/2010 14:00	1.75	10/9/2011 8:00	1.99	6/7/2012 1:00	1.68	1/9/2013 7:00	1.19	10/13/2014 11:00
	12	1.41	1/3/2005 19:00	2.63	11/6/2006 11:00	2.66	6/27/2007 9:00	3.66	11/11/2008 12:00	2.27	5/3/2009 3:00	3.45	9/8/2010 14:00	2.53	10/9/2011 14:00	2.62	3/20/2012 11:00	2.27	1/9/2013 11:00	1.21	5/13/2014 6:00
	24	1.85	1/3/2005 23:00	3.67	2/25/2006 21:00	3.48	6/27/2007 21:00	3.66	11/11/2008 12:00	3.17	10/22/2009 10:00	4.41	9/8/2010 14:00	3.24	10/9/2011 17:00	2.96	3/20/2012 14:00	2.89	9/21/2013 1:00	1.21	5/13/2014 6:00
44	1	0.69	8/16/2005 1:00	0.89	11/6/2006 6:00	1.41	6/26/2007 23:00	1.68	11/11/2008 2:00	1.20	8/1/2009 2:00	0.89	9/8/2010 11:00	0.84	4/11/2011 7:00	1.06	6/6/2012 21:00	0.79	11/22/2013 3:00	0.63	10/13/2014 8:00
	6	1.29	1/3/2005 16:00	2.51	11/6/2006 11:00	2.33	6/27/2007 3:00	3.35	11/11/2008 6:00	2.01	9/12/2009 6:00	1.93	9/8/2010 11:00	1.87	10/9/2011 8:00	1.93	6/7/2012 1:00	1.66	1/9/2013 7:00	1.24	10/13/2014 11:00
	12	1.30	1/3/2005 19:00	2.51	11/6/2006 11:00	2.64	6/27/2007 9:00	3.70	11/11/2008 12:00	2.32	10/22/2009 9:00	3.43	9/8/2010 14:00	2.66	10/9/2011 14:00	2.66	3/20/2012 11:00	2.23	1/9/2013 11:00	1.28	5/13/2014 6:00
	24	1.74	1/3/2005 23:00	3.58	2/25/2006 21:00	3.39	6/27/2007 21:00	3.70	11/11/2008 12:00	3.43	10/22/2009 10:00	4.42	9/8/2010 14:00	3.42	10/9/2011 18:00	3.02	3/20/2012 14:00	2.83	1/9/2013 16:00	1.29	5/13/2014 6:00
45	1	0.73	8/16/2005 1:00	0.89	11/6/2006 6:00	1.37	6/26/2007 23:00	1.55	11/11/2008 2:00	1.06	9/12/2009 1:00	0.83	9/8/2010 11:00	0.87	4/11/2011 7:00	1.02	6/6/2012 21:00	0.75	11/22/2013 3:00	0.74	9/6/2014 22:00
	6	1.17	1/3/2005 16:00	2.39	11/6/2006 11:00	2.30	6/27/2007 3:00	3.37	11/11/2008 6:00	2.10	9/12/2009 6:00	1.94	9/8/2010 11:00	1.99	10/9/2011 8:00	1.86	6/7/2012 1:00	1.64	1/9/2013 7:00	1.35	9/7/2014 2:00
	12	1.18	1/3/2005 19:00	2.46	2/25/2006 11:00	2.61	6/27/2007 9:00	3.74	11/11/2008 12:00	2.51	10/22/2009 9:00	3.41	9/8/2010 14:00	2.79	10/9/2011 14:00	2.71	3/20/2012 11:00	2.19	1/9/2013 11:00	1.38	9/7/2014 6:00
	24	1.63	1/3/2005 23:00	3.49	2/25/2006 21:00	3.31	6/27/2007 21:00	3.74	11/11/2008 12:00	3.70	10/22/2009 10:00	4.44	9/8/2010 14:00	3.60	10/9/2011 18:00	3.08	3/20/2012 14:00	2.78	1/9/2013 16:00	1.38	9/7/2014 6:00
46	1	0.68	6/5/2005 12:00	0.88	11/6/2006 6:00	1.45	6/26/2007 23:00	1.80	11/11/2008 2:00	1.43	8/1/2009 2:00	1.00	7/9/2010 22:00	0.80	4/11/2011 7:00	1.09	6/6/2012 21:00	0.85	5/16/2013 5:00	0.62	10/13/2014 8:00
	6	1.40	1/3/2005 16:00	2.63	11/6/2006 11:00	2.36	6/27/2007 2:00	3.33	11/11/2008 6:00	2.12	5/3/2009	1.92	9/8/2010 14:00	1.75	10/9/2011 8:00	1.99	6/7/2012 1:00	1.68	1/9/2013 7:00	1.19	10/13/2014 11:00
	12	1.41	1/3/2005 19:00	2.63	11/6/2006 11:00	2.66	6/27/2007 9:00	3.66	11/11/2008 12:00	2.27	5/3/2009 3:00	3.45	9/8/2010 14:00	2.53	10/9/2011 14:00	2.62	3/20/2012 11:00	2.27	1/9/2013 11:00	1.21	5/13/2014 6:00
	24	1.85	1/3/2005 23:00	3.67	2/25/2006 21:00	3.48	6/27/2007 21:00	3.66	11/11/2008 12:00	3.17	10/22/2009 10:00	4.41	9/8/2010 14:00	3.24	10/9/2011 17:00	2.96	3/20/2012 14:00	2.89	9/21/2013 1:00	1.21	5/13/2014 6:00
47	1	0.68	6/5/2005 12:00	0.88	11/6/2006 6:00	1.45	6/26/2007 23:00	1.80	11/11/2008 2:00	1.43	8/1/2009 2:00	1.00	7/9/2010 22:00	0.80	4/11/2011 7:00	1.09	6/6/2012 21:00	0.85	5/16/2013 5:00	0.62	10/13/2014 8:00
	6	1.40	1/3/2005 16:00	2.63	11/6/2006 11:00	2.36	6/27/2007 2:00	3.33	11/11/2008 6:00	2.12	5/3/2009	1.92	9/8/2010 14:00	1.75	10/9/2011 8:00	1.99	6/7/2012 1:00	1.68	1/9/2013 7:00	1.19	10/13/2014 11:00
	12	1.41	1/3/2005 19:00	2.63	11/6/2006 11:00	2.66	6/27/2007 9:00	3.66	11/11/2008 12:00	2.27	5/3/2009 3:00	3.45	9/8/2010 14:00	2.53	10/9/2011 14:00	2.62	3/20/2012 11:00	2.27	1/9/2013 11:00	1.21	5/13/2014 6:00
	24	1.85	1/3/2005 23:00	3.67	2/25/2006 21:00	3.48	6/27/2007 21:00	3.66	11/11/2008 12:00	3.17	10/22/2009 10:00	4.41	9/8/2010 14:00	3.24	10/9/2011 17:00	2.96	3/20/2012 14:00	2.89	9/21/2013 1:00	1.21	5/13/2014 6:00
48	1	0.55	6/5/2005 11:00	0.62	11/6/2006 6:00	1.52	6/26/2007 23:00	1.41	4/24/2008 2:00	1.39	5/2/2009 23:00	0.97	9/8/2010 11:00	0.80	4/11/2011 7:00	1.34	6/6/2012 21:00	0.86	11/22/2013 3:00	1.00	5/12/2014 21:00
	6	1.08	6/5/2005 14:00	2.51	11/6/2006 11:00	2.39	6/27/2007 3:00	2.53	11/11/2008 6:00	2.13	5/3/2009	2.14	9/8/2010 11:00	2.02	10/9/2011 8:00	2.35	6/7/2012 1:00	1.73	1/9/2013 7:00	1.67	5/13/2014 1:00
	12	1.08	6/5/2005 14:00	2.52	11/6/2006 14:00	2.66	6/27/2007 9:00	2.70	11/11/2008 12:00	2.29	5/3/2009 5:00	3.97	9/8/2010 14:00	2.97	10/9/2011 14:00	2.87	3/20/2012 11:00	2.36	1/9/2013 11:00	1.77	5/13/2014 7:00
	24	1.29	1/3/2005 23:00	3.08	2/25/2006 21:00	3.51	6/27/2007 21:00	2.71	11/11/2008 14:00	3.27	10/22/2009 10:00	5.13	9/8/2010 14:00	3.84	10/9/2011 18:00	3.23	3/20/2012 14:00	3.02	1/9/2013 16:00	1.78	5/13/2014 11:00
49	1	0.68	6/5/2005 12:00	0.88	11/6/2006 6:00	1.45	6/26/2007 23:00	1.80	11/11/2008 2:00	1.43	8/1/2009 2:00	1.00	7/9/2010 22:00	0.80	4/11/2011 7:00	1.09	6/6/2012 21:00	0.85	5/16/2013 5:00	0.62	10/13/2014 8:00
	6	1.40	1/3/2005 16:00	2.63	11/6/2006 11:00	2.36	6/27/2007 2:00	3.33	11/11/2008 6:00	2.12	5/3/2009	1.92	9/8/2010 14:00	1.75	10/9/2011 8:00	1.99	6/7/2012 1:00	1.68	1/9/2013 7:00	1.19	10/13/2014 11:00
	12	1.41	1/3/2005 19:00	2.63	11/6/2006 11:00	2.66	6/27/2007 9:00	3.66	11/11/2008 12:00	2.27	5/3/2009 3:00	3.45	9/8/2010 14:00	2.53	10/9/2011 14:00	2.62	3/20/2012 11:00	2.27	1/9/2013 11:00	1.21	5/13/2014 6:00

	24	1.85	1/3/2005 23:00	3.67	2/25/2006 21:00	3.48	6/27/2007 21:00	3.66	11/11/2008 12:00	3.17	10/22/2009 10:00	4.41	9/8/2010 14:00	3.24	10/9/2011 17:00	2.96	3/20/2012 14:00	2.89	9/21/2013 1:00	1.21	5/13/2014 6:00
50	1	0.68	6/5/2005 12:00	0.88	11/6/2006 6:00	1.45	6/26/2007 23:00	1.80	11/11/2008 2:00	1.43	8/1/2009 2:00	1.00	7/9/2010 22:00	0.80	4/11/2011 7:00	1.09	6/6/2012 21:00	0.85	5/16/2013 5:00	0.62	10/13/2014 8:00
	6	1.40	1/3/2005 16:00	2.63	11/6/2006 11:00	2.36	6/27/2007 2:00	3.33	11/11/2008 6:00	2.12	5/3/2009	1.92	9/8/2010 14:00	1.75	10/9/2011 8:00	1.99	6/7/2012 1:00	1.68	1/9/2013 7:00	1.19	10/13/2014 11:00
	12	1.41	1/3/2005 19:00	2.63	11/6/2006 11:00	2.66	6/27/2007 9:00	3.66	11/11/2008 12:00	2.27	5/3/2009 3:00	3.45	9/8/2010 14:00	2.53	10/9/2011 14:00	2.62	3/20/2012 11:00	2.27	1/9/2013 11:00	1.21	5/13/2014 6:00
	24	1.85	1/3/2005 23:00	3.67	2/25/2006 21:00	3.48	6/27/2007 21:00	3.66	11/11/2008 12:00	3.17	10/22/2009 10:00	4.41	9/8/2010 14:00	3.24	10/9/2011 17:00	2.96	3/20/2012 14:00	2.89	9/21/2013 1:00	1.21	5/13/2014 6:00
51	1	0.73	8/16/2005 1:00	0.89	11/6/2006 6:00	1.37	6/26/2007 23:00	1.56	11/11/2008 2:00	1.06	9/12/2009 1:00	0.83	9/8/2010 11:00	0.86	4/11/2011 7:00	1.03	6/6/2012 21:00	0.76	11/22/2013 3:00	0.72	9/6/2014 22:00
	6	1.19	1/3/2005 16:00	2.40	11/6/2006 11:00	2.30	6/27/2007 3:00	3.37	11/11/2008 6:00	2.09	9/12/2009 6:00	1.94	9/8/2010 11:00	1.97	10/9/2011 8:00	1.87	6/7/2012 1:00	1.64	1/9/2013 7:00	1.33	9/7/2014 2:00
	12	1.19	1/3/2005 19:00	2.47	2/25/2006 11:00	2.61	6/27/2007 9:00	3.74	11/11/2008 12:00	2.49	10/22/2009 9:00	3.41	9/8/2010 14:00	2.78	10/9/2011 14:00	2.71	3/20/2012 11:00	2.19	1/9/2013 11:00	1.36	9/7/2014 6:00
	24	1.64	1/3/2005 23:00	3.50	2/25/2006 21:00	3.32	6/27/2007 21:00	3.74	11/11/2008 12:00	3.67	10/22/2009 10:00	4.43	9/8/2010 14:00	3.58	10/9/2011 18:00	3.08	3/20/2012 14:00	2.79	1/9/2013 16:00	1.36	9/7/2014 6:00
52	1	0.68	6/5/2005 12:00	0.88	11/6/2006 6:00	1.45	6/26/2007 23:00	1.80	11/11/2008 2:00	1.43	8/1/2009 2:00	1.00	7/9/2010 22:00	0.80	4/11/2011 7:00	1.09	6/6/2012 21:00	0.85	5/16/2013 5:00	0.62	10/13/2014 8:00
	6	1.40	1/3/2005 16:00	2.63	11/6/2006 11:00	2.36	6/27/2007 2:00	3.33	11/11/2008 6:00	2.12	5/3/2009	1.92	9/8/2010 14:00	1.75	10/9/2011 8:00	1.99	6/7/2012 1:00	1.68	1/9/2013 7:00	1.19	10/13/2014 11:00
	12	1.41	1/3/2005 19:00	2.63	11/6/2006 11:00	2.66	6/27/2007 9:00	3.66	11/11/2008 12:00	2.27	5/3/2009 3:00	3.45	9/8/2010 14:00	2.53	10/9/2011 14:00	2.62	3/20/2012 11:00	2.27	1/9/2013 11:00	1.21	5/13/2014 6:00
	24	1.85	1/3/2005 23:00	3.67	2/25/2006 21:00	3.48	6/27/2007 21:00	3.66	11/11/2008 12:00	3.17	10/22/2009 10:00	4.41	9/8/2010 14:00	3.24	10/9/2011 17:00	2.96	3/20/2012 14:00	2.89	9/21/2013 1:00	1.21	5/13/2014 6:00
53	1	0.78	8/16/2005 1:00	0.90	11/6/2006 6:00	1.39	3/31/2007 1:00	1.40	11/11/2008 2:00	1.07	9/12/2009 1:00	0.83	9/2/2010 10:00	0.90	4/11/2011 7:00	0.98	6/6/2012 21:00	0.71	11/22/2013 3:00	0.92	9/6/2014 22:00
	6	1.04	8/16/2005 6:00	2.24	11/6/2006 11:00	2.26	6/27/2007 3:00	3.40	11/11/2008 6:00	2.21	9/12/2009 6:00	1.96	9/8/2010 11:00	2.12	10/9/2011 8:00	1.79	6/7/2012 1:00	1.62	1/9/2013 7:00	1.60	9/7/2014 2:00
	12	1.08	8/16/2005 10:00	2.45	2/25/2006 11:00	2.58	6/27/2007 9:00	3.79	11/11/2008 12:00	2.74	10/22/2009 9:00	3.39	9/8/2010 14:00	2.96	10/9/2011 15:00	2.76	3/20/2012 11:00	2.14	1/9/2013 10:00	1.62	9/7/2014 6:00
	24	1.49	1/3/2005 23:00	3.38	2/25/2006 21:00	3.22	6/27/2007 21:00	3.79	11/11/2008 12:00	4.00	10/22/2009 10:00	4.45	9/8/2010 14:00	3.81	10/9/2011 18:00	3.15	3/20/2012 14:00	2.72	1/9/2013 16:00	1.62	9/7/2014 6:00
54	1	0.75	8/16/2005 1:00	0.89	11/6/2006 6:00	1.37	3/31/2007 1:00	1.51	11/11/2008 2:00	1.06	9/12/2009 1:00	0.80	9/8/2010 11:00	0.88	4/11/2011 7:00	1.01	6/6/2012 21:00	0.74	11/22/2013 3:00	0.79	9/6/2014 22:00
	6	1.13	1/3/2005 16:00	2.34	11/6/2006 11:00	2.29	6/27/2007 3:00	3.38	11/11/2008 6:00	2.14	9/12/2009 6:00	1.95	9/8/2010 11:00	2.03	10/9/2011 8:00	1.84	6/7/2012 1:00	1.63	1/9/2013 7:00	1.42	9/7/2014 2:00
	12	1.14	1/3/2005 19:00	2.46	2/25/2006 11:00	2.60	6/27/2007 9:00	3.75	11/11/2008 12:00	2.58	10/22/2009 9:00	3.40	9/8/2010 14:00	2.84	10/9/2011 14:00	2.73	3/20/2012 11:00	2.17	1/9/2013 11:00	1.45	9/7/2014 6:00
	24	1.59	1/3/2005 23:00	3.46	2/25/2006 21:00	3.28	6/27/2007 21:00	3.75	11/11/2008 12:00	3.79	10/22/2009 10:00	4.44	9/8/2010 14:00	3.66	10/9/2011 18:00	3.10	3/20/2012 14:00	2.76	1/9/2013 16:00	1.45	9/7/2014 6:00

References

Adams B.J., Howard, C.D.D., 1986. Design Storm Pathology, Canadian Water Resources Journal Revue canadienne des ressources hydriques, 11:3, 49-55, DOI: 10.4296/cwrj1103049

Alila, Y., 1999. A hierarchical approach for the regionalization of precipitation annual maxima in Canada. J. Geophys. Res. 104 (D24), 31645–31655. http://dx.doi.org/10.1029/1999JD900764.

Allen, R.J., DeGaetano, A.T., 2005. Considerations for the use of radar-derived precipitation estimates in determining return intervals for extreme areal precipitation amounts. J. Hydrol. 315(1), 203-219.

Asquith, W.H., 1998. Depth-Duration Frequency of Precipitation for Texas: U.S. Geological Survey Water-Resources Investigations Report 98–4044.

Asquith, W.H., Famiglietti, J.S., 2000. Precipitation areal reduction factor estimation using an annual-maxima centered approach: J. Hydrol. 230, 55–69.

Asquith, W.H., Roussel, M.C., 2004. Atlas of depth-duration frequency of precipitation annual maxima for Texas: U.S. Geological Survey Scientific Investigations Report 2004–5041, 106.

Basu, B., Srinivas, V.V., 2015. A recursive multi-scaling approach to regional flood frequency analysis. J. of Hydrol. 529, 373-383.

Breidenbach, J.P., Seo, D.J., Fulton, R. A., 1998. Stage II and III post processing of the NEXRAD precipitation estimates in the modernized National Weather Service, 14th Conf on IIPS, AMS, Phoenix, Jan.

Brodie, I.M., 2013. Rational Monte Carlo method for flood frequency analysis in urban catchments. J. of Hydrol. 486, 306-314.

Chow, V.T., Maidment, D.R., and Mays, L.W., 1988. Applied Hydrology. New York: McGraw-Hill, 1988. Print.

Durrans, S.R., Julian, L.T., Yekta, M., 2002. Estimation of depth-area relationships using radar-rainfall data. Journal of Hydrologic Engineering, 7(5), 356-367.

Eagleson, P.S., Dynamic Hydrology, McGraw-Hill, New York, 462p., 1970.

Eldardiry, H., Habib, E., Zhang, Y., 2015. On the Use of Radar-Based Quantitative Precipitation Estimates for Precipitation Frequency Analysis. J. Hydrol. 531, 441-453. DOI: 10.1016/j.jhydrol.2015.05.016

England, J.F., Julien, P.Y., Velleux, M.L., 2014. Physically-based Extreme Flood Frequency with Stochastic Storm Transposition and Paleoflood Data on Large Watersheds. J. Hydrol. 510, 228-45.

Franchinia, M., Helmlingerb, K.R., Foufoula-Georgioub, E., Todini, E., 1996. Stochastic storm transposition coupled with rainfall-runoff modeling for estimation of exceedance probabilities of design floods, J. Hydrol. 175(1-4), 511–532, doi:10.1016/S0022-1694(96)80022-9.

Frederick, R.H., Myers, V.A., Auciello, E.P., 1977. Five- to Sixty-Minute Precipitation Frequency for the Eastern and Central United States. Silver Spring, MD: U.S. Dept. of Commerce, National Oceanic and Atmospheric Administration, 1977. Print.

Fulton, R.A., 2002. Activities to improve WSR-88D radar rainfall estimation in the National Weather Service. In: Proceedings of the Second Federal Interagency Hydrologic Modeling Conference, Las Vegas, Nevada, July 28–August 1.

Fulton, R.A., Ding, F., and Miller, D.A., 2003. Truncation errors in historical WSR-88D rainfall products. 31st Conference on Radar Meteorology, Amer. Meteor. Soc., Seattle, WA, August 2003.

Foufoula-Georgiou, E., 1989. A probabilistic storm transposition approach for estimating exceedance probabilities of extreme precipitation depths. Water Resour. Res., 25(5), 799–815, doi:10.1029/WR025i005p00799.

Fowler, H.J., Kilsby, C.G., 2003. A regional frequency analysis of United Kingdom extreme rainfall from 1961 to 2000. Int. J. Climatol. 23, 1313–1334. http://dx.doi.org/10.1002/joc.943.

Gellens, D., 2002. Combining regional approach and data extension procedure for assessing GEV distribution of extreme precipitation in Belgium. J. Hydrol. 268, 113–126. http://dx.doi.org/10.1016/S0022-1694(02)00160-9.

Greene, D.R., Huldow, M.D., 1982. Hydrolometeorologic grid mapping procedure. American Water Resours. Assn. Int. Symp. On Hydrolometeorol. AURA, Herndon, Va.

Gutknecht, D., 1977. Ein Computermodell zur Erzeugung einer Folge von Regenereignissen, Tech. Report, Inst. f. Hydraulik, Technical University of Vienna.

Habib, E., Larsona, B.F., Graschelb, J., 2009. Validation of NEXRAD multisensor precipitation estimates using an experimental dense rain gauge network in south Louisiana. J. Hydrol. 373 (3-4), 463-478.

Habib, E., Qin, L., Seo, D.J., Ciach, G.J., Nelson, B., 2013. Independent Assessment of Incremental Complexity in NWS Multisensor Precipitation Estimator Algorithms. J. Hydrol. Eng. 18, 143-155.

Hansen, E.M., 1987. Probable maximum precipitation for design floods in the united states. J. Hydrol. 96, 267–278.

Hao, Z., Singh, V.P., 2013. Entropy-based method for extreme rainfall analysis in Texas. J. Geophys. Res-Atmos. 118, 263–273, doi:10.1029/2011JD017394.

Hershfield, D.M., Wilson, W.T., Hiatt, W.E., 1958. Rainfall Intensity-frequency Regime. Part 2 - Southeastern United States. Washington, D.C.: U. S. Department of Commerce, Weather Bureau.

Hershfield, D.M., 1961. Rainfall Frequency Atlas of the United States: For Durations from 30 Minutes to 24 Hours and Return Periods from 1 to 100 Years. Washington: Dept. of Commerce, Weather Bureau.

Hershfield, D.M., 1962. Rainfall frequency atlas of the united states for Durations from 30 Minutes to 24 Hours and Return Periods from 1 to 100 Years. Technical Report No. 40. U.S. Department of Commerce.

iSWM Technical Manual, 2014. http://iswm.nctcog.org/Documents/technical_manual/Hydrology_9-2014.pdf

Kappel, Bill, Ed Tomlinson, Courtney Jalbert, and Louie Verreault. Site-Specific PMP for North Texas: Bringing HMR 51 into the 21st Century. Proc. of United States Society on Dams 2012 Annual Meeting and Conference, New Orleans, LA. Monument, CO: Applied Weather Associates, 2012.

Klazura, G.E., Imy, D.A, 1993. A description of the initial set of analysis products available from the NEXRAD WSR-88D System. Bull. Amer. Meteorol. Soc. 74, 1293-1312.

Koutsoyiannis, D., 2004. Statistics of extremes and estimation of extreme rainfall: II. Empirical investigation of long rainfall records. Hydrol. Sci. J. 49 (4), 591–610. http://dx.doi.org/10.1623/hysj.49.4.575.54430.

Marra, F., Morin, E., 2015. Use of radar QPE for the derivation of Intensity–Duration–Frequency curves in a range of climatic regimes. J. Hydrol. 531, 427-440.

Nguyen, C.C., Gaume, E., Payrastre, O., 2014. Regional flood frequency analyses involving extraordinary flood events at ungauged sites: further developments and validations. J. Hydrol. 508, 385-396.

Olivera, F., Choi, J., Kim, D., Li, M.H., 2008. Estimation of average rainfall areal reduction factors in Texas using NEXRAD data. J. Hydrol. Eng. 13(6), pp. 438-448.

Overeem, A., Buishand, T.A., Holleman, I., 2009. Extreme rainfall analysis and estimation of depth–duration–frequency curves using weather radar. Water Resour. Res. 45, W10424. http://dx.doi.org/10.1029/2009WR007869.

Paixao, E., Qader Mirza M.M., Shephard, M.W., Auld, H., Klaassen , J., Smith, G., 2015. An integrated approach for identifying homogeneous regions of extreme rainfall events and estimating IDF curves in Southern Ontario, Canada: Incorporating radar observations. J. of Hydrol. 528, 734-750.

Perica, S., Martin, D., Pavlovic, S., Roy, I., Laurent, M., Trypaluk, C., Unruh, D., Yekta, M., Bonnin, G., 2013. Precipitation-frequency atlas of the United States, NOAA Atlas 14, Volume 9, Version 2: Southeastern States, Silver Spring, Maryland, 2013: U.S. Department of Commerce, National Oceanic and Atmospheric Adminstration, National Weather Service.

Rafieeinasab, A., Norouzi, A., Seo, D.J., Nelson, B., 2015. Improving high-resolution quantitative precipitation estimation via fusion of multiple radar-based precipitation products. J. Hydrol. 531, 320-336.

Reed, S.M., Maidment, D.R., 1999. Coordinate Transformations for Using NEXRAD Data in GIS-Based Hydrologic Modeling. Journal of Hydrologic Engineering, Vol. 4, No. 2, pp. 174-182, (doi: http://dx.doi.org/10.1061/(ASCE)1084-0699(1999)4:2(174))

Seo, D.J., Seed, A., Delrieu, G., 2010. Radar-based rainfall estimation, chapter in AGU Book Volume on Rainfall: State of the Science, F. Testik and M. Gebremichael, Editors. Geophys. Monogr. Ser. 191. doi:10.1029/GM191.

Sivapalan, M., B1oschl, G., 1998. Transformation of point rainfall to areal rainfall: Intensity-duration-frequency curves. J. Hydrol. 204, 150-167.

Stedinger, J.R., Vogel, R.M., Foufoula-Georgio, E., 1993. Frequency analysis of extreme events. In: D. R. Maidment, ed. Handbook of Hydrology. New York: McGraw-Hill, p. 18.1 – 18.66.

Feldman, A.D., 1979. Flood hydrograph and peak flow analysis. Technical Report 62.

Olson, D., Norman W.J., Korty, B., 1995. Evaluation of 33 Years of Quantitative Precipitation Forecasting at the NMC". Weather and Forecasting. 09/1995; 10(3), 498-511

U. S. Weather Bureau, 1957. Rainfall intensity-frequency regime. 1. The Ohio Valley; 2. Southeastern United States. Tech. Paper No. 29, U. S. Dept. of Commerce, Washington, D.C.

US Army Corps of Engineers, HMR52, 1984. Probable Maximum Storm (Eastern United States).

Villarini, G., Smith, J.A., Serinaldi, F., Bales, J., Bates, P.D., Krajewski, W.F., 2009. Flood frequency analysis for nonstationary annual peak records in an urban drainage basin. Advances in Water Resources 32, 1255–1266.

Wang, X., Xie, H., Sharif, H., Zeitler, J., 2008. Validating NEXRAD MPE and stage III precipitation products for uniform rainfall on the Upper Guadalupe River Basin for the Texas Hill Country. J. Hydrol. 348, 73-86.

Westcott, N.E., Knapp, H.V., Hillberg, S.D., 2008. Comparison of gage and multi-sensor precipitation estimates over a range of spatial and temporal scales in the Midwestern United States. J. Hydrol. 351, 1-12.

Wright, D.B., Smith, J.A., Villarini, G., Baeck, M.L., 2013. Estimating the frequency of extreme rainfall using weather radar and stochastic storm transposition, J. Hydrol. 488, 150–165, doi:10.1016/j.jhydrol.2013.03.003.

Wright, D.B., Smith, J.A., Baeck, M.L., 2014. Flood Frequency Analysis Using Radar Rainfall Fields and Stochastic Storm Transposition. Water Resources Research 50(2), 1592-1615.

Zhang, Y., Reed, S., Kitzmiller, D., 2011. Effects of retrospective gauge-based readjustment of multi-sensor precipitation estimates on hydrologic simulations. J. Hydrometeorol. 12(3), 429–443.

Zhang Q., Gu X., Singh V.P., Xiao, M., 2014. Flood frequency analysis with consideration of hydrological alterations: Changing properties, causes and implications. J. Hydrol. 519, 803-813.

Zhang, J., Howard, K., Langston, C., Kaney, B., Qi, Y., Tang, L., Grams, H., Wang, Y., Cocks, S., Martinaitis, S., Arthur, A., Cooper, K., Brogden, J., Kitzmiller, D., 2015. Multi-Radar Multi-Sensor (MRMS) Quantitative Precipitation Estimation: Initial Operating Capabilities, submitted to Bulletin of the American Meteorological Society.

Biographical Information

Morteza Kiani, obtained B.Sc. degree in Water Drainage Network Engineering at University of Zabol in 2005. He pursued graduate studies in Water Engineering at Azad University, Central Branch and obtained M.Sc. degree in 2010 in Civil Engineering (Hydraulics) .In addition to his academic experience. He worked for three years at ReyAb Consultant company and involved in numerous practical the projects such drainage network systems for three municipality zones 7,18,21) at city of Tehran and developing river inundation maps for Qom rivers . He also worked for as developer at Iran's and Water Research Institute (ministry of energy) as a programmer to develop a flood forecasting system for many provinces in Iran. He started his Master program in spring 2014 under supervision of Dr. Nick Fang and gained significant experience in hydrologic modeling.